

34 ELECTRON TRANSFER IN ION-ATOM COLLISIONS

by

LAURA NORMAN TUNNELL

B.S., East Texas State University, 1976

A MASTER'S THESIS

submitted in partial fulfillment of the

requirements for the degree

MASTER OF SCIENCE

Department of Physics

KANSAS STATE UNIVERSITY
Manhattan, Kansas

1979

Approved:


Major Professor

Spm Cell
LD
266T
.T4
1977
T85
e.2

TABLE OF CONTENTS

LIST OF FIGURESii
LIST OF TABLESiii
ACKNOWLEDGEMENTSiv
I. INTRODUCTION	1
II. DESCRIPTION OF THE TSAE METHOD	12
A. Derivation of the Coupled Equations	12
B. Comparison of the TSAE Expression With Various Born Theories	18
III. NUMERICAL METHOD	21
A. Potential and Wavefunction	21
B. Matrix Elements	23
C. Numerical Integration of the Coupled Equations	28
IV. RESULTS	30
A. Gross Features of Electron Transfer Cross Sections	30
B. Comparison of K-K Results Using Different Atomic Models	34
C. Outer Shell Capture	43
V. DISCUSSION AND SUMMARY	54
A. Atomic Model	55
B. Scattering Model	55
REFERENCES	57
APPENDIX I	66
APPENDIX II	78
APPENDIX III	124
ABSTRACT	

LIST OF FIGURES

I.1	Fluorine X-Ray Spectra Resulting From the Bombardment of Neutral Helium by F^{4+} and F^{9+}	2
I.2	Copper K X-Ray Production as a Function of Projectile Charge State	5
I.3	Comparison of Various Theoretical Results With Experimental Data for the Capture of Hydrogen K Shell Electrons by Protons	9
II.1	The Coordinate System Used to Perform the Calculations	13
III.1	Rotation of the Lab Coordinates With Respect to the Coordinate System Used to Perform the Calculations	26
IV.1	General Characteristics of the Electron Transfer Cross Section as a Function of Projectile Energy	32
IV.2	Comparison of the Screened Hydrogenic and Herman-Skillman Potentials for Neutral Argon	36
IV.3	Comparison of the Argon 1s Wavefunction Using the Screened Hydrogenic and Herman-Skillman Models	36
IV.4	K-K Capture Cross Sections for $P + Ar$ and $F^{9+} + Ar$	38
IV.5	The Potential Curves for $P + Ar$ and $F^{9+} + Ar$ in the Screened Hydrogenic and Herman-Skillman Models	41
IV.6	Cross Sections For Electron Transfer for $P + Ar$	45
IV.7	The Weighted Capture Probability as a Function of Impact Parameter for $P + Ar$	47
IV.8	Electron Capture From the Outermost Shells of Neon and Krypton by Protons	52

LIST OF TABLES

III.1	Comparison of Orbital Energies For the Bound States of Argon59
III.2	Exponents and Expansion Coefficients For Neutral Argon60
IV.1	K-K Capture Cross Sections For Bare Projectiles on Noble Gases61
IV.2	Target Ionicity Dependence of K-K Capture Cross Sections For $P^{9+} + Ar$62
IV.3	Subshell Capture Cross Sections Per Target Atom For $P + Ar$63
IV.4	Subshell Capture Cross Sections Per Target Atom For Protons on Krypton and Neon64
IV.5	Z_p Dependence of the Argon ($N = 2$) $\rightarrow Z_p(N = 1)$ Capture Cross Sections Per Target Atom65

ACKNOWLEDGEMENTS

The author wishes to express appreciation to Dr. C. D. Lin for his patience and guidance throughout the course of this work. She is grateful to the U. S. Department of Energy, Division of Chemical Sciences for financial support under contract no. EY-76-S-02-2753. Use of the computer facilities at Argonne National Laboratory and the assistance of Drs. K. T. Lu and K. T. Cheng are also appreciated. The author wishes to thank Richard Vore for his technical assistance and Rhonda Born for the painstaking job of typing this thesis.

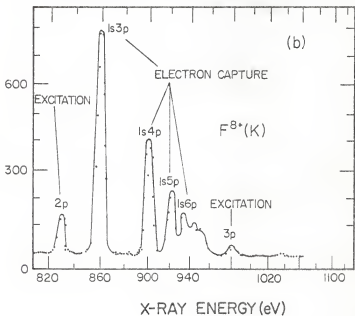
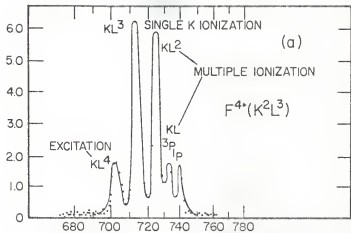
CHAPTER I: INTRODUCTION

Electron capture has been a subject of interest for both experimentalists and theoreticians in recent years. The transfer of an electron from the bound state of one system to the bound state of another is of fundamental interest; it is the very basis of many chemical processes. An understanding of charge exchange is needed in order to explain the bulk behavior of plasmas in thermonuclear reactions. It is also an important inelastic process occurring in ion-atom collisions.

Along with the widespread use of tandem Van de Graaff accelerators in recent years, ion-atom collisions have been investigated by experimentalists over a spectrum of projectile velocities and charge states. In a violent ion-atom collision electrons in both the target and projectile can undergo a variety of single or multiple events. These processes are generally classified as excitation, ionization, or charge transfer. To illustrate this point Figs. I.1a and I.1b show the K-shell x-ray spectra of fluorine ions resulting from the bombardment of neutral helium by F^{4+} and F^{8+} , respectively, at a projectile energy of 15 Mev.¹ In addition to single excitation and ionization events Fig. I.1a displays prominent features at higher x-ray energies which are the result of multiple ionization. Fig. I.1b exhibits peaks due to single excitation similar to those of Fig. I.1a, as well as structure from excited states of F^{7+} formed during the collision by the transfer of a target electron to the projectile.

Figure I.1: X-ray spectra resulting from the bombardment of helium by (a), F^{4+} and (b), F^{8+} at an incident energy of 15 Mev. The data are from the work of Richard, et. al.¹.

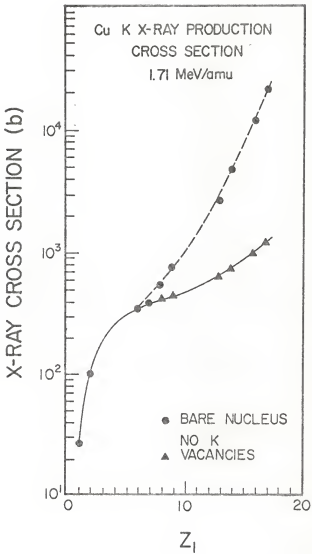
X-RAY COUNTS/RECOIL He



Direct Coulomb ionization is known to be the primary mechanism for inner shell vacancy production in targets bombarded by lighter ions. As the nuclear charge of the projectile increases, however, the electron capture mechanism is found to be important as well. Fig. I.2 shows the Cu K x-ray production cross section as a function of projectile atomic number for velocities corresponding to 1.71 Mev/amu^2 . Two types of projectiles are used, one with and one without K shell vacancies. The K x-rays in the target follow as the result of vacancies created by excitation, ionization, or capture of a Cu K shell electron. The contribution from each of these mechanisms to the total production of target K vacancies is approximately the same for both types of projectiles with the exception of the K-K capture process. The latter can occur only if the impinging ion has a K vacancy. As the collision becomes more symmetric, the K-K transfer process becomes more important to the production of target K vacancies.

Over the years various theoretical models have been proposed to explain vacancy production in ion-atom collisions. The electron promotion model of Fano and Lichten³ has been very successful in providing a qualitative description for collision velocities which are much less than the characteristic orbital velocity of the electron under observation. This theory has recently been put in quantitative form by Briggs and Macek.⁴ The First Born theory has been adequate to describe the excitation and ionization mechanisms of asymmetric systems at higher collision velocities.⁵ A description of the charge transfer mechanism, however, is much more complex.^{5,6,7}

Figure 1.2: Cu K x-ray production as a function of projectile charge at projectile velocities corresponding to 1.71 Mev/amu. As the atomic number increases, the data exhibit a pronounced distinction between projectiles with and without K shell vacancies. The experimental points are from Gardner, et. al.².



Like ionization and excitation, the charge transfer process was originally described by the First Born Approximation. From the beginning questions arose concerning the presence of an internuclear interaction in the electronic transition amplitude. It was argued that an interaction between the colliding nuclei could not directly affect an electronic transition except to deflect the projectile. This is the reasoning which led to the Oppenheimer⁸, Brinkman, and Kramers (OBK) Approximation.⁹ Other authors, however, preferred to retain the internuclear term. Bates and Dalgarno¹⁰ argued that, in some way, it compensated for the nonorthogonality between the initial and final state wavefunctions. (The appearance of this term can be traced to the fact that this nonorthogonality was not formally recognized.) Jackson and Schiff (JS)¹¹ believed that retaining the internuclear interaction improved the convergence of the Born series. The JS method appeared to be successful for the simple transfer process



while the OBK results were an order of magnitude too high. Despite its success for K-K capture by protons on hydrogen, the straightforward generalization of the JS method to arbitrary systems again failed.^{11,12,13}

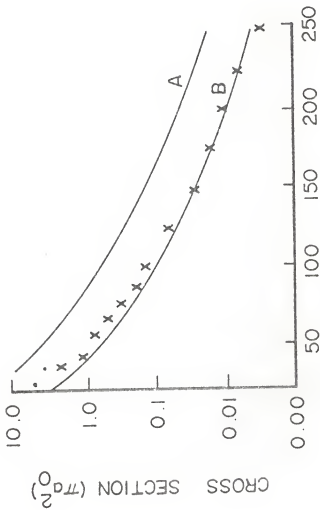
In 1958 D. R. Bates reformulated the electron transfer problem.¹⁴ Whereas the First Born theory solved the time dependent Schrödinger equation by means of a perturbation expansion, Bates employed a truncated eigenfunction expansion to solve the time dependent Schrödinger equation. Unlike the various Born formulations, Bates' Two State Atomic Expansion

(TSAE) method took formal cognizance of the nonorthogonality between the initial and final states of a captured electron. The resulting expression for the capture probability is easily shown to be independent of any internuclear interaction. Thus, the difficulty formerly associated with this term was resolved. When minimal approximations are made, the TSAE expression is equivalent to the Distorted Wave Born Approximation (DWBA)¹⁵ of Bassel and Gerjuoy. The TSAE results simulate the JS and OBK expressions when further approximations are made. Results of the OBK, the JS, and the TSAE methods are compared with data in Fig. I.3 for K-K capture by fast protons incident on atomic hydrogen. The two curves, labeled A and B, are results of the OBK and JS¹⁶ methods respectively. For this case the TSAE¹⁷ and JS results are indistinguishable to the scale drawn.

In this work the TSAE method has been generalized to study single electron transfer in multielectron ion-atom collisions. The multielectron systems are described within the independent particle approximation in order to avoid undue mathematical complications. For collision velocities of interest the motion of the nuclei can be treated within the impact parameter approximation. This is a semi-classical method in which the nuclear motion is treated classically and the electronic motion, quantum mechanically. The projectile is deflected very little by the target at these velocities; thus straight line trajectories are adopted.

The earlier work of this type²⁰ generalized the TSAE method to transfer processes involving multielectron systems and was applied to K-K capture by fast protons on carbon, nitrogen, oxygen, neon, and argon targets. Because K-shell electronic motion is dominated by the influence of the

Figure I.3: The total cross section for electron capture by protons from atomic hydrogen. Curve A results from the Brinkman-Kramers approximation; curve B, the Two State and the Born approximation. The latter two are indistinguishable to the scale shown and are drawn as one. Experimental data are from refs. no. 18 and 19.



INCIDENT ENERGY (KeV)

nucleus rather than the aggregate influence of the passive electrons, it was reasoned that a screened hydrogenic wavefunction and potential would give an adequate description of the multielectron targets. Results of these calculations agreed reasonably well with experimental data.

As opposed to the description of inner shell capture processes, a description of outer shell capture requires a more complex atomic model. Whereas a K-shell electron's interaction with the nucleus is much stronger than its interaction with the other electrons, the influence of neighboring electrons on an outer shell electron is comparable to that of the nucleus. In this work it was assumed that the most important effect of the passive electrons on the electron under observation was to provide screening of the nuclear potential. This screening, described by a Herman-Skillman screening function,²¹ enabled a study of transfer from outer shells. Comparison with earlier K-K calculations was made as well in order to verify the validity of the simple atomic model used to describe inner shell capture processes.

In Chapter II the details of the TSAE method are given. Chapter III describes the numerical techniques employed in this work to perform the calculations. A discussion of the results is given in Chapter IV and Chapter V summarizes the work. Appendix I contains the derivations of the relevant formulas. The computer coding written to perform the calculations is listed in Appendix II and the publication connected with this work is given in Appendix III. Atomic units will be used.

CHAPTER II: DESCRIPTION OF THE TSAE METHOD

In this study the single electron transfer problem is treated within the independent particle approximation. Only one electron is considered active. The presence of the passive electrons is acknowledged through the screening of the nuclear potential.

A. Derivation of the Coupled Equations. In the impact parameter approximation the electronic wavefunction satisfies the time dependent Schrödinger equation

$$i \frac{\partial}{\partial t} \psi(\vec{r}, t) = H(t) \psi(\vec{r}, t) \quad \text{II.1}$$

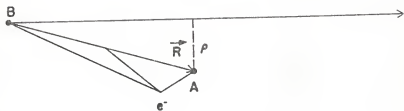
where $H(t)$ is assumed to have the form

$$H(t) = -1/2 \nabla^2 + V_A(\vec{r}_A) + V_B(\vec{r}_B) \quad \text{II.2}$$

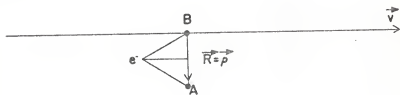
The time dependence of the Hamiltonian occurs through the change of the internuclear distance as the collision progresses. $V_A(\vec{r}_A)$ connects the electron to the target (projectile) as shown in Fig. II.1. $V_B(V_B)$ is the potential experienced by the electron at infinite internuclear separation when it is bound to nucleus A(B).

Eqn. II.1 can be conveniently solved by the method of eigenfunction expansions. The type of basis set to be chosen in a truncated expansion depends on the ratio of the projectile's velocity to the characteristic orbital velocity of the electron under consideration. When this ratio is small, a molecular basis set is appropriate. Atomic basis sets are used for moderate to high collision velocities. In describing the charge cap-

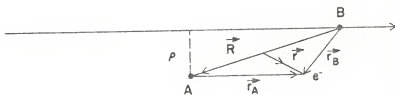
Figure II.1: The coordinate system used to calculate electron capture probabilities within the impact parameter formulation. ρ is the impact parameter, \vec{R} is the internuclear line joining the target, A, to the projectile, B, and \vec{r}_A (\vec{r}_B) connects nucleus A(B) with the electron. \vec{r} is the position vector of the electron with respect to the origin of this coordinate system, the mid-point of the internuclear axis.



$t=0$



$t>0$



ture process, it is convenient to use an expansion centered about both the target and the projectile. This insures that each term in the expansion will be an eigenfunction of H in the limit of infinite internuclear separation. With this in mind, the electronic wavefunction can be written

$$\begin{aligned} \psi(\vec{r}, t) = & \sum_i a_i(t) \psi_i(\vec{r}_A) e^{-i\epsilon_i^A t} \\ & + \sum_j b_j(t) \psi_j(\vec{r}_B) e^{-i\epsilon_j^B t} \end{aligned} \quad \text{II.3}$$

Each ψ_i (ψ_j) is a product of a stationary state wavefunction centered about nucleus A(B) and a 'plane-wave-like' phase factor. These phase factors, necessary to insure translational invariance of the system, represent the momentum that the electron has by virtue of being bound to one or the other of the two nuclei at infinite internuclear separation.

$$\begin{aligned} \psi_i(\vec{r}_A) &= \phi_i(\vec{r}_A) e^{i \left[\frac{\vec{v}}{2} \cdot \vec{r} - 1/2 \left(\frac{v}{2} \right)^2 t \right]} \\ \psi_j(\vec{r}_B) &= \phi_j(\vec{r}_B) e^{-i \left[\frac{\vec{v}}{2} \cdot \vec{r} + 1/2 \left(\frac{v}{2} \right)^2 t \right]} \end{aligned} \quad \text{II.4}$$

where \vec{v} is the collision velocity and \vec{r} , the position of the electron with respect to the origin, (the midpoint of the internuclear axis, R, as shown in Fig. II.1).

$\phi_i(\vec{r}_A)$ and $\phi_j(\vec{r}_B)$ are stationary eigenstates satisfying

$$\begin{aligned} [-1/2v_A^2 + V_A(\vec{r}_A) - \epsilon_i^A] \phi_i(\vec{r}_A) &= 0 \\ [-1/2v_B^2 + V_B(\vec{r}_B) - \epsilon_j^B] \phi_j(\vec{r}_B) &= 0 \end{aligned} \quad \text{II.5}$$

In the Two State Approximation only one term from each sum in Eqn. II.3

is retained, those representing the initial and final state of a captured electron. (Henceforth, the subscripts i and j will be replaced by A and B.) This truncated version of the wavefunction is substituted into the Schrödinger equation, II.1. The result is

$$\begin{aligned}
 i[\dot{a} \psi_A e^{-i\epsilon_A t} + \dot{b} \psi_B e^{-i\epsilon_B t}] \\
 = a V_B \psi_A e^{-i\epsilon_A t} + b V_A \psi_B e^{-i\epsilon_B t}
 \end{aligned}
 \tag{II.6}$$

The overlap of this equation is taken with $\psi_A^* e^{i\epsilon_A t}$ and $\psi_B^* e^{i\epsilon_B t}$, respectively, resulting in the final set of coupled equations

$$\begin{aligned}
 i(a + S_{AB} \dot{b}) &= H_{AA} a + H_{AB} b \\
 i(S_{BA} \dot{a} + \dot{b}) &= H_{BA} a + H_{BB} b,
 \end{aligned}
 \tag{II.7}$$

where $S_{AB} = S_{BA}^*$ is the overlap between the initial and final states

$$S_{AB} = \int d\tau \phi_A^* \phi_B e^{i(\vec{v} \cdot \vec{r} + \omega t)}
 \tag{II.8}$$

and $\omega = \epsilon_A - \epsilon_B$. The diagonal and off-diagonal elements of H are the direct and exchange elements of the interaction matrix.

$$\begin{aligned}
 H_{AA} &= \int d\tau \phi_A^* V_B \phi_A \\
 H_{BB} &= \int d\tau \phi_B^* V_A \phi_B \\
 H_{AB} &= \int d\tau \phi_A^* V_A \phi_B e^{+i(\vec{v} \cdot \vec{r} + \omega t)} \\
 H_{BA} &= \int d\tau \phi_B^* V_B \phi_A e^{-i(\vec{v} \cdot \vec{r} + \omega t)}
 \end{aligned}
 \tag{II.9}$$

The integrations in the above matrix elements are over the electronic

coordinates. Eqns. II.7 can be further simplified by the unitary transformation

$$a(t) = A(t) \exp(-i \int^t dt' \alpha(t')) \quad \text{II.10}$$

$$b(t) = B(t) \exp(-i \int^t dt' \beta(t'))$$

where

$$(1 - |s|^2) \alpha(t) = H_{AA} - S_{AB} H_{BA} \quad \text{II.11}$$

$$(1 - |s|^2) \beta(t) = H_{BB} - S_{BA} H_{AB}$$

The resulting set of equations now read

$$i \dot{A}(t) = X_{AB} B(t) \quad \text{II.12}$$

$$i \dot{B}(t) = X_{BA} A(t)$$

where

$$(1 - |s|^2) X_{AB} = (H_{AB} - S_{AB} H_{BB}) e^{+i\delta} \quad \text{II.13}$$

$$(1 - |s|^2) X_{BA} = (H_{BA} - S_{BA} H_{AA}) e^{-i\delta}$$

and

$$\delta(t) = \int^t dt' [\alpha(t') - \beta(t')] \quad \text{II.14}$$

Eqns. II.11 are to be solved subject to the initial conditions

$$A(-\infty) = 1 \quad \text{II.15}$$

$$B(-\infty) = 0$$

The total capture cross section at projectile energy, E , is given by

$$Q(E) = 2\pi \int_0^{\infty} \rho d\rho P(\rho) \quad \text{II.16}$$

where ρ is the impact parameter and P , the probability for single electron transfer. The functional form of P depends upon the number of equivalent electrons available for capture. For a one electron target

$$P(\rho) = p(\rho) = |B(\infty)|^2 \quad \text{II.17}$$

In multielectron targets there are two equivalent electrons for every set of principal, orbital, and magnetic quantum numbers. p is the probability that an electron is transferred and $1-p$ is the probability that it is not. Therefore, the probability for only one of the two equivalent electrons to be captured is given by

$$P(\rho) = 2p(1-p) \quad \text{II.18}$$

where the factor of two arises because there are two possible arrangements for a single electron to be transferred.

B. Comparison of the TSAE Expression With Various Born Theories. Eqns. II.12 are exact within the TSAE approximation. When the capture probability is expected to be small, $A(t)$ can be set equal to one for all t and $B(\infty)$ obtained by first order perturbation

$$B(\infty) = -i \int_{-\infty}^{\infty} dt' X_{BA}(t') \quad \text{II.19}$$

where $X_{BA}(t)$ can be written explicitly as II.20

$$X_{BA} = \frac{e^{-i(\omega t + \delta)}}{1 - |S|^2} \int dt' \langle \psi_B^* | V_B - \langle \psi_A | V_B | \psi_A \rangle | \psi_A \rangle e^{-i \vec{v} \cdot \vec{r}}$$

This expression for the capture amplitude, unlike other Born theories, is independent of any internuclear term or other constant potential added to the original Hamiltonian, Eqn. II.2. The addition of an internuclear

term would have the effect of replacing V_B in the previous expression by $V_B + V(R)$, where $V(R)$ is the internuclear interaction. The inner bracketed terms in Eqn. II.20 would become

$$\begin{aligned}
 & V_B + V(R) - \langle \phi_A | V_B + V(R) | \phi_A \rangle \\
 &= V_B + V(R) - \langle \phi_A | V_B | \phi_A \rangle - \langle \phi_A | \phi_A \rangle V(R) \quad \text{II.21} \\
 &= V_B - \langle \phi_A | V_B | \phi_A \rangle
 \end{aligned}$$

as before. This stems from the fact that formal recognition has been taken of the nonzero overlap between the initial and final state wavefunctions at small internuclear separation.

When δ is neglected and the denominator of Eqn. II.20 set equal to unity, the TSAE expression is equivalent to the Distorted Wave Born Approximation (DWBA) of Bassel and Gerjuoy. Both are characterized by a potential term, $\langle \phi_A | V_B | \phi_A \rangle$, in addition to the projectile-electron interaction, V_B . However, it must be recognized that the physical interpretation of this term is entirely different. In the DWBA, the term $\langle \phi_A | V_B | \phi_A \rangle$ arises because the distortion of the projectile is included in the formalism. In Eqn. II.20 this term arises from proper treatment of the nonorthogonality between the initial and final state wavefunction. If the nonorthogonality is ignored, Eqn. II.20 can be justified by identifying the interaction for charge transfer as $V_B - \langle \phi_A | V_B | \phi_A \rangle$. This fictitious potential is sometimes called the 'Bates - Born' potential.⁵ Eqn. II.20 can be compared to other Born theories as well. For the K-K capture process of protons on hydrogen $w = \delta = 0$. When the denominator of Eqn. II.20 is approximated by unity and $\langle \phi_A | V_B | \phi_A \rangle$ by

its large R limit, $-1/R$, Eqns. II.19 and II.20 reduce to the result of Jackson and Schiff. If $\langle \phi_A | V_B | \phi_A \rangle$ is set equal to zero the OBK expression is recovered.

CHAPTER III: NUMERICAL METHOD

In order to solve Eqns. II.12 within the independent electron approximation an appropriate local potential for the active electron must be obtained, the matrix elements defined by Eqns. II.9 must be evaluated, and the coupled equations must be numerically integrated. Sections III.A, III.B, and III.C describe the techniques employed in this work to do each step.

A. Potential and Wavefunction. A local potential in a multielectron atom can be expressed as

$$V(r) = -\frac{Z}{r} U(r) \tag{III.1}$$

where the screening function, $U(r)$ has the limiting forms

$$\begin{aligned} U(r) &\rightarrow 1 & r \rightarrow 0 \\ U(r) &\rightarrow I/Z & r \rightarrow r_0 \end{aligned} \tag{III.2}$$

r_0 is roughly the size of the atom and $(I-1)$ is its charge. In this work the potential and subsequent wavefunctions were obtained by fitting the Herman-Skillman²¹ screening function to the form

$$Z U(r) = I + (Z - I) p(r) e^{-\lambda v r} \tag{III.3}$$

where

$$p(r) = 1 + c_1 r + c_2 r^2 + c_3 r^3$$

This particular form was chosen for its correct asymptotic behavior and its compatibility to the techniques employed for the evaluation of the

matrix elements.

The screening function drops rapidly from 1 at the origin and smooths out to $1/Z$ as r approaches the size of the atom. These characteristics can be adequately reproduced if the parameter λ_v and the coefficients c_λ are well chosen. A proper choice for λ_v insures the sharp decline of the screening function in the small r region. The c_λ are chosen to fit the intermediate region of r .

In order to determine λ_v the $r \rightarrow 0$ limit of Eqn. III.3 is considered. In this limit $p \rightarrow 1$ and the resulting expression can be rearranged to give

$$-\lambda_v r = \ln \left| \frac{UZ - I}{Z - I} \right| \quad \text{III.4}$$

λ_v is obtained by calculating the slope of the right hand side of the above equation. Eqn. III.3 is then linearized and the coefficients of the polynomial determined by the least squares fitting procedure.

The angular dependence of the wavefunctions for a central potential such as Eqn. III.1 are the spherical harmonics, $Y_{\ell m}(\Omega)$. The radial dependence can be conveniently expressed as a sum of Slater type orbitals.

$$P_{n\ell}(r) = \sum_{\lambda} A_{n\lambda} r^{n_\lambda} e^{-\alpha_\lambda r} \quad \text{III.5}$$

where the parameters n_λ and α_λ were chosen from the work of Clementi and Roetti.²² The remaining parameters, $A_{n\lambda}$, were left free to absorb any necessary adjustments. These, as well as the eigenenergies were obtained by diagonalization of the radial Schrödinger Equation

$$H_\ell(r) P_{n\ell}(r) = E_{n\ell} P_{n\ell}(r) \quad \text{III.6}$$

The details of this derivation are given in Appendix I.A.

Fitting the Herman-Skillman screening function in this manner gives energy eigenvalues which are very close to both the Hartree-Fock and original Herman-Skillman numbers. As a typical example Table III.1 lists the orbital energies and Table III.2, the wavefunction parameters for the bound states of neutral argon. A comparison is made between the results of this method and the afore-mentioned works. As can be seen, the agreement between the orbital energies is very good for all values of n and ℓ . A plotted comparison of the original and fitted Herman-Skillman wavefunctions reveals few discernible differences. The coding written to perform these calculations is listed in Appendix II.A.

B. Matrix Elements. The two centered matrix elements in Eqns. II.9 can be conveniently evaluated using prolate spheroidal coordinates λ , μ , and ϕ defined by

$$\lambda = \frac{r_A + r_B}{R} \quad \mu = \frac{r_A - r_B}{R} \quad \text{III.7}$$

ϕ is the azimuthal angle. These coordinates have ranges

$$1 \leq \lambda < \infty \quad -1 \leq \mu \leq 1 \quad 0 \leq \phi < 2\pi \quad \text{III.8}$$

and volume element $d\tau = R^3/8(\lambda^2 - \mu^2) d\lambda d\mu d\phi$. Other quantities of interest are

$$r_Y \cos \theta_Y = R/2 (\lambda \mu \pm 1) \quad r_Y \sin \theta_Y = R/2 \sqrt{(\lambda^2 - 1)(1 - \mu^2)} \quad \text{III.9}$$

$$\hat{v} \cdot \hat{z} = 1/2v^2 \epsilon_{\lambda\mu} + v_0/2 \sqrt{(\lambda^2 - 1)(1 - \mu^2)}$$

where the subscript γ represents either A or B. The upper signs are taken for A and the lower signs, for B. These derivations can be found in the monograph by McDowell and Coleman.⁵

The diagonal matrix elements appearing in Eqns. II.9 can be evaluated analytically. The integration over ϕ normalizes to unity. The two remaining integrals are a linear combination of products of incomplete gamma functions. As an example, the diagonal matrix elements for the K-K transfer of a hydrogen electron to a proton are

$$H_{AA} = H_{BB} = -R^2/2 (f_1 g_0 + g_1 f_0)$$

where

III.10

$$g_n = \int_1^{\infty} d\lambda \lambda^n e^{-R\lambda}$$

$$f_n = \int_{-1}^1 d\mu \mu^n$$

The off-diagonal terms are much more complex. In spite of the difficulties which arise because of the factor $e^{+i \hat{v} \cdot \hat{r}}$, two of the three integrals can be done analytically. The integration over ϕ is done with the help of Bessel's integral

$$2\pi i^{l-m} |J_{|m|}(\alpha)| (\alpha) = \int_0^{2\pi} d\phi e^{i[\alpha \cos \phi + \pi \phi]} \quad \text{III.11}$$

and, over μ ²³

$$\begin{aligned} 2i^{\ell-m} J_{\ell}(\tau) P_{\ell}^m(\cos X) \\ = \int_{-1}^1 d\mu J_m(\tau \sin X \sqrt{1-\mu^2}) P_{\ell}^m(\mu) e^{i\mu \tau \cos X} \end{aligned} \quad \text{III.12}$$

where j_ℓ is the spherical Bessel function and P_ℓ^m is the associated Legendre polynomial. The integration over λ is done by making a simple change of variable and using Gauss-Laguerre quadrature. For the process mentioned above the off-diagonal matrix elements are

$$S_{AB} = S_{BA}^* = R^3/2 \int_1^\infty d\lambda \Delta(\lambda) e^{-R\lambda}$$

$$H_{AB} = H_{BA} = -R^2 \int_1^\infty d\lambda h(\lambda) e^{-R\lambda}$$
III.13

where

$$\Delta(\lambda) = [\lambda^2 - 1/3] j_0(T) + 2/3 j_2(T) P_2(\cos \chi)$$

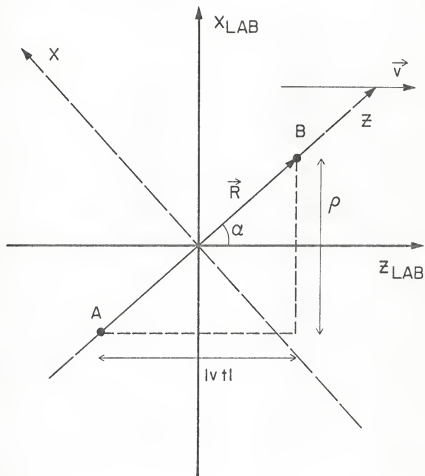
$$h(\lambda) = j_0(T) - i j_1(T) P_1(\cos \chi)$$

$$T = v/2 [\lambda^2 R^2 - \rho^2]^{1/2} \quad \cos \chi = \lambda v \tau [\lambda^2 R^2 - \rho^2]^{-1/2}$$

(S, by definition, is Hermitian. In general, however, H is neither symmetric nor Hermitian.)

An additional complexity is manifested for processes involving non-spherical wavefunctions. The Schrödinger Equation, II.1, is written in terms of the laboratory coordinates. In the lab system, the Z-axis is defined to be in the direction of the projectile's incident velocity. The matrix elements, however, are derived in a coordinate system which defines the Z-axis to be along the internuclear line, R, as shown in Fig. II.1. Since R changes angle continuously with respect to the projectile's velocity vector during the course of the collision, the two coordinate systems rotate with respect to each other as shown in Fig. III.1. This rotation can be handled in one of two ways; either the coordinate

Figure III.1: The rotation of the laboratory coordinates with respect to the coordinate system used to perform the calculations as shown in Figure II.1. In this illustration $\sin \alpha = \rho/R$ and $\cos \alpha = vt/R$.



system or the wavefunctions in Eqns. II.1 can undergo a rotational transformation. In this work the latter method has been chosen.

Firstly, the stationary state part of the wavefunctions in Eqn. II.6 can be expressed as

$$\phi_{\gamma}(\mathbf{r}_{\gamma}) = G(\mathbf{r}_{\gamma}) F(x_{\gamma}, y_{\gamma}, z_{\gamma}) \quad \text{III.14}$$

where the subscript γ represents either A or B. From Fig. III.1 it is apparent that

$$\begin{pmatrix} x_{\gamma} \\ y_{\gamma} \\ z_{\gamma} \end{pmatrix} = \begin{pmatrix} \cos \alpha & 0 & -\sin \alpha \\ 0 & 1 & 0 \\ \sin \alpha & 0 & \cos \alpha \end{pmatrix} \begin{pmatrix} x \\ y \\ z \end{pmatrix} \quad \text{III.15}$$

Thus, to account for this rotation x_{γ} and z_{γ} should be expressed in terms of x and z . The y components are perpendicular to the plane of scattering; thus, they do not contribute to the capture cross section and need not be considered. For spherically symmetric states, $F = 1$ in Eqn. III.14. Accordingly, capture processes involving only states with spherical symmetry do not exhibit the effects of this rotation and it can be ignored.

In Appendix I.B matrix elements for transfer processes of the form

$$B^{+} + A(ns) \rightarrow B(n'\ell) + A^{+} \quad \text{III.16}$$

have been derived. Program listings for the specific cases of $\ell = 0$ and $\ell = 1$ are given in Appendices II.B and II.C.

C. Numerical Integration of the Coupled Equations. Eqns. II.12 are solved in one of two ways; when the capture probability is expected

to be less than 1/10, $A(t)$ can be set equal to unity and the solution found by repeated iteration. For larger capture probabilities the coupled equations are integrated directly by the Gill-Runga-Kutta method. The coding written for the iterative method is listed in Appendices II.B and II.C. Appendix II.B includes the coding used for the direct integration method.

CHAPTER IV: RESULTS

The Two State Atomic Expansion method described in the previous chapters has been applied to the study of electron transfer cross sections in ion-atom collisions. The discussions in this chapter are divided into three parts; A, gross features of the capture cross section as functions of projectile velocity; B, the sensitivity of the calculations to the type of atomic model used; and C, outer shell capture. Comparison of the theoretical results with experimental data is presented in Sections B and C.

A. Gross Features of Electron Transfer Cross Sections. Massey's criterion states that the electron capture cross section peaks at projectile velocities approximately equal to the characteristic orbital velocity of the active electron. To elucidate this point Eqns. II.12 are rewritten in slightly different form

$$\begin{aligned} i \dot{A} &= X_{AB} B \\ i \dot{B} &= X_{BA} A \end{aligned} \tag{IV.1}$$

where

$$\begin{aligned} [1 - |S|^2] X_{AB} &= \int dt \int_A^{\infty} [V_A - \langle \psi_B | V_A | \psi_B \rangle] \psi_B e^{-i[\vec{v} \cdot \vec{r} + W(R)/v]} \\ [1 - |S|^2] X_{BA} &= \int dt \int_B^{\infty} [V_B - \langle \psi_A | V_B | \psi_A \rangle] \psi_A e^{-i[\vec{v} \cdot \vec{r} + W(R)/v]} \end{aligned} \tag{IV.2}$$

and

$$W(R) = -\frac{R}{a} \frac{xdx}{x^2 - a^2} [U_A - U_B] \tag{IV.3}$$

$$U_A = \epsilon_A + \langle \phi_A | V_B | \phi_A \rangle$$

IV.4

$$U_B = \epsilon_B + \langle \phi_B | V_A | \phi_B \rangle$$

From Eqns. IV.2 it can be seen that the velocity dependence of the coupling matrix elements, X_{AB} and X_{BA} , occurs primarily through the exponential factors, $e^{\pm i(\vec{v} \cdot \vec{r} + W(R)/v)}$. At high collision energies their magnitude is greatly reduced by cancellation in the integrand due to oscillation of the exponential, $e^{\pm i(\vec{v} \cdot \vec{r})}$. This factor is responsible for the rapid decrease of the transfer cross section with increasing projectile velocity. The magnitude of $X_{AB}(X_{BA})$ is reduced at low collision energies through the oscillation of $e^{\pm i(W(R)/v)}$. The cross section peak occurs at v_0 , the velocity at which oscillations from the two terms add destructively. Taking $r=R$, a rough estimate can be made for v_0 .

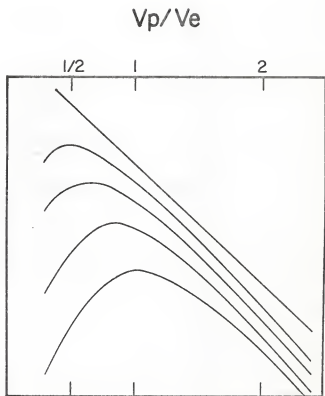
$$\begin{aligned} \vec{v}_0 \cdot \vec{r} &\approx W(R)/v_0 \\ v_0 R &= (\epsilon_A - \epsilon_B) R/v_0 \\ v_0 &= \sqrt{|\epsilon_A - \epsilon_B|} \end{aligned} \quad \text{IV.5}$$

Fig. IV.4 illustrates the general behavior of the electron transfer cross section as a function of projectile energy per amu, (or equivalent-ly, projectile velocity), for varying types of colliding systems. For symmetrically resonant transfer the cross section does not peak: it exhibits a monotonic decrease with increasing projectile energy. For non-resonant transfer the cross section peak shifts to higher collision velocities with decreasing symmetry of the system. This behavior is consistent with Eqn. IV.5.

The high velocity damping factor, $e^{-i(\vec{v} \cdot \vec{r})}$, is not very sensitive

Figure IV.1: Gross features of the electron capture cross section as functions of projectile energy per amu, (or equivalently, projectile velocity). Resonantly symmetric collisions exhibit a monotonic increase with decreasing energy as typified by the uppermost curve. As the colliding system becomes less symmetric, the peak of the capture cross section shifts toward the energy corresponding to $v_p/v_e = 1$ where v_p (v_e) is the velocity of the projectile (electron).

CAPTURE CROSS SECTION
(arbitrary units)



ENERGY/MASS
(arbitrary units)

to the type of atomic model used in the description of the multielectron atom. As can be seen from its definition, however, the low velocity damping factor, $e^{+i(W(R)/v)}$, is extremely model dependent. U_A and U_B in Eqn. IV.4 can, in fact, be identified as the 'potential curves' defined within this theory. They represent the distortion of the electron cloud in the initial (final) state by the projectile (target) nucleus. In anticipation of the following discussion, therefore, the calculations can be expected to show sensitivity to the atomic model at low collision velocities.

B. Comparison of K-K Results Using Different Atomic Models. The TSAE method has been applied to the description of K-K capture processes for bare projectiles on multielectron targets. The potential of the bare projectile is given by $V_B = -Z_B/r_B$. Within the independent electron approximation, the target potential can be expressed in several ways. In the early work of Lin et. al.²⁰ a screened hydrogenic potential, $V_A = -Z_A^*/r_A$, (where $Z_A^* = Z_A - 5/16$), was used. This potential includes the mutual screening of the K shell electrons and the corresponding wavefunction is known to represent the actual 1s orbital very well. However, the screening of the outer electrons is not acknowledged by this treatment; thus, the corresponding energy, $\epsilon_A = -Z_A^{*2}/2$, is quite different from the experimental value. It was recognized in the earlier work that this discrepancy would not arise with the use of a proper multielectron theory. Therefore, experimental K shell binding energies were substituted for ϵ_A . It should be noted, however, that by choosing ϵ_A and V_A inconsistently the unitarity condition of the calculation was destroyed.

To ascertain the importance of these approximations on the capture

probability a comparison between this work and the earlier one is made. The Herman-Skillman potential differs from the hydrogenic potential primarily by its inclusion of outer as well as inner shell screening. In Fig. IV.2 the hydrogenic, (dashed lines), and Herman-Skillman, (solid lines), potentials for neutral argon are compared. The differences are most significant in the region outside the K shell radius. The corresponding 1s wavefunction for each potential is compared in Fig. IV.3. The reason for the apparent agreement between the wavefunctions can be attributed to the approximately hydrogenic behavior of the Herman-Skillman potential within the region of the 1s amplitude.

The statement was made in Section IV.A that discrepancies between calculations using different atomic models should occur at low collision velocities due to the increased importance of the factor, $e^{-i(W(R)/v)}$. By considering the above comments and the V_A dependence of $W(R)$, it can be seen that these discrepancies are caused by the differing behavior of the hydrogenic and Herman-Skillman potentials. Fig. IV.4 compares the electron transfer cross sections calculated in the two models for two widely varying systems, $P + Ar$ and $F^{9+} + Ar$. As anticipated in the comments at the end of Section IV.A, the agreement between the models is good in the high energy region. At low collision energies, however, significant discrepancies exist, particularly for $F^{9+} + Ar$. To further illustrate this point the calculated values of the transfer cross sections in the two models are listed in Table IV.1. Though the agreement does improve with increasing projectile velocity, the disagreement in the low energy region is substantial.

The discrepancy between the two models is generally small for very

Figure IV.2: Comparison of the screened hydrogenic and Herman-Skillman potentials for neutral argon. It should be noted that the former is much stronger than the latter, particularly in the large r region.

Figure IV.3: Comparison of the screened hydrogenic and Herman-Skillman wavefunctions of argon. (The screened charge is taken to be 17.6875). Unlike their corresponding potentials, the agreement between the wavefunctions is very good. The K shell radius, r_K , is indicated.

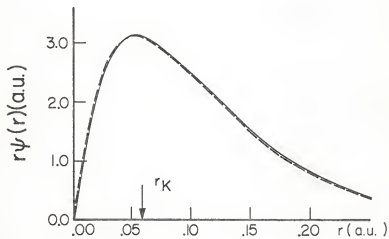
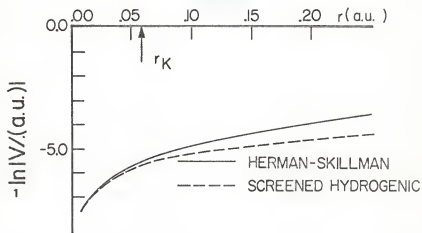
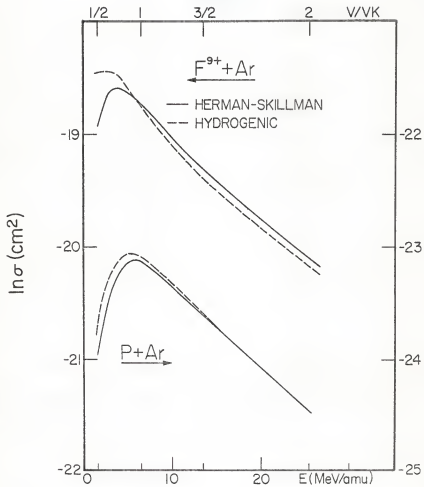


Figure IV.4: K-K cross sections for electron transfer as functions of collision energy for $F^{9+} + Ar$ and $P + Ar$ calculated using the Herman-Skillman and hydrogenic models. (v is the collision velocity and v_K is the characteristic orbital velocity of the K shell electron.)

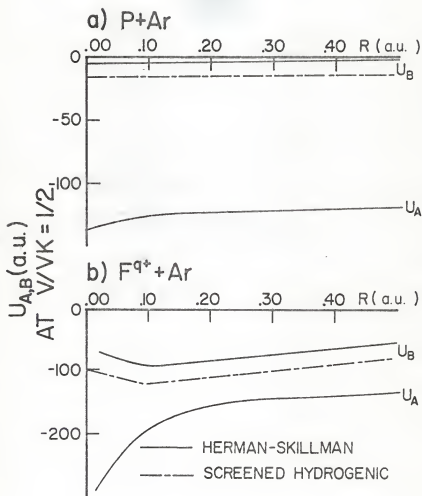


asymmetric systems such as P + Ar. As the symmetry of the system increases, however, the differences are significant. The reason for this can be elucidated by considering Fig. IV.5. The potential curves, U_A and U_B , are plotted for P + Ar and F^{9+} + Ar using both the hydrogenic and Herman-Skillman models. The discrepancies between the models is much more significant for F^{9+} + Ar than P + Ar. This is due to the increased importance of terms containing V_A for the former system than the latter.

Table. IV.1 lists theoretical cross sections for several other systems along with experimental data. Though the Herman-Skillman is a more realistic potential, these results do not show improvement with experimental measurements. The Herman-Skillman calculations were done under the assumption that the active electron experiences the potential of a neutral target. It is known that the target becomes multiply ionized during the course of the collision. Table IV.2 compares several Herman-Skillman calculations for F^{9+} + Arⁿ⁺ for varying values of n. As evidenced by these results, the capture cross section does not exhibit a strong dependence on the final charge state of the target. This point is further discussed in Chapter V.

Though it is important to use a more realistic model for more symmetric systems, the computer time involved in such a calculation poses practical difficulties. It therefore remained desirable to find a simpler way to give an adequate description of the multielectron system. As evidenced by Figs. IV.2 and IV.3, the most significant difference between the two models occurs in the behavior of the multielectron potential, V_A . The idea was therefore proposed of using a 'hybrid' model— a screened hydrogenic wavefunction with a Herman-Skillman potential. This proved to

Figure IV.5: The potential curves for $F^{9+} + Ar$ and $P + Ar$ in the Herman-Skillman and hydrogenic models at an incident energy corresponding to $v/v_K = 1/2$. U_A is indistinguishable for the two models to the scale shown and are drawn as one.



be quite successful. For the particular case of $F^{9+} + Ar$ at a collision velocity of $v = v_K/2$, the agreement with the full Herman-Skillman calculation was better than 2% and the computer time reduced by more than 80%. In view of these considerations it is clear that the most practical way of insuring an adequate description of K-K capture processes involving multielectron atoms is to use a screened hydrogenic wavefunction, (with screened charge $Z^* = Z-5/16$), and a Herman-Skillman description of the potential.

C. Outer Shell Capture. The Herman-Skillman model provides a satisfactory description of the potential in the large r region of a multielectron atom, thus enabling a study of electron capture from outer shells. Section IV.C discusses charge transfer from the outermost shells of neon, argon, and krypton to the K shell of hydrogen. The capture cross sections for these systems can be expected to be important because the energy defects between the initial and final states are small.

There are many studies of this type for low collision energies which are based on the MO theory. Except for the simplistic OBK method,⁵ however, there are no theoretical investigations for more energetic collisions. The assumptions on which the OBK theory is based are invalid for systems such as these because the capture probabilities are not small and the potential experienced by an outer shell electron is not Coulombic. This is an effort to describe outer shell electron transfer in which more realistic assumptions are made.

It was emphasized in Section IV.A that charge transfer cross sections are sensitive to both the energy defect between the initial and final states as well as the velocity of the incoming projectile. In low

energy collisions between protons and argon atoms, for example, the capture process is dominated by electron transfer from the Ar(3p) to the H(1s) state. Capture to excited states of the projectile is much less important, as is capture from more tightly bound states of the target, because the energy defects are larger. In faster collisions, however, outer shell electrons have very little time to react to the field of the impinging ion; thus, the more energetic L and K shell electrons are transferred. Because the energy defects are larger for these processes, the magnitude of the total capture cross sections are reduced.

Table IV.3 lists the electron transfer cross sections from the K, L, and M shells of argon to the K shell of hydrogen. Comparison between these results and the available experimental data is shown in Fig. IV.6. At low collision velocities capture from the Ar(3p) state, (dashed line), dominates the total electron transfer cross section, (dot-dashed line), entirely masking the Ar(3s), (dashed line), contribution. This is consistent with the foregoing discussion concerning energy defects. As the collision energy increases, L shell capture begins to take over. Again, most of the capture occurs from the p state though the s state contribution is not negligible. At still higher proton velocities transfer from the K shell begins to be important. The fine details of this study warrant improvement; however, the overall agreement with experimental data is satisfactory.

In Figs. IV.7a, IV.7b, and IV.7c the impact parameter dependence of the weighted capture probability, $2P(1-P)_0$, is illustrated for the transfer of K, L, and M shell electrons. These figures indicate some general trends. The maxima of the weighted probability for a given state moves in to smaller impact parameters with increasing projectile velocity. Accom-

Figure IV.6: The energy dependence of the capture cross section for electron transfer from the K, L, and M shells of argon atoms to the K shell of hydrogen. Calculated total cross sections from each shell are indicated, (---), along with individual subshell contributions, (---). The experimental data, (—), from the K and L shells are from Macdonald et. al.²⁸ and Rodbro et. al.²⁹.

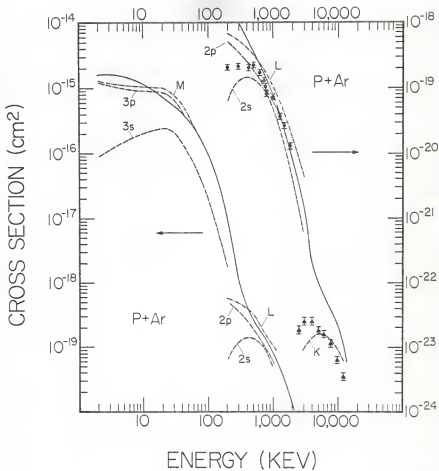
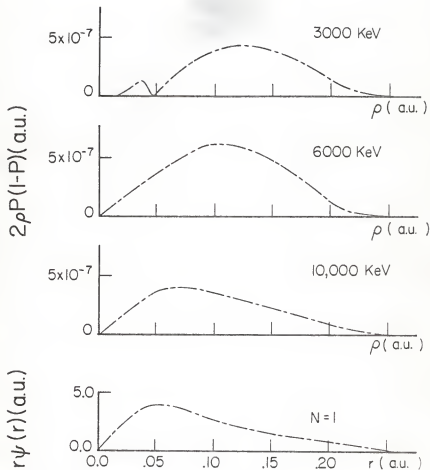
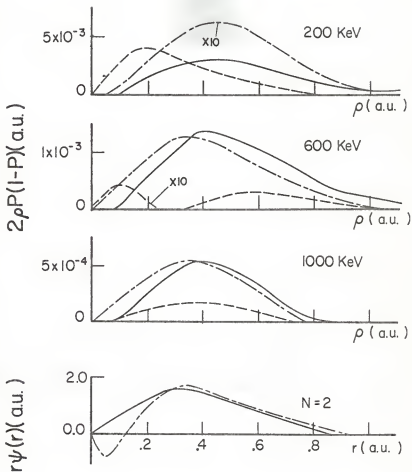
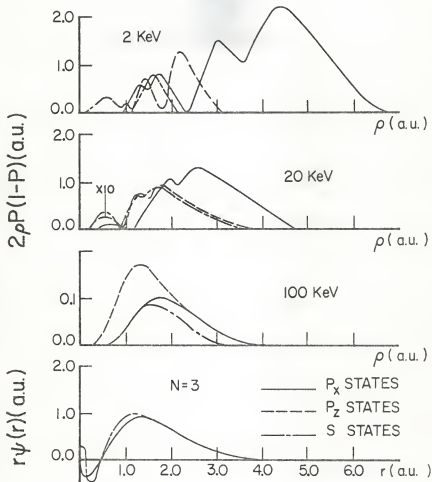


Figure IV.7: The weighted capture probability, $2P(1-P)\rho$, for electron transfer from the $N = 3, 2,$ and 1 states of argon to the $N = 1$ state of hydrogen. The radial distribution of the target wavefunction for each corresponding orbital is illustrated in the lower figures.





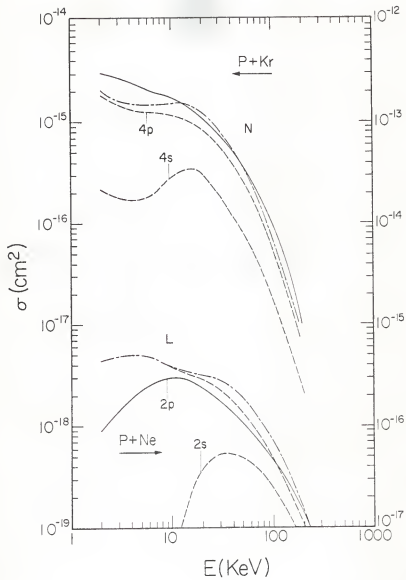


panied by this is the disappearance of oscillation in the probability function.

Fig. IV.8 presents results from a similar study of electron transfer from the outermost shells of neon and krypton to the K shell of hydrogen. The subshell contributions are listed in Table IV.4 for selected collision energies. The agreement with experimental data is good for P + Kr though the shape of the curve is somewhat questionable. This is not the case for P + Ne. The disagreement between theoretical and experimental results is substantial, particularly for proton energies less than 10 kev. Capture from the L shell of neon is a much more asymmetric process than the other two systems discussed in this section. Usage of the single particle approximation is known to be a limitation in this formulation as is the retainment of only two states in the multistate expansion, Eqn. II.3. Chapter V discusses these points in further detail.

A preliminary study of the Z_B dependence of electron transfer from the L shell of argon to the K shell of various ions has been made. The OBK theory predicts these cross sections to be scaled by Z_B^5 when Z_B/Z_A is small and the projectile velocity is large. Table IV.5 presents the results of this study for three collision velocities. These calculations are not in accord with the Z_B^5 scaling estimate nor do they exhibit any such simplistic Z_B dependence.

Figure IV.8: The energy dependence of the charge transfer cross section from the outermost shells of neon and krypton to the K shell of hydrogen. The total transfer cross section from each shell is indicated, (— - — -), along with the individual subshell contributions, (— — — —). The experimental data, (————), are from the compilation by Tawara and Russek³⁰.



CHAPTER V: DISCUSSION AND SUMMARY

In this work the Two State Atomic Expansion method has been applied to the study of electron capture within the independent particle approximation. A Herman-Skillman model has been used to describe charge transfer processes involving multielectron ions. Wide ranges of collision energies have been covered in order to observe the shell dependence of the total capture cross section. Two different models, the Herman-Skillman and the screened hydrogenic, were compared for the description of the K-K transfer process. It was observed that, except for very asymmetric systems, the capture probabilities are sensitive to the type of atomic model used for the multielectron atoms. Prior to this there are few serious attempts to describe charge transfer from outer shells and it is hoped that a more in depth study will emerge from this preliminary work.

A comment on the experimental data is in order. Particularly for the K-K transfer process, comparison of theoretical and experimental results is difficult. The experimental values in Table IV.1, for instance, were deduced from either x-ray or Auger cross sections. A single fluorescence yield or Auger rate was assumed in determining the total vacancy production. This assumption is open to question. For example, it has been shown by Tawara et. al.³¹ that in $F^{9+} + Si$ collisions the fluorescence yield for Si K x-rays changes from $1.7w_0$ to $1.9w_0$ with the removal of 5 and 6 target electrons, respectively. (w_0 is the fluorescence yield for neutral Silicon.) In $F^{9+} + Ar$ collisions it was estimated that 6-8 target electrons are removed with the production of one K shell vacancy.

This discussion implies that, theoretically, ionization and inner shell capture should be considered simultaneously. Such a formulation, however, is impossible at present.

The preliminary study of outer shell capture done in this work is the first of its kind. Both the atomic and scattering models are as simple as possible without being unrealistic. However, improvements in the description of capture from both outer and inner shells can be made.

A. Atomic Model. The primary defects of the atomic model are due to the single particle approximation. Because outer shell capture occurs at low projectile velocities, usage of antisymmetrized wavefunctions would probably improve the agreement with experimental data. The effect of the neighboring electrons on the active electron may be comparable to the perturbation caused by the impinging ion as well, particularly for low collision velocities. (For example, this may be important in the capture of neon L shell electrons by protons.) Thus, the formulation of a many electron theory of charge transfer is warranted. The difficulties involved in such a calculation, however, are formidable.

B. Scattering Model. The major approximation made in the scattering model is the retainment of only two terms in the multistate expansion, Eqn. II.3. For instance, the initial and final state wavefunctions in very asymmetric collisions are severely different in size; therefore, it may be necessary to include intermediate states in the multistate expansion for the purpose of 'filling the gaps'. This type of approach should improve the description of a process such as the K-K transfer of argon electrons to protons.

As is evidenced by Figs. IV.7, the impact parameters important to

the transfer process become small with increasing projectile velocity. The Two State Approximation is not adequate to describe this region well. At high collision velocities, therefore, the inclusion of states which have amplitude in the small impact parameter region should improve the results. For the description of outer shell electron transfer this would mean the inclusion of lower orbital states and for transfer of inner shell electrons, the inclusion of pseudostates.

REFERENCES

1. Richard, et. al. (to be published)
2. Gardner, et. al. (to be published)
3. U. Fano and W. Lichten, Phys. Rev. Lett. 14, 627 (1965).
4. J. S. Briggs and J. H. Macek, J. Phys. B 5, 579 (1972).
See also the review by J. S. Briggs in Rep. Prog. Phys. 39, 217 (1976).
5. M.R.C. McDowell and J. P. Coleman, Introduction to the Theory of Ion-Atom Collisions (North-Holland, Amsterdam, 1970).
6. See the review by R. A. Mapleton, Theory of Charge Exchange (Wiley-Interscience, New York, 1972).
7. B. H. Bransden, Rep. Prog. Phys. 35, 949 (1972).
8. J. R. Oppenheimer, Phys. Rev. 31, 349 (1928).
9. H. C. Brinkman and H. A. Kramers, Proc. Acad. Sci. (Amsterdam) 33, 973 (1930).
10. D.R. Bates and A. Dalgarno, Proc. Phys. Soc. Lond. A 65, 919 (1952).
11. J. D. Jackson and H. Schiff, Phys. Rev. 89, 359 (1953).
12. Y. B. Band, Phys. Rev. Lett. 37, 634 (1976).
13. A. Halpern and J. Law, Phys. Rev. A 12, 1776 (1975).
14. D. R. Bates, Proc. R. Soc. A 274, 294 (1958).
15. R. H. Bassel and E. Gerjuoy, Phys. Rev. 117, 749, (1960).
16. R. McCarroll, Proc. R. Soc. A 264, 547 (1961).
17. R. A. Mapleton, Phys. Rev. 126, 1477 (1962).
18. J. P. Coleman and S. A. Trelease, Atom. Molec. Phys. 1, 172 (1968).
19. A. B. Wittkower, G. Ryding and H. B. Gilbody, Proc. Phys. Soc. 89, 541 (1966).
20. C. D. Lin, S. C. Soong, and L. N. Tunnell, Phys. Rev. A 17, 1646 (1978).
21. F. Herman and S. Skillman, Atomic Structure Calculations (Prentice-Hall, New Jersey, 1963).
22. E. Clementi and C. Roetti, Atomic Data and Nuclear Data Tables 14, 177 (1974).
23. G. N. Watson, Treatise on the Theory of Bessel Functions (Cambridge Univ. Press, Cambridge, 1944).
24. C. W. Woods, R. L. Kauffman, K. A. Jamison, N. Stolterfoht and P. Richard, Phys. Rev. A 13, 1358-69 (1976).

25. T. G. Winter and N. F. Lane, Phys. Rev. A, (January 1978).
26. F. Hopkins, N. Cue and V. Dutkiewica, Phys. Rev. A 12, 1710-2 (1976a).
27. F. Hopkins, R. Breen, A. R. Wittlemore, N. Cue, V. Dutkiewica and R. Chaturvedi, Phys. Rev. A 13 74-85 (1976b).
28. J. R. Macdonald, C. L. Cocke, and W. W. Eidson, Phys. Rev. Lett. 32, 648 (1974).
29. M. Rodbro, E. Pederson, and J. R. Macdonald: Proc. X ICPEAC, p. 48, Paris (1977).
30. Compilation from Tawara and Russek, Rev. Mod. Phys. 45, 178 (1973).
31. H. Tawara, P. Richard, J. R. Macdonald, R. Dillingham, and P. Pepmiller; to be published in Phys. Rev. A (1979).

TABLE III. 1

COMPARISON OF ORBITAL ENERGIES
FOR THE BOUND STATES OF ARGON

<u>ORBITAL</u>	<u>HARTREE-FOCK*</u>	<u>HERMAN-SKILLMAN**</u>	<u>THIS WORK</u>
1s	- 118.61	- 116.28	- 117.77
2s	- 12.32	- 11.44	- 11.11
3s	- 1.28	- 1.05	- 1.07
2p	- 9.57	- 9.10	- 9.01
3p	- .59	- .53	- .56

* ref. no. 22

** ref. no. 21

TABLE III. 2

EXONENTS AND EXPANSION
COEFFICIENTS FOR NEUTRAL ARGON*

<u>EXONENTS</u>	<u>1s</u>	<u>2s</u>	<u>3s</u>
1s 18.01640	.97349(.97824)	.27635(.28011)	.08634(.09449)
3s 22.04650	.01684(.01148)	.00289(.00069)	.00186(.00042)
3s 16.08250	.02422(.02659)	-.03421(-.03907)	-.01540(-.01478)
3s 11.63570	-.00114(-.00685)	-.33229(-.35409)	-.10236(-.12777)
3s 7.70365	.00123(.00259)	-.65828(-.62148)	-.27614(-.28171)
3s 4.87338	-.00039(-.00122)	-.06834(-.08899)	-.11879(-.10256)
3s 3.32987	.00010(.00054)	.00623(.14479)	.68436(.74965)
3s 2.02791	-.00003(-.00011)	-.00174(-.00198)	.52050(.45017)

<u>EXONENTS</u>	<u>2p</u>	<u>3p</u>
2p 9.05477	.64116(.68865)	-.17850(-.20725)
4p 15.54410	.00865(.00241)	-.00812(-.00801)
4p 12.39770	.04186(.03307)	.00520(.01045)
4p 8.56120	.31735(.28159)	-.10986(-.10940)
4p 5.94658	.09642(.09553)	.10944(.15359)
4p 3.42459	.00003(-.00285)	.56149(.59541)
4p 1.96709	.00053(.00101)	.46314(.39726)
4p 1.06717	-.00013(-.00029)	.02951(.02429)

* The entries to the left of the parenthesis are the expansion coefficients, A_i in Eqn. III.5, from reference no. 21. Those in parenthesis are the expansion coefficients obtained in this work by the procedure described in Section III.A.

TABLE IV. 1

K-K CAPTURE CROSS SECTIONS FOR
BARE PROJECTILES ON NOBLE GASES⁺

PROJECTILE + TARGET	E (MEV)	V/V _K	σ_H^*	σ_{HS}^{**}	σ_{EXP}
N ⁷⁺ + Ne	14	.79	368	284	355 ^a
	19	.92	343	223	350
N ⁷⁺ + Ar	14.7	.42	5.1	1.4	3.2 ^b
	26.3	.56	12.6	3.4	13.2
F ⁹⁺ + Ar	20	.42	23.1	5.6	9.7 ^c
	30	.52	34.7	10.0	29.0
	36	.57	38.6	16.0	30.4
	46	.64	40.4	22.0	47.7
	56	.71	38.7	26.0	53.6
	66	.77	35.0	27.0	48.8
	80	.85	30.0	27.0	--
	86	.88	28.0	--	--
	114	1.01	20.0	21.0	--
F ⁹⁺ + Kr	46	.30	.074	.029	.010
	56	.33	.079	.037	.037
	66	.36	.075	.040	.064
	76	.39	.068	.038	.061
Cl ¹⁷⁺ + Kr	100	.33	1.55	0.52	0.60 ^d
	120	.36	1.40	0.59	1.15
	140	.39	1.62	0.60	1.90
	160	.42	2.50	0.60	3.80

+ Units are 10⁻²⁰ cm² per target electron.

* Calculations done using a hydrogenic model.

** Calculations done using a Herman-Skillman model.

a) Woods et. al. (1976)

b) Woods et. al. (1973)

c) Hopkins et. al. (1976a)

d) Hopkins et. al. (1976b)

TABLE IV. 2

TARGET IONICITY DEPENDENCE OF
K-K CAPTURE CROSS SECTIONS FOR $F^{9+} + Ar^{n+*}$

v/v_k	Target Ionicity			
	0^+	7^+	10^+	13^+
.42	5.2	5.8	5.6	5.3
.57	14.5	16.1	15.5	13.6
.77	24.9	25.8	25.5	24.3
1.01	18.8	19.0	18.9	18.7

*Units are 10^{-20} cm^2 per target electron.

TABLE IV. 3

SUBSHELL CAPTURE CROSS SECTIONS PER
TARGET ATOM FOR PROTONS ON ARGON (cm^2)*

TARGET	ENERGY(KEV)	σ_s	σ_{px}	σ_{pz}	σ_T
Ar(n=3)	2.0	8.9(-17)	9.7(-16)	2.4(-16)	1.3(-15)
	5.0	1.5(-16)	7.0(-16)	3.0(-16)	1.1(-15)
	10.0	2.0(-16)	6.4(-16)	2.7(-16)	1.1(-15)
	20.0	2.4(-16)	4.8(-16)	2.8(-16)	1.0(-15)
	50.0	1.0(-16)	1.4(-16)	1.4(-16)	3.8(-16)
	75.0	2.2(-17)	3.2(-17)	4.1(-17)	9.5(-17)
	100.0	1.0(-17)	1.5(-17)	2.4(-17)	4.9(-17)
200.0	8.8(-19)	1.7(-18)	4.1(-18)	6.7(-18)	
Ar(n=2)	200.0	5.8(-20)	3.2(-19)	2.9(-19)	6.7(-19)
	400.0	1.4(-19)	2.2(-19)	3.4(-20)	4.0(-19)
	600.0	1.2(-19)	1.3(-19)	3.3(-21)	2.5(-19)
	1000.0	4.5(-20)	4.6(-20)	1.4(-20)	1.1(-19)
	3000.0	5.7(-22)	1.5(-21)	2.9(-21)	5.0(-21)

*The numbers in paranthesis are the exponents of the cross sections.

TABLE IV. 4

SUBSHELL CAPTURE CROSS SECTIONS PER TARGET ATOM FOR PROTONS ON KRYPTON AND NEON (cm²)*

TARGET	ENERGY(KEV)	σ_s	σ_{px}	σ_{pz}	σ_T
K _r (n=4)	2.0	2.1(-16)	1.2(-15)	6.2(-16)	2.0(-15)
	5.0	1.7(-16)	8.9(-16)	3.9(-16)	1.5(-15)
	12.5	3.2(-16)	7.3(-16)	4.1(-16)	1.5(-15)
	25.0	2.6(-16)	4.0(-16)	3.2(-16)	9.7(-16)
	50.0	7.2(-17)	1.3(-16)	1.5(-16)	3.5(-16)
	100.0	2.1(-17)	2.2(-17)	4.0(-17)	8.0(-17)
	200.0	2.2(-18)	2.0(-18)	4.5(-18)	8.7(-18)
N _e (n=2)	2.0	---	1.6(-16)	2.7(-16)	4.3(-16)
	5.0	1.4(-18)	3.5(-16)	1.3(-16)	4.8(-16)
	10.0	4.4(-18)	3.4(-16)	2.8(-17)	3.7(-16)
	30.0	5.3(-17)	2.1(-16)	2.1(-17)	2.9(-16)
	60.0	4.3(-17)	8.0(-17)	2.2(-17)	1.5(-16)
	100.0	2.3(-17)	3.1(-17)	1.6(-17)	7.0(-17)

*The numbers in paranthesis are the exponents of the cross sections.

TABLE IV. 5

Z_p DEPENDENCE OF THE ARGON ($N=2$) \rightarrow Z_p ($N=1$)
CAPTURE CROSS SECTIONS PER TARGET ELECTRON (cm^2)*

E(MEV/AMU)	Z_p	σ_{2s}	σ_{2px}	σ_{2pz}	σ_T	$\sigma_T/2^5$
200	1	5.8(-20)	3.2(-19)	2.9(-19)	6.7(-19)	6.7(-19)
	2	2.3(-18)	9.6(-18)	1.9(-18)	1.4(-17)	4.4(-19)
	3	1.5(-17)	3.0(-17)	3.5(-18)	4.8(-17)	2.0(-19)
	4	3.4(-17)	3.6(-17)	1.4(-17)	8.4(-17)	8.2(-20)
	5	3.5(-17)	3.7(-17)	2.3(-17)	9.5(-17)	3.0(-20)
400	1	1.4(-19)	2.2(-19)	3.4(-20)	4.0(-19)	4.0(-19)
	2	2.0(-18)	4.9(-18)	7.0(-20)	7.0(-18)	2.2(-19)
	3	8.2(-18)	1.7(-17)	3.7(-18)	2.9(-17)	1.2(-19)
	4	1.5(-17)	2.7(-17)	1.5(-17)	5.7(-17)	5.6(-20)
	5	1.6(-17)	2.7(-17)	2.1(-17)	6.4(-17)	2.0(-20)
600	1	1.2(-19)	1.3(-19)	3.3(-21)	2.5(-19)	2.5(-19)
	2	1.2(-18)	2.6(-18)	2.6(-19)	4.1(-18)	1.3(-19)
	3	4.2(-18)	9.8(-18)	3.8(-18)	1.8(-17)	7.4(-20)
	4	7.2(-18)	1.7(-17)	1.2(-17)	3.7(-17)	3.6(-20)
	5	8.3(-18)	2.0(-17)	1.7(-17)	4.5(-17)	1.4(-20)

*The numbers in paranthesis are the exponents of the cross sections.

APPENDIX I

A. Potential and Wavefunctions. This section outlines the procedure used to determine the wavefunction parameters, A_i , in Eqn. III.5 and the corresponding energy eigenvalue. Within the independent electron approximation, the wavefunction for the active electron is written

$$\Psi_{nlm}(r) = \frac{P_{nl}(r)}{r} Y_{lm}(\vartheta) \quad \text{A.1}$$

$P_{nl}(r)$ satisfies $\{H_l - E_{nl}\} P_{nl} = 0$ where

$$H_l(r) = -\frac{1}{2} \frac{d^2}{dr^2} + \frac{l(l+1)}{2r^2} + V(r) \quad \text{A.2}$$

The first part of program HERMAN in App. II.A fits the potential of Herman and Skillman to the form

$$-rV(r) = I + (Z-I)e^{-\alpha r} \left\{ 1 + \sum_{k=1}^3 C_k r^k \right\} \quad \text{A.3}$$

$P_{nl}(r)$ is expressed as a sum of Slater type orbitals

$$P_{nl}(r) = \sum_i A_i \chi_i \quad \text{A.4}$$

The column matrix, A, is obtained from the solution of the eigenvalue equation

$$S^{-1}HA = EA \quad A.5$$

where S and H are defined as

$$S_{ij} = \langle \chi_i | \chi_j \rangle \quad A.6$$

$$H_{ij} = \langle \chi_i | H_e | \chi_j \rangle \quad A.7$$

Eqn. A.5 is inconvenient to solve because the basis functions, $\{\chi_i\}$, are not orthogonal. Though programs are available to diagonalize matrices of the form $A^{-1}B$, Eqn. A.5 can also be solved by expressing the $\{\chi_i\}$ in terms of an orthonormal basis set, $\{\phi_i\}$

$$\chi_i = \sum_j a_{ij} \phi_j \quad A.8$$

where the a_{ij} are determined by the procedure of Schmidt orthogonalization. Both the χ_i and ϕ_i are of the form

$$\chi_i = N_i \sum_n c_{in} e^{-i\mathbf{r}_n} \quad A.9$$

where the parameters n_i and α_i are taken from the tables by Clementi and Roetti.²² The basic integrals to be solved are

$$\begin{aligned}
 S_{ij} &= \langle \chi_i | \chi_j \rangle \\
 &= N_i N_j \int_0^\infty dr r^{n_i+n_j} e^{-(\alpha_i+\alpha_j)r} \\
 &= N_i N_j \frac{\Gamma(n+1)}{\alpha^{n+1}}
 \end{aligned}
 \tag{A.10}$$

where $n = n_i + n_j$ and $\alpha = \alpha_i + \alpha_j$.

$$\begin{aligned}
 H_{ij} &= \langle \chi_i | H_e | \chi_j \rangle \\
 &= \langle \chi_i | -\frac{1}{2} \frac{d^2}{dr^2} + \frac{l(l+1)}{2r^2} + V(r) | \chi_j \rangle \\
 &= H_{ij}^1 + H_{ij}^2 + H_{ij}^3
 \end{aligned}
 \tag{A.11}$$

H_{ij}^1 , H_{ij}^2 , and H_{ij}^3 are defined

$$\begin{aligned}
 H_{ij}^1 &= \langle \chi_i | -\frac{1}{2} \frac{d^2}{dr^2} | \chi_j \rangle \\
 &= -\frac{1}{2} \langle \frac{d}{dr} \chi_i | \frac{d}{dr} \chi_j \rangle \\
 &= \frac{N_i N_j}{-2} \left\{ n_i n_j \frac{\Gamma(n-1)}{\alpha^{n-1}} \right. \\
 &\quad \left. - (n_i \alpha_j + n_j \alpha_i) \frac{\Gamma(n)}{\alpha^n} + \alpha_i \alpha_j \frac{\Gamma(n+1)}{\alpha^{n+1}} \right\}
 \end{aligned}
 \tag{A.12}$$

$$\begin{aligned}
 H_{ij}^2 &= \langle \chi_i | \frac{l(l+1)}{2r^2} | \chi_j \rangle & \text{A.13} \\
 &= N_i N_j \frac{l(l+1)}{2} \frac{\Gamma(n-1)}{\alpha^{n-1}}
 \end{aligned}$$

$$\begin{aligned}
 H_{ij}^3 &= \langle \chi_i | V(r) | \chi_j \rangle & \text{A.14} \\
 &= - \langle r^{-1} \chi_i | \mathbb{I} + (z-\mathbb{I}) z^{-1} r^2 \left\{ 1 + \sum_{k=1}^3 c_k r^k \right\} | \chi_j \rangle \\
 &= - N_i N_j \left\{ \mathbb{I} \frac{\Gamma(n)}{\alpha^n} \right. \\
 &\quad \left. + (z-\mathbb{I}) \left[\frac{\Gamma(n)}{\alpha^n} + \sum_{k=1}^3 c_k \frac{\Gamma(n+k)}{\alpha^{n+k}} \right] \right\}
 \end{aligned}$$

where $\alpha' = \alpha + \lambda_{\nu}$. Evaluation of these matrices and the diagonalization of Eqn. A.5 is performed in the second part of program HERMAN listed in App. II.A.

B. Evaluation of the Matrix Elements. The two centered matrix elements appearing in Eqn. II.9 can be evaluated in prolate spheroidal coordinates. The procedure used to derive the off-diagonal terms of both the overlap and interaction matrices is similar because of the common factor $e^{i \vec{v} \cdot \vec{r}}$. These matrix elements are evaluated in Appendix I.B.1. The derivation of the diagonal terms is given in Appendix I.B.2.

B.1. Off-Diagonal Terms. The following definitions necessary for the evaluation of the off-diagonal matrix elements in Eqns. II.9 can be found in the monograph by McDowell and Coleman.⁵

$$\begin{aligned}
 \vec{r} \cdot \vec{r} &= \frac{1}{2} a^2 (\lambda + \mu) + a^2 / 2 \sqrt{\lambda^2 - 1} \sqrt{1 - \mu^2} \cos \phi & \text{A.15} \\
 r_A &= \frac{a}{2} (\lambda + \mu) \\
 r_B &= \frac{a}{2} (\lambda - \mu) \\
 r_B \cos \theta_B &= \frac{a}{2} (\lambda \mu - 1) \\
 r_B \sin \theta_B &= \frac{a}{2} \sqrt{\lambda^2 - 1} \sqrt{1 - \mu^2}
 \end{aligned}$$

It is convenient to define the function

$$\begin{aligned}
 4\pi G_{\lambda\mu}(\delta_+ \delta_-) &= \int_1^{\infty} d\lambda \lambda^k (\lambda^2 - 1)^{m/2} e^{-\lambda \delta_+} & \text{A.16} \\
 &\times \int_0^1 d\mu \mu^k (1 - \mu^2)^{m/2} \int_0^{2\pi} d\phi (-1)^m \sin^m \phi e^{i \vec{v} \cdot \vec{r} - \mu \delta_-}
 \end{aligned}$$

where

$$\begin{aligned}
 i\hat{a}\hat{a} - \mu\delta_0 &= i T \sin \chi \sqrt{1-\mu^2} \cos \phi + i \mu T \cos \chi \\
 T \cos \chi &= \frac{1}{2} \mu^2 \lambda + i \delta_0 \\
 T \sin \chi &= \frac{1}{2} \mu \rho \sqrt{\lambda^2 - 1}
 \end{aligned}
 \tag{A.17}$$

Using Bessel's integral

$$\begin{aligned}
 2\pi i^{l+m} J_{l+m}(T \sin \chi \sqrt{1-\mu^2}) \\
 = \int_0^{2\pi} d\phi \exp i \{ T \sin \chi \sqrt{1-\mu^2} \cos \phi + m \phi \}
 \end{aligned}
 \tag{A.18}$$

the integration over ϕ is easily performed. $\mu^L (-)^m (1-\mu^2)^{m/2}$ is expanded in an associated Legendre series

$$\mu^L (-)^m (1-\mu^2)^{m/2} = \sum_{l=m}^{L+m} \frac{2l+1}{2} a_{l2} P_l^m(\mu)
 \tag{A.19}$$

where $a_{l2} = 0$ for $L+l$ odd. For $L+l$ even

$$a_{l2} = \frac{1}{2^m} \frac{\Gamma\left(\frac{1+l}{2}\right)}{\Gamma\left(\frac{2+l+m-l}{2}\right)} \frac{\Gamma\left(\frac{2+l}{2}\right)}{\Gamma\left(\frac{3+l+m+l}{2}\right)}
 \tag{A.20}$$

The μ integration is done with the help of an identity given by Watson²⁴.

$$\begin{aligned}
 & 2i^{l-m} j_l(\tau) P_l^m(\cos \chi) \\
 & = \int_{-1}^1 d\mu J_m(\tau \mu \chi \sqrt{1-\mu^2}) P_l^m(\mu) e^{i\mu \tau \cos \chi}
 \end{aligned}
 \tag{A.21}$$

The resulting expression is the same regardless of whether m is positive or negative.

$$\begin{aligned}
 & G_{\kappa L}(\delta_+ \delta_-) \\
 & = \sum_{l=m}^{\delta_+ m} i^l a_{lL} \frac{2l+1}{2} \int_0^{\infty} d\lambda e^{-\lambda \delta_+} (\lambda^2)^{l/2} j_l(\tau) P_l^m(\cos \chi)
 \end{aligned}
 \tag{A.22}$$

The integration over λ is done by making a simple change of variables and using Gauss-Laguerre quadrature.

In this work only processes of the form

$$B^+ + A(n_s) \rightarrow B(n'l) + A^+
 \tag{A.23}$$

and their time reversed counterparts have been considered. Though the programs in Appendix II.B and II.C are written for the specific cases of $\delta = 0$ and $\lambda = 1$, it is simplest to derive the matrix elements for the more general processes, Eqn. A.23 and then specialize.

The initial and final state wavefunctions for the reaction, A.23 are

$$\psi_{n_A 00}^A = \frac{P_n(\lambda_A)}{\lambda_A} Y_{00}(\Omega_A)
 \tag{A.24}$$

$$Y_{n_x l m}^\beta = \frac{P_{n_B}(\alpha_B)}{r_B} Y_{l m}(\Omega_B) \quad \text{A.25}$$

where

$$P_{n_x}^\lambda(\alpha_x) = \sum_k C_{n_x k} r^{n_k} e^{-\delta_k \alpha_x} \quad n_x \leq n_k \quad \text{A.26}$$

γ stands for either A or B. The standard series representation is used for $Y_{l m}(\Omega_B)$.

$$Y_{l m}(\Omega_B) = \frac{(-)^m e^{i m \phi} (\sin \theta_B)^m}{\sqrt{4\pi}} \sum_{k=m}^{l-m} b_{l m}^k (c \cos \theta_B)^{l-m-2k} \quad \text{A.27}$$

where

$$b_{l m}^k = \frac{\sqrt{2l+1} \sqrt{(l-m)!}}{2^{2l} l! \sqrt{(l+m)!}} \binom{l}{k} \frac{(-)^k (2l-2k)!}{(l-m-2k)!}$$

Using the definitions A.15 and repeated applications of the binomial expansion to r_A , r_B , and $\cos \theta_B$, the expression for the wavefunctions are cast into the form

$$\sqrt{4\pi} r_A Y_{n_A 0 0}^A = \sum_i A_i \binom{n_i}{l} \sum_{p=0}^{n_i} \binom{n_i}{p} \lambda^{n_i-p} \mu^p e^{-\alpha_i r_A} \quad \text{A.28}$$

$$\sqrt{4\pi} r_0 \psi_{nlm}^B = \sum_j B_j \left[\frac{r_0}{z} \right]^j \sum_{k=0}^{l-m} C_{lm}^k \sum_{g=0}^{n_1} \binom{n_1}{g} \sum_{r=0}^{n_2} \binom{n_2}{r} (-)^{n_2-r+g} \lambda^{n_1+n-g} \mu^{n+g} \{(\lambda^2-1)(1-\mu^2)\}^{m/2} (-)^m e^{i m \phi} e^{-\beta_j r_0} \quad \text{A.29}$$

where

$$\begin{aligned} n_1 &= n_j - l + 2k \\ n_2 &= l - m - 2k \end{aligned}$$

It is convenient as well to express V_A and V_B in powers of λ and μ .

$$\begin{aligned} -\lambda_A V_A &= I_A + (z_A - I_A) e^{-\lambda_V r_A} \sum_{s=0}^3 c_A^s \left[\frac{r_0}{z} \right]^s \sum_{s'=0}^s \binom{s}{s'} \lambda^{s-s'} \mu^{s'} \quad \text{A.30} \\ -\lambda_B V_B &= I_B + (z_B - I_B) e^{-\lambda_V r_B} \sum_{t=0}^3 c_B^t \left[\frac{r_0}{z} \right]^t \sum_{t'=0}^t \binom{t}{t'} \lambda^{t-t'} (-\mu)^{t'} \end{aligned}$$

where $c_0^A = c_0^B = 1$.

Substitution of Eqns. A.28 - A.30 into Eqns. II.9 gives for the off-diagonal terms

$$\begin{aligned} S_{AB} &= R/z F_{00}^0 \\ H_{AB} &= -F_{10}^A \\ H_{BA}^* &= -F_{01}^B \end{aligned} \quad \text{A.31}$$

where

$$F_{n'_1 n'_2}^X = \sum_i A_i \sum_j B_j \left[\frac{R}{2} \right]^{n_i + n_j} \quad \text{A. 32}$$

$$\times \sum_{k=0}^{n_1 - n'_1} \sum_{l=0}^{n_2 - n'_2} \sum_{p=0}^{n_i - n'_i} \sum_{g=0}^{n_j - n'_j} \sum_{r=0}^{n_2} \binom{n_2}{r} (-)^{n_2 + r + g}$$

$$\times \left\{ I_{\lambda} G_{N - n'_1 - n'_2, M}(\delta_+ \delta_-) + \left(\frac{2}{\lambda} I_{\lambda} \right) \sum_{A=0}^3 C_{\lambda}^X \left[\frac{R}{2} \right]^A \sum_{t=0}^A \binom{A}{t} \pi_{\lambda}^t G_{N^t - n'_1 - n'_2, M}(\delta_+^t \delta_-^t) \right\}$$

and

$$\begin{aligned} \pi_A &= 1 & I_0 &= 1 \\ \pi_B &= -1 & C_{\lambda}^0 &= 0 \quad \lambda = 0, 1, 2, 3 \end{aligned}$$

$$\begin{aligned} \delta_{\pm} &= \frac{R}{2} (\alpha_i \pm \beta_j) & N &= n_1 + n_2 - g + n_i - p \\ \delta_+^X &= \delta_+ + \lambda_v^X \frac{R}{2} & M &= p + r + g \\ \delta_-^A &= \delta_- + \lambda_v^A \frac{R}{2} & N^t &= N + A - t \\ \delta_-^B &= \delta_- - \lambda_v^B \frac{R}{2} & M^t &= M + t \end{aligned} \quad \text{A. 33}$$

B.2 Diagonal Terms. It is convenient to define the function

$$\begin{aligned}
 h_{N_1, N_2}(\delta_+, \delta_-) &= \frac{1}{4\pi} \int_0^{2\pi} d\phi \int_1^{\infty} d\lambda \lambda^{N_1} e^{-\lambda \delta_+} \int_{-1}^1 d\mu \mu^{N_2} e^{-\mu \delta_-} \\
 &= \frac{1}{2} g_{N_1}(\delta_+) f_{N_2}(\delta_-)
 \end{aligned}
 \tag{A.34}$$

where

$$\begin{aligned}
 g_n(x) &= \int_1^{\infty} d\lambda \lambda^n e^{-x\lambda} \\
 f_n(x) &= \int_{-1}^1 d\mu \mu^n e^{-x\mu}
 \end{aligned}
 \tag{A.35}$$

The g 's and f 's satisfy the recursion relations

$$\begin{aligned}
 dg_n &= (n-1)g_{n-1} + e^{-x} \\
 \alpha f_n &= (n-1)f_{n-1} - (1)^n e^{-x} - e^{-x}
 \end{aligned}
 \tag{A.36}$$

where

$$\begin{aligned}
 dg_0 &= e^{-x} \\
 \alpha f_0 &= e^{-x} - e^{-x}
 \end{aligned}
 \tag{A.37}$$

Using Eqns. A.34 and A.28-29, it is straightforward to derive the analytical expression for the diagonal terms.

$$H_{AA} = - \sum_{i,i'} A_i A_{i'} \left[\frac{R}{2} \right]^{n_i + n_{i'}} \sum_{p=0}^{n_i} \binom{n_i}{p} \sum_{p'=0}^{n_{i'}-1} \binom{n_{i'}-1}{p'} \quad \text{A.38}$$

$$\times \left\{ I_B h \left(\frac{\delta_+ \delta_-}{N_1 N_2} \right) + (Z_B - I_B) \sum_{\lambda=0}^C C_{\lambda}^B \left[\frac{R}{2} \right]^{\lambda} \sum_{\lambda'=0}^{\lambda} \binom{\lambda}{\lambda'} (-1)^{\lambda'} h \left(\frac{\delta_+^B \delta_-^B}{N_1 + A - \lambda', N_2 + \lambda'} \right) \right\}$$

where

$$\delta_{\pm} = \frac{R}{2} (\alpha_i + \alpha_{i'}) \quad N_2 = p + p'$$

$$\delta_{\pm}^B = \gamma_{\pm}^B \pm \frac{1}{\lambda} \frac{R}{2} \quad N_1 = n_i + n_{i'} - 1 - N_2$$

A.39

$$H_{BB} = - \sum_{j,j'} B_j B_{j'} \left[\frac{R}{2} \right]^{n_j + n_{j'}} \sum_{k=0}^{l-2} b_k^k b_{l-k}^{l-k} \sum_{g=0}^{n_j} \binom{n_j}{g} \sum_{g'=0}^{n_{j'}-1} \binom{n_{j'}-1}{g'} \sum_{n_2=0}^{n_2} \binom{n_2}{n_2} \sum_{n_1=0}^{n_1} \binom{n_1}{n_1} \sum_{s=0}^m \binom{m}{s} (-1)^s$$

$$\times \sum_{s=0}^m \binom{m}{s} \left\{ I_A h \left(\frac{\gamma_+ \gamma_-}{N_1 N_2} \right) + (Z_A - I_A) \sum_{t=0}^C C_t^A \left[\frac{R}{2} \right]^t \sum_{t'=0}^t \binom{t}{t'} (-1)^{t'} h \left(\frac{\gamma_+^A \gamma_-^A}{N_1 + t - t', N_2 + t'} \right) \right\}$$

where

$$\delta_{\pm} = \frac{R}{2} (\beta_j + \beta_{j'}) \quad n_2 = l - m - 2k$$

$$\gamma_{\pm}^A = \gamma_{\pm}^A \pm \frac{1}{\lambda} \frac{R}{2} \quad n_1 = l - m - 2k'$$

$$n_i = n_j - l + 2k \quad N_1 = n_i + n_{i'} + n + n' - g - g' - 1 + 2(m - s)$$

$$n_{i'} = n_{j'} - l + 2k' \quad N_2 = g + g' + n + n' + 2s'$$

The coding written to perform these calculations is listed in Appendices II.B and II.C.

APPENDIX II

Appendix II lists the computer coding written to perform the calculations of Appendix I. Appendix II.A begins on p. 79, Appendix II.B, on p. 89; and Appendix II.C begins on p. 108.

CC
CC

HERMAN

PURPOSE: THIS PROGRAM DIAGONALIZES THE HAMILTONIAN FOR ANY
POTENTIAL WHICH CAN BE FITTED TO THE FORM

$$V(R) = [(1+Z^2)^{-1} * (1 + \lambda R)] * \exp(-\mu R) \quad \text{EQN. 1}$$

WHERE F(R) IS A POLYNOMIAL OF ORDER THREE.
THE RADIAL WAVEFUNCTIONS ARE EXPRESSED AS SUMS OF
SLATER TYPE ORBITALS.

$$\Psi(R) = \sum C(I) * X(I) \quad \text{EQN. 2}$$

EACH ORBITAL IS OF THE FORM

$$X(I) = \text{NORM} * R^{*M} * \exp(-A * R) \quad \text{EQN. 3}$$

WHERE NORM IS A NORMALIZATION FACTOR, THE SCREENING
FUNCTION CORRESPONDING TO EQN. 1 IS READ IN AS WELL AS
THE PARAMETERS A AND M IN EQN. 3. THE PROGRAM PUNCHES OUT
QLM, THE COEFFICIENTS IN F(R), AND THE
INFORMATION NECESSARY FOR THE DESCRIPTION OF THE WAVEFUNCTION.

CARD 1: (LABEL(1), I=1,10), Z, RM, NUNTIM, NU, NZ (10AN, 2FS, 0, 6LS)
LABEL: PROGRAM TITLE
Z: CHARGE OF THE NUCLEUS
NUNTIM: THE NUMBER OF L VALUES FOR WHICH THE DIAGONALIZATION
IS PERFORMED
IZ: THE IONICITY OF THE ATOM
NU: THE NUMBER OF VALUES OF THE SCREENING FUNCTION TO BE READ
CARD 2: (I(1), I=1, NU) (P(1), 3)
I(1): VALUES OF THE SCREENING FUNCTION
FOR A HYDROGENIC POTENTIAL; ONE BLANK CARD
SHOULD BE READ IN.

THE NEXT CARDS ARE INPUTTED IN SETS OF THREE. THERE ARE NUNTIM SETS.

CARD A: NTRMS, L (1615)
NTRMS: THE UPPER LIMIT OF THE SUM IN EQN. 2
L: THE CRIBITAL ANGULAR MOMENTUM QUANTUM NUMBER
CARD B: (NDP(I), I=1, NTRMS)
NDP(I): THE N IN EQN. 3
CARD C: (AKP(I), I=1, NTRMS)
AKP(I): THE A IN EQN. 3

FOR EACH L VALUE, THERE WILL BE X NUMBER OF BOUND STATES. FOUR CARDS
WILL BE OUTPUTTED FOR EACH STATE BEGINNING WITH THE ONE HAVING
THE MOST NEGATIVE ENERGY EIGENVALUE.

CARD AA: EVAL, 0, (CV(1), J=1, 3), QNZ
EVAL: ENERGY EIGENVALUE FOR A GIVEN STATE.
Q: THE FLOATING POINT EQUIVALENT OF NTRMS
CV: DEFINED IN EQN. 1
CV: THE COEFFICIENTS IN F(R) OF EQN. 1
QNZ: THE FLOATING POINT EQUIVALENT OF NZ
CARD BB: IMAGE OF CARD B
CARD CC: IMAGE OF CARD C
CARD DD: (EVCT(I), I=1, NTRMS)
THE C(I) IN EQN. 2 FOR A GIVEN STATE K

CARD IMAGES OF THE OUTPUT ARE PRINTED IN THE PROGRAM AFTER THE LISTING
OF THE WAVEFUNCTIONS FOR EACH L VALUE. EACH SET OF FOUR CARDS ARE THEN
USED AS INPUT FOR ANS0NS AND ANS0NP.

WRITTEN BY LAURA TUNHELL (1976)

CC
CC

```

IMPLICIT REAL*8(A-H,O-Z)
COMMON/AF/ALF(10),AXP(20),ANRM(20),NOP(20),LOPI(20),L,NTRMS
COMMON/MSV/CV(10),OLM(2),Z1,RM,U(225),NV,NU
COMMON/LCM/A(225),G(225),X(225),EVAL(20),EVCT(12,12),NM
DIMENSION LABEL(20)
1 FORMAT(10I5)
2 FORMAT(8F10.5)
3 FORMAT(10A,2F5.0,0I5)
4 FORMAT(//10A, ' Z =',F3.0/)
5 FORMAT(//'/L',10A, ' L =',F3.0/)
220 FORMAT(//'/ ' /)

NV=3
OLM=0.000
GC 20 I=1,10
20 CV(1)=0.000
READ(5,3) (LABEL(I),I=1,10),Z,RM,NUMTIM,NU,NZ
1FERM.EQ.0.000) RM=1.000
1FNUMTIM.EQ.0) NUMTIM=1
1FNV.EQ.0) NV=1
GNZ=Z
Z1=GNZ
READ(5,2) (U(I),I=1,NU)
PRINT 22C
PRINT 200
200 FORMAT(' (LABEL(I),I=1,10),Z,RM,NUMTIM,NU,NZ *')
PRINT 3, (LABEL(I),I=1,10),Z,RM,NUMTIM,NU,NZ
PRINT 210
210 FORMAT(' (U(I),I=1,NU) ')
PRINT 2, (U(I),I=1,NU)
PRINT 22C
PRINT 4, (LABEL(I),I=1,10),Z
1F(U(1).EQ.1.000) CALL YFCTN
GC 12 N=1,NUMTIM
READ(5,1) NTRMS,L
READ(5,1) INDP(I),I=1,NTRMS)
READ(5,2) (AXP(I),I=1,NTRMS)
PRINT 220
PRINT 221
221 FORMAT(' NTRMS,L *')
PRINT 1, NTRMS,L
PRINT 222
222 FORMAT(' INDP(I),I=1,NTRMS) *')
PRINT 1, INDP(I),I=1,NTRMS)
PRINT 223
223 FORMAT(' (AXP(I),I=1,NTRMS) *')
PRINT 2, (AXP(I),I=1,NTRMS)
PRINT 220
GC 10 J=1,NTRMS
AI=(2.000/AXP(I))**2*INDP(J)+1)
A2=0.0A1/G(LCAT(2*INDP(J)+1))
10 ANRM(J)=CSQR(A1/A2)
PRINT 5, (LABEL(I),I=1,10),L
CALL CDEP
GC 12 I=1,NTRMS
I=(I+NTRMS)-1)
1F(EVAL(I).GT.0.000) GO TO 12
EVALI=EVAL(I)
DPLICAT(NTRMS)
PUNCH 2, EVALI,D,OLM,(CV(I),J=1,3),CAZ
PUNCH 1, INDP(J),J=1,NTRMS)
PUNCH 2, (AXP(J),J=1,NTRMS)
PUNCH 2, (EVCT(I),J=1,NTRMS)
PRINT 2, EVALI,D,OLM,(CV(J),J=1,3),GNZ
PRINT 1, INDP(J),J=1,NTRMS)
PRINT 2, (AXP(J),J=1,NTRMS)
PRINT 2, (EVCT(I),J=1,NTRMS)
12 CONTINUE

STOP
END

SUBROUTINE COEF
IMPLICIT REAL*8(A-H,O-Z)
COMMON/AF/ALF(10),AXP(20),ANRM(20),NOP(20),LOPI(20),L,NTRMS
COMMON/MSV/CV(10),OLM(2),Z1,RM,U(225),NV,NU
COMMON/LCM/A(225),G(225),X(225),EVAL(20),EVCT(12,12),NM
DIMENSION A(225),FCTN(10,10)
DIMENSION ALF(12,12),OLP(12,12),H(12,12),R(12,12)
COMMON/H/EVL(10),OLM(2),Z1,RM,U(225),NV,NZ
DIMENSION R(12),V(12),V(12),V(12)
DIMENSION R1(10)
3 FORMAT(10E14,1P(14.5))
4 FORMAT(10E14,1P(12.5))

```

```

NM=NTRMS
DO 10 J=1,NTRMS
DO 30 J=1,NTRMS
NO=NOP(1)+NOP(J)+1
N1=NO-1
N2=N-1
AA=AXP(1)+AXP(J)
RF(1)=1.000/AA
DO 11 K=1,NO
KK=K-1
11 RF(K)= (DFLCAT(KK+1)/AA)*RF(K)
H1=NOP(1)+NOP(J)+AF(N2)-(NOP(1)+AXP(J)+NOP(J)+AXP(1))*RF(N1)
*AXP(J)*AXP(J)*RF(N1)
H2=DFLCAT(L*(L+1))*RF(N2)
VA=OLM*AA
VF(1)=1.000/VA
NMW=NV*NO
DO 12 K=1,NV
KK=K-1
12 VF(K)= (DFLCAT(KK+1)/VA)*VF(K)
N11=NO+1
M11=NMW+1
M3=O.CDO
DO 13 K=1,NV
13 H3=H3+CV(F(1)+VF(N1)+K)
H3=2*(H3-F(1))+(-2)*VF(N1)+H3
AN=ANRM(1)+ANRM(J)
H4(J)=AN*(H3+H2-2+ODD*M3)/2.000
R(J,J)=AN*RP(NC)
H(J,J)=H(1,J)
R(J,J)=R(1,J)
10 CONTINUE
ALP(1,1)=1.000
DO 30 N=2,NTRMS
ALP(N,N)=1.000
N1=N-1
ONRM=1.000
DO 30 J=1,N-1
A(J)=0.000
DO 35 J=1,J
15 A(J)=A(J)+ALP(J,J)*R(J,N)
30 ONRM=ONRM+A(J)*A(J)
ONRM=OSQRT(CABS(ONRM))
DO 21 K=1,N1
ALP(N,K)=0.000
ALP(N,K)=0.000
DO 21 K=1,N1
21 ALP(N,K)=ALP(N,K)-A(J)*ALP(J,K)
DO 30 K=1,N
30 ALP(N,K)=ALP(N,K)/ONRM
DO 70 I=1,NTRMS
DO 70 J=1,J
OLP(J,J)=0.000
DO 70 K=1,J
EVCT(K,J)=0.000
DO 75 L=1,J
EVCT(K,J)=EVCT(K,J)+H(K,L)*ALP(J,L)
75 CONTINUE
OLP(J,J)=OLP(J,J)+ALP(J,K)*EVCT(K,J)
70 CONTINUE
PRINT 5
5 FORMAT(// ' HAMILTONIAN ' //)
K=0
DO 80 J=1,NTRMS
PRINT 6, (OLP(I,J),J=1,J)
DO 80 J=1,J
K=K+1
80 A(K)=OLP(J,J)
NM=NTRMS+NTRMS
CALL E(CENHTRMS,0)
NM=NTRMS+NTRMS
NMAX=1
KK=0
LL=0
DO 90 J=1,NTRMS
LL=LL+J
EVAL(J)=ALL)
JF(EVAL(J),GT,3.000) NMAX=J
DO 90 J=1,NTRMS
90 OLP(J,J)=X(1+(J-1)*NTRMS)
N1=NMAX+1
DO 92 J=1,NTRMS
DO 92 J=1,J*IFR=J
EVCT(J,J)=0.000
DO 100 K=1,NTRMS

```

```

EVCT(I,J)=CVCT(I,J)+DLPI(I,K)*ALPIK,JJ
193 CONTINUE
92 CONTINUE
PRINT 91
FCRMAT(// ' ENERGY EIGENVALUES ' //)
PRINT 6, (EVAL(I),I=1,NTRMS)
PRINT 93
93 FCRMAT(// ' COEFFICIENTS FOR BASIS SET ' //)
DO 94 I=1,NTRMS
96 PRINT 3, (EVCT(I,J),J=1,NTRMS)
S=0.000
P=DARCD(SI-1.000)
FMJ=(2.000*DLG(I3+000*P(I)-OLDG(I2)-7.000*DLG(I2,000)))/3.000
FMJ=DEXP(FMJ)
DO 106 J=1,8
SA=2.000*(J-1)
S=S*SA,CD=02
DO 106 I=1,10
IJ=I+J-1)*1.00+01
A(I,J)=S
R(I,I)=FMJ*S
106 S=S*SA
NU=I*J-1
N2=NTRMS-ANAX
PRINT 210
DC 96 K=1,NU
FLM=DLN*(R(I,K)
IF(FLM,DE=1.400+32) DO=0.000
IF(FLM,LT=1.400+32) CD=DEXP(-FLM)
U3=R(I,K)*CV(I)+R(I,K)*C(VL2)+R(I,K)*C(VL3))
U(K)=(Z2+Z-21)*CD*(1.000+U11)/2
DO 96 J=K1,NTRMS
WFCTN(K,J)=0.000
DO 96 I=1,NTRMS
W=0.000
IF(AMPI(I)*R(I,K),LE=1.200+02) W=DEXP(-AMPI(I)*R(I,K))
WFCTN(K,J)=WFCTN(I,J)+EVCT(I,J)*W*(R(I,K)*WDP(I))**
96 CONTINUE
PRINT 103
103 FCRMAT(// ' X R(X) U(X) P(X) ' //)
A1=0.000
DO 97 I=1,NJ
97 PRINT 3, A(I),R(I,1),U(I),A1,(WFCTN(I,J),J=N1,NTRMS)
NL=NTRMS-1
PRINT 210
SSUM=0.000
NUL=NUL-1
DO 220 I=2,NUL
X1=R(I,1)-1)
X2=R(I,1)
X3=R(I,1)+1)
Y1=WFCTN(I-1,NTRMS)
Y2=WFCTN(I,NTRMS)
Y3=WFCTN(I+1,NTRMS)
Y1=Y1*Y1
Y2=Y2*Y2
Y3=Y3*Y3
220 SSUM=SSUM+SUM(X1,X2,X3,Y1,Y2,Y3)
PRINT 225, SSUM
225 FCRMAT(// ' SSUM= ', 1PD12.5//)
210 FCRMAT(// ' //)
RETURN
END
REAL FUNCTION $A*(X1,X2,X3,Y1,Y2,Y3)
IMPLICIT REAL*8 (A-H,O-Z)
IF(DABS((X3-X2)-(X2-X1))-LT.1.0E-8) GO TO 10
A=Y1/(X1-X2)*X1-X3)
B=Y2/((X2-X3)*(X2-X1))
C=Y3/(X3-X1)*(X3-X2)
D=A*B*C
E=A*(X2+X3)-B*(X1+X3)-C*(X2+X1)
F=A*B*C*X3+D*(X1+X3)+E*(X2+X1)
SUM=(D*(X2**2+X1*(X2+X1)))/3.000+B*(X2+X1)/2.000+F*(X2-X1)
RETURN
10 O=X2-X1
SUM=D*(5*Y1+8*Y2-Y3)/12.000
RETURN
END
SUBROUTINE VFCTN
IMPLICIT REAL*8(A-H,O-Z)
COMMON/MSW/DV(I,1),DLN,Z,Z1,DMAX,UT(Z25),NV,N
DIMENSION LADL(20),EAL(50)

```

```

DIMENSION R(225),X(225),UU(225)
DIMENSION A(225,10),B(10,10),C(225),F(225)
DIMENSION I(1,3),JK(3),SS(3),ZS(3),OL(10,3)
DIMENSION SUMA(50),Z(50),G(225),CV(10,6)
3 FORMAT(1X,1P012.5)
305 FORMAT(1X,*)

XMAX=1.000
NC=3
ZZ=1.000/Z
S=0.000
PI=0.0ARCSIN(1.000)
OMU=(2.000*LOG(3.000*PI)-LOG(Z))-7.000*LOG(2.000)/3.000
OMU=EXP(OMU)
NU=0
DO 6 J=1,12
  SA=2.000**J-1
  SA=SA*1.00-02
  DO 6 I=1,10
    IJ=I+J-1*10
    R(IJ)=OMU**S
    X(IJ)=S
    S=S+SA
    IF(NU.EQ.0) GO TO 6
    IF(R(IJ).GE.XMAX) NU=IJ
6 CONTINUE
  NNU=IJ
  IF(NU.EQ.0) NU=IJ
  DO 5 I=1,NU
5 U(I)=ZZ
  OBTAIN OLN
  S=0.000
  U1=0.000
  DO 32 I=2,NU
    R1=R(I-1)
    R2=R(I)
    U2=(U(I)*2-Z1)/(2-Z1)
    U2=OLCGT(ABS(U2))
    Z2=(U2-U1)/(R2-R1)
    S=S+Z2
    IF(U(I).LE.2.000/Z) GO TO 33
32 U1=U2
33 Z2=-S/DFLOAT(I-1)
    DO 7 I=1,NU
      OLN=Z2**R(I)
      IF(OLN.GT.1.400*Z2) GO TO 8
      OLN=EXP(OLN)
7 U(I)=(U(I)*2-Z1)*OLN/(2-Z1)-1.000
8 NR=I-1
  CCNSTRUCT BASIS VECTORS
  DO 10 I=1,NNU
    DO 10 J=1,NC
      A(I,J)=R(I)**J
10 CONTINUE
  PERFORM MULTIPLICATION PROCEDURE
  DO 20 I=1,NC
    DO 20 J=1,NC
      B(I,J)=0.000
      DO 21 K=1,NR
21 B(I,J)=B(I,J)+A(K,I)**R(K,J)
      B(I,J)=B(I,J)
      F(I)=0.000
      DO 22 K=1,NR
22 F(I)=F(I)+A(K,I)**U(K)
20 CONTINUE
  DO 30 J=1,NC
    DO 30 I=1,NC
      I=I+J-1**NC
      C(I,J)=B(I,J)
30 CONTINUE
  NNC=NC*NC
  LI=NC
  KK=II
  SOLVE EQUATIONS FOR THE COEFFICIENTS
  CALL SOLVEGF,C,NC,NNC,1,1.0E-03,ITER)
  SQRA(II)=0.000
  CS=1.000
  SGG=0.000
  DO 40 I=1,N*MM
    OLN=Z2**R(I)
    IF(OLN.LE.1.400*Z2) GO=0.000
    IF(OLN.LT.1.400*Z2) GO=EXP(-OLN)
    GO=0.000
  DO 50 J=1,NC

```



```

CWEJ,11)=FJ11
90 GOMG+F(1,1)M11,J1
G11)=(Z1+(Z-21)*D0*(1.000+G11)/Z
IF(1.GE.NU) GO TO 40
SGM11)=SGM111)+(U(11)-GG)**2)*CS
40 CONTINUE
PRINT 305
309 FOMAT(1111111111) FIT TO THE HERMAN-SKILLMAN POTENTIAL 1/1
PRINT 315, RMAX,OMU,ZZ
315 FOMAT(1111111111) RMAX= 1.1P012.5, OMU= 1.1P012.5, DLN= 1.1P012.5)
PRINT 310
310 FOMAT(1111111111) X=.....R=..... MN-SK=.....FITTED=..... 1/1
DO 311 I=1,NNU
311 PRINT 3, X(I),R(I),NR,U(I),G(I)
PRINT 301
301 FOMAT(1111111111) COEFFICIENTS FOR THE POTENTIAL 1/1
PRINT 3, ECVI,AKI,J=1,NC)
PRINT 305
DLN=ZZ
DO 320 I=1,3
320 DV(I)=CV(I,AKI)
5000 CONTINUE
RETURN
END

```

..... DELG 10
DELG 20
DELG 30
SUBROUTINE DGELG DELG 40
PURPOSE DELG 50
TO SOLVE A GENERAL SYSTEM OF SIMULTANEOUS LINEAR EQUATIONS. DELG 60
DELG 70
USAGE DELG 80
CALL DGELG(A,P,N,EPS,IER) DELG 100
DELG 110
DESCRIPTION OF PARAMETERS DELG 120
R - DOUBLE PRECISION M BY N RIGHT HAND SIDE MATRIX DELG 130
(DESTROYED). ON RETURN A CONTAINS THE SOLUTIONS DELG 140
OF THE EQUATIONS. DELG 150
A - DOUBLE PRECISION M BY M COEFFICIENT MATRIX DELG 160
(DESTROYED). DELG 170
M - THE NUMBER OF EQUATIONS IN THE SYSTEM. DELG 180
N - THE NUMBER OF RIGHT HAND SIDE VECTORS. DELG 190
EPS - SINGLE PRECISION INPUT CONSTANT WHICH IS USED AS DELG 200
RELATIVE TOLERANCE FOR TEST ON LOSS OF DELG 210
SIGNIFICANCE. DELG 220
IER - RESULTING ERROR PARAMETER CODED AS FOLLOWS DELG 230
IER=0 - NO ERROR. DELG 240
IER=-1 - NO RESULT BECAUSE OF M LESS THAN 1 OR DELG 250
PIVOT ELEMENT AT ANY ELIMINATION STEP DELG 260
EQUAL TO 0. DELG 270
IER=K - WARNING DUE TO POSSIBLE LOSS OF SIGNIFI- DELG 280
CANCE INDICATED AT ELIMINATION STEP K+1, DELG 290
WHERE PIVOT ELEMENT WAS LESS THAN OR DELG 300
EQUAL TO THE INTERNAL TOLERANCE EPS TIMES DELG 310
ABSOLUTELY GREATEST ELEMENT OF MATRIX A. DELG 320
DELG 330
REMARKS DELG 340
INPUT MATRICES R AND A ARE ASSUMED TO BE STORED COLUMNWISE DELG 350
IN MMN RESP. MMN SUCCESSIVE STORAGE LOCATIONS. ON RETURN DELG 360
SOLUTION MATRIX A IS STORED COLUMNWISE TOO. DELG 370
THE PROCEDURE GIVES RESULTS IF THE NUMBER OF EQUATIONS M IS DELG 380
GREATER THAN 0 AND PIVOT ELEMENTS AT ALL ELIMINATION STEPS DELG 390
ARE DIFFERENT FROM 0. HOWEVER WARNING IER=K - IF GIVEN - DELG 400
INDICATES POSSIBLE LOSS OF SIGNIFICANCE. IN CASE OF A WELL DELG 410
SCALED MATRIX AND APPROPRIATE TOLERANCE EPS, IER=K MAY BE DELG 420
INTERPRETED THAT MATRIX A HAS THE RANK N. NO WARNING IS DELG 430
GIVEN IN CASE M=1. DELG 440
DELG 450
SUBROUTINES AND FUNCTION SUBPROGRAMS REQUIRED DELG 460
NCHE DELG 470
DELG 480
METHOD DELG 490
SOLUTION IS DONE BY MEANS OF GAUSS-ELIMINATION WITH DELG 500
COMPLETE PIVOTING. DELG 510
DELG 520
..... DELG 530
SUBROUTINE DGELG(A,P,N,EPS,IER) DELG 540
DELG 550
DELG 560
DOUBLE PRECISION PIV,TOL,PIV1 DELG 570
DOUBLE PRECISION A(M),R(M), DELG 580
IF(M)Z,C1,C1 DELG 600

```

SEARCH FOR GREATEST ELEMENT IN MATRIX A
1 IER=0
PIV=0.00
NN=MM
MM=MM
DO 3 L=1,MM
TB=0ABS(A(L))
IF(TB=PIV)3,3,2
2 PIV=TB
I=L
3 CONTINUE
TCL=EPS*PIV
A(I) IS PIVOT ELEMENT. PIV CONTAINS THE ABSOLUTE VALUE OF A(I).
DELG 610
DELG 620
DELG 630
DELG 640
DELG 650
DELG 660
DELG 670
DELG 680
DELG 690
DELG 700
DELG 710
DELG 720
DELG 730
DELG 740
DELG 750
DELG 760
DELG 770
DELG 780
DELG 790
DELG 800
DELG 810
DELG 820
DELG 830
DELG 840
DELG 850
DELG 860
DELG 870
DELG 880
DELG 890
DELG 900
DELG 910
DELG 920
DELG 930
DELG 940
DELG 950
DELG 960
DELG 970
DELG 980
DELG 990
DELG1000
DELG1010
DELG1020
DELG1030
DELG1040
DELG1050
DELG1060
DELG1070
DELG1080
DELG1090
DELG1100
DELG1110
DELG1120
DELG1130
DELG1140
DELG1150
DELG1160
DELG1170
DELG1180
DELG1190
DELG1200
DELG1210
DELG1220
DELG1230
DELG1240
DELG1250
DELG1260
DELG1270
DELG1280
DELG1290
DELG1300
DELG1310
DELG1320
DELG1330
DELG1340
DELG1350
DELG1360
DELG1370
DELG1380
DELG1390
DELG1400
DELG1410
DELG1420
DELG1430
DELG1440
DELG1450

START ELIMINATION LOOP
LST=1
DO 17 K=1,M
TEST ON SINGULARITY
IF(PIV)23,23,4
4 IF(IER)7,7,7
5 IF(PIV=TCL)6,6,7
6 IER=-1
7 PIV=1.00/A(I)
J=(I-1)/P
I=I-J*M-K
J=J+I-K
I+K IS ROW-INDEX, J+K COLUMN-INDEX OF PIVOT ELEMENT
DELG 980
DELG 990
DELG1000
DELG1010
DELG1020
DELG1030
DELG1040
DELG1050
DELG1060
DELG1070
DELG1080
DELG1090
DELG1100
DELG1110
DELG1120
DELG1130
DELG1140
DELG1150
DELG1160
DELG1170
DELG1180
DELG1190
DELG1200
DELG1210
DELG1220
DELG1230
DELG1240
DELG1250
DELG1260
DELG1270
DELG1280
DELG1290
DELG1300
DELG1310
DELG1320
DELG1330
DELG1340
DELG1350
DELG1360
DELG1370
DELG1380
DELG1390
DELG1400
DELG1410
DELG1420
DELG1430
DELG1440
DELG1450

PIVOT ROW REDUCTION AND ROW INTERCHANGE IN RIGHT HAND SIDE R
DO 8 L=K,MM,M
LL=L+1
TB=PIV*A(LL)
R(LL)=R(L)
8 R(LL)=TB
DELG 980
DELG 990
DELG1000
DELG1010
DELG1020
DELG1030
DELG1040
DELG1050
DELG1060
DELG1070
DELG1080
DELG1090
DELG1100
DELG1110
DELG1120
DELG1130
DELG1140
DELG1150
DELG1160
DELG1170
DELG1180
DELG1190
DELG1200
DELG1210
DELG1220
DELG1230
DELG1240
DELG1250
DELG1260
DELG1270
DELG1280
DELG1290
DELG1300
DELG1310
DELG1320
DELG1330
DELG1340
DELG1350
DELG1360
DELG1370
DELG1380
DELG1390
DELG1400
DELG1410
DELG1420
DELG1430
DELG1440
DELG1450

IS ELIMINATION TERMINATED
IF(K=MM,18,18)
DELG 980
DELG 990
DELG1000
DELG1010
DELG1020
DELG1030
DELG1040
DELG1050
DELG1060
DELG1070
DELG1080
DELG1090
DELG1100
DELG1110
DELG1120
DELG1130
DELG1140
DELG1150
DELG1160
DELG1170
DELG1180
DELG1190
DELG1200
DELG1210
DELG1220
DELG1230
DELG1240
DELG1250
DELG1260
DELG1270
DELG1280
DELG1290
DELG1300
DELG1310
DELG1320
DELG1330
DELG1340
DELG1350
DELG1360
DELG1370
DELG1380
DELG1390
DELG1400
DELG1410
DELG1420
DELG1430
DELG1440
DELG1450

COLUMN INTERCHANGE IN MATRIX A
LEND=LST+M-K
IF(J)12,12,10
10 I=J*M
DO 11 L=LST,LEND
TB=A(L)
LL=L+I
A(L)=A(LL)
11 A(LL)=TB
DELG 980
DELG 990
DELG1000
DELG1010
DELG1020
DELG1030
DELG1040
DELG1050
DELG1060
DELG1070
DELG1080
DELG1090
DELG1100
DELG1110
DELG1120
DELG1130
DELG1140
DELG1150
DELG1160
DELG1170
DELG1180
DELG1190
DELG1200
DELG1210
DELG1220
DELG1230
DELG1240
DELG1250
DELG1260
DELG1270
DELG1280
DELG1290
DELG1300
DELG1310
DELG1320
DELG1330
DELG1340
DELG1350
DELG1360
DELG1370
DELG1380
DELG1390
DELG1400
DELG1410
DELG1420
DELG1430
DELG1440
DELG1450

ROW INTERCHANGE AND PIVOT ROW REDUCTION IN MATRIX A
12 DO 13 L=LST,M,M
LL=L+1
TB=PIV*A(LL)
A(LL)=A(L)
13 A(L)=TB
DELG 980
DELG 990
DELG1000
DELG1010
DELG1020
DELG1030
DELG1040
DELG1050
DELG1060
DELG1070
DELG1080
DELG1090
DELG1100
DELG1110
DELG1120
DELG1130
DELG1140
DELG1150
DELG1160
DELG1170
DELG1180
DELG1190
DELG1200
DELG1210
DELG1220
DELG1230
DELG1240
DELG1250
DELG1260
DELG1270
DELG1280
DELG1290
DELG1300
DELG1310
DELG1320
DELG1330
DELG1340
DELG1350
DELG1360
DELG1370
DELG1380
DELG1390
DELG1400
DELG1410
DELG1420
DELG1430
DELG1440
DELG1450

SAVE COLUMN INTERCHANGE INFORMATION
A(LST)=J
DELG 980
DELG 990
DELG1000
DELG1010
DELG1020
DELG1030
DELG1040
DELG1050
DELG1060
DELG1070
DELG1080
DELG1090
DELG1100
DELG1110
DELG1120
DELG1130
DELG1140
DELG1150
DELG1160
DELG1170
DELG1180
DELG1190
DELG1200
DELG1210
DELG1220
DELG1230
DELG1240
DELG1250
DELG1260
DELG1270
DELG1280
DELG1290
DELG1300
DELG1310
DELG1320
DELG1330
DELG1340
DELG1350
DELG1360
DELG1370
DELG1380
DELG1390
DELG1400
DELG1410
DELG1420
DELG1430
DELG1440
DELG1450

ELEMENT REDUCTION AND NEXT PIVOT SEARCH
PIV=0.00
LST=LST+1
J=0
DO 16 I=LST,LEND
PIV=-A(I)
IST=I+M
J=J+1
DO 15 L=LST,M,M
LL=L+1
A(L)=A(L)+PIV*A(LL)
TB=0ABS(A(L))
IF(TB=PIV)13,13,14
14 PIV=TB
I=L
15 CONTINUE
DO 16 L=LST,M,M
LL=L+1
A(LL)=A(LL)+PIV*A(LL)
LST=LST+M
END OF ELIMINATION LOOP
DELG 980
DELG 990
DELG1000
DELG1010
DELG1020
DELG1030
DELG1040
DELG1050
DELG1060
DELG1070
DELG1080
DELG1090
DELG1100
DELG1110
DELG1120
DELG1130
DELG1140
DELG1150
DELG1160
DELG1170
DELG1180
DELG1190
DELG1200
DELG1210
DELG1220
DELG1230
DELG1240
DELG1250
DELG1260
DELG1270
DELG1280
DELG1290
DELG1300
DELG1310
DELG1320
DELG1330
DELG1340
DELG1350
DELG1360
DELG1370
DELG1380
DELG1390
DELG1400
DELG1410
DELG1420
DELG1430
DELG1440
DELG1450

BACK SUBSTITUTION AND BACK INTERCHANGE
DELG 980
DELG 990
DELG1000
DELG1010
DELG1020
DELG1030
DELG1040
DELG1050
DELG1060
DELG1070
DELG1080
DELG1090
DELG1100
DELG1110
DELG1120
DELG1130
DELG1140
DELG1150
DELG1160
DELG1170
DELG1180
DELG1190
DELG1200
DELG1210
DELG1220
DELG1230
DELG1240
DELG1250
DELG1260
DELG1270
DELG1280
DELG1290
DELG1300
DELG1310
DELG1320
DELG1330
DELG1340
DELG1350
DELG1360
DELG1370
DELG1380
DELG1390
DELG1400
DELG1410
DELG1420
DELG1430
DELG1440
DELG1450

```

```

16 IF(M-1)23,22,19
19 IST=MM+M
   LST=M+1
   DD Z1 I=2,M
   I=LST-1
   IST=IST-LST
   L=IST-M
   L=A(L)*.5DD
   DD Z1 J=I,MM,M
   TB=R(I)
   LL=J
   DD ZD K=IST,MM,M
   LL=LL+1
20 TB=TB-A(I)*R(LL)
   M=J+L
   R(J)=R(K)
21 A(K)=TB
22 RETURN

ERRDR RETURN
18 IER=-
23 RETURN
END

```

```

DELG1460
DELG1470
DELG1480
DELG1490
DELG1500
DELG1510
DELG1520
DELG1530
DELG1540
DELG1550
DELG1560
DELG1570
DELG1580
DELG1590
DELG1600
DELG1610
DELG1620
DELG1630
DELG1640
DELG1650
DELG1660
DELG1670
DELG1680
DELG1690

```

```

.....
EIGE 10
EIGE 20
EIGE 30
EIGE 40
EIGE 50
EIGE 60
EIGE 70
EIGE 80
EIGE 90
EIGE 100
EIGE 110
EIGE 120
EIGE 130
EIGE 140
EIGE 150
EIGE 160
EIGE 170
EIGE 180
EIGE 190
EIGE 200
EIGE 210
EIGE 220
EIGE 230
EIGE 240
EIGE 250
EIGE 260
EIGE 270
EIGE 280
EIGE 290
EIGE 300
EIGE 310
EIGE 320
EIGE 330
EIGE 340
EIGE 350
EIGE 360
EIGE 370
EIGE 380
EIGE 390
EIGE 400

```

.....

SUBROUTINE EIGEN

PURPOSE
 COMPUTE EIGENVALUES AND EIGENVECTORS OF A REAL SYMMETRIC
 MATRIX

USAGE
 GALL EIGEN(A,R,N,MV)

DESCRIPTION OF PARAMETERS
 A - ORIGINAL MATRIX (SYMMETRIC), DESTROYED IN COMPUTATION.
 RESULTANT EIGENVALUES ARE DEVELOPED IN DIAGONAL OF
 MATRIX A IN DESCENDING ORDER.
 R - RESULTANT MATRIX OF EIGENVECTORS (STORED COLUMNWISE,
 IN SAME SEQUENCE AS EIGENVALUES)
 N - ORDER OF MATRICES A AND R
 MV- INPUT CODE
 0 COMPUTE EIGENVALUES AND EIGENVECTORS
 1 COMPUTE EIGENVALUES ONLY (R NEED NOT BE
 DIMENSIONED BUT MUST STILL APPEAR IN CALLING
 SEQUENCE)

REMARKS
 ORIGINAL MATRIX A MUST BE REAL SYMMETRIC (STORAGE MODE=1)
 MATRIX A CANNOT BE IN THE SAME LOGICION AS MATRIX R

SUBROUTINES AND FUNCTION SUBPROGRAMS REQUIRED
 NONE

METHOD
 DIAGONALIZATION METHOD ORIGINATED BY JACOBI AND ADAPTED
 BY VON NEUMANN FOR LARGE COMPUTERS AS FOUND IN "MATHEMATICAL
 METHODS FOR DIGITAL COMPUTERS", EDITED BY A. RALSTON AND
 H.S. WILF, JOHN WILEY AND SONS, NEW YORK, 1962, CHAPTER 7

```

.....
SUBROUTINE EIGEN(A,RV)
  DOUBLE PRECISION A,R,J,ANORM,ANRMA,THR,X,Y,SENK,SINXZ,CCSX,
  1 COSXZ,SINCZ,RANGE,AAAA,EVAL
  COMMON/EQN/(A(225),U(225),R(225),EVAL(22),AAAA(12),MM10
  GENERATE IDENTITY MATRIX
  5 RANGE=1,CC=6
  IF(MV=1) 10,25,10
  10 IQ=M
  DD ZD J=I,M
  IQ=IQ+N
  DD ZD I=1,N
  I=IQ+1
  R(I,J)=0,C
  IF(I=J) 20,15,20
  15 R(I,J)=I,C
  20 CONTINUE
  COMPUTE INITIAL AND FINAL NORMS (ANDRM AND ANRMA)
EIGE 640
EIGE 650
EIGE 660
EIGE 680
EIGE 690
EIGE 700
EIGE 710
EIGE 720
EIGE 730
EIGE 740
EIGE 750
EIGE 760
EIGE 770
EIGE 780
EIGE 790

```

```

25 ANGRM=0.000
DO 35 I=1,N
DO 35 J=1,N
IF(I=J) 30,35,30
30 IA=1+(J-I)/2
ANGRM=ANGRM+IA)*A(IA)
35 CONTINUE
IF(ANGRM) 105,105,40
40 ANGRM=1.414*OSQRT(ANGRM)
ANRMX=ANGRM*ANWE/OFLCATEN
INITIALIZE INDICATORS AND COMPUTE THRESHOLD, THR
IN0=0
THR=ANGRM
45 THR=THR/OFLCATEN
50 L=1
55 M=L+1
COMPUTE SIN AND COS
60 M0=(M-N)/2
L0=(L-L)/2
L=L+M0
62 IF(OABS(A(L))>THR) 130,65,65
65 IN0=L
LL=L+L0
MM=M+M0
X0=5*PI*(L0)-(MM)
68 Y=-A(L)/OS CRT(A(L)*A(L)*X*X)
IF(X) 70,75,75
70 Y=Y
75 SINX=Y/OSQRT(1.0+(1.0+OSQRT(1.0+Y*Y)))
SINX2=SINX*SINX
78 COSX=OSQRT(1.0-SINX2)
COSX2=COSX*COSX
SINCX = SINX*COSX
ROTATE L AND M COLUMNS
ILO=M*(L-1)
IMO=M*(M-1)
DO 125 I=1,N
IO=(I-1)/2
IF(I=1) 80,115,80
80 IF(I=3) 85,115,90
85 IM=I+M0
GO TO 95
90 IM=M+IQ
95 IF(I=1) 100,105,105
100 IL=I+L0
GO TO 110
105 IL=L+I0
110 X=A(IL)*COSX-A(IM)*SINX
A(IM)=A(IL)*SINX+A(IM)*COSX
A(IL)=X
115 IF(MV=1) 120,125,120
120 ILR=IL+1
IMR=IM+1
X=A(ILR)*COSX-R(IMR)*SINR
R(IMR)=A(ILR)*SINR+A(IMR)*COSX
R(ILR)=X
125 CONTINUE
X=2.0*A(L0)*SINCX
Y=A(L0)*COSX2-A(M0)*SINX2-X
X=A(L0)*SINX2+A(M0)*COSX2+X
A(L0)=A(L0)-A(M0)/SINCX+A(L0)*COSX2-SINX2)
A(L0)=Y
A(M0)=X
TESTS FOR COMPLETION
TEST FOR M = LAST COLUMN
130 IF(M=N) 135,140,135
135 M=M+1
GO TO 80
TEST FOR L = SECCND FROM LAST COLUMN
140 IF(L=(M-1)) 145,150,145
145 L=L+1
GO TO 55
150 IF(IN0=1) 160,155,160

```

```

EIGL 800
EIGL 820
EIGL 830
EIGL 840
EIGL 850
EIGL 860
EIGL 870
EIGL 880
EIGL 910
EIGL 920
EIGL 930
EIGL 940
EIGL 950
EIGL 970
EIGL 980
EIGL 990
EIGL1000
EIGL110
EIGL120
EIGL130
EIGL140
EIGL160
EIGL170
EIGL180
EIGL190
EIGL200
EIGL210
EIGL220
EIGL230
EIGL240
EIGL250
EIGL260
EIGL270
EIGL280
EIGL290
EIGL300
EIGL310
EIGL320
EIGL330
EIGL340
EIGL350
EIGL360
EIGL370
EIGL380
EIGL390
EIGL400
EIGL410
EIGL420
EIGL430
EIGL440
EIGL450
EIGL460
EIGL470
EIGL480
EIGL490
EIGL500
EIGL510
EIGL520
EIGL530
EIGL540
EIGL550
EIGL560
EIGL570
EIGL580
EIGL590
EIGL600
EIGL610
EIGL620
EIGL630
EIGL640

```

155	IND=0	EIGEL690
	GD TO 50	EIGEL690
	COMPARE THRESHOLD WITH FINAL NORM	EIGEL690
160	IF(THR-ANMX) 165,165,45	EIGEL690
	SORT EIGENVALUES AND EIGENVECTORS	EIGEL710
165	IG=-N	EIGEL730
	DO 165 I=1,N	EIGEL740
	IQ=IG+N	EIGEL750
	LL=(I+I-1)/2	EIGEL760
	JQ=N*(I-2)	EIGEL770
	DO 185 J=1,N	EIGEL780
	JC=JQ+N	EIGEL790
	HR=J+(J-J)/2	EIGEL800
	IF(A(LL)-A(HR)) 170,185,185	EIGEL810
170	M=ALL	EIGEL820
	A(LL)=A(HR)	EIGEL830
	A(HR)=M	EIGEL840
	A(M)=M	EIGEL850
	A(MV-1) 175,185,175	EIGEL860
175	DO 180 K=L,N	EIGEL870
	ILR=IQ+K	EIGEL880
	IHR=JQ+K	EIGEL890
	X=R(ILR)	EIGEL900
	R(ILR)=R(IHR)	EIGEL910
180	R(IHR)=X	EIGEL920
185	CONTINUE	EIGEL930
	RETURN	EIGEL940
	END	EIGEL950

CC
CC

ANSBNS

PURPOSE: TO COMPUTE CAPTURE CROSS SECTIONS FOR PROCESSES OF THE FORM
B* + A(INS) -> B(N'S) + A*
OR THEIR TIME REVERSED COUNTERPARTS.

- CARD 1: NLG (1615)
NUMBER OF INTEGRATION POINTS FOR GAUSS-LAGUERRE QUADRATURE
- CARD 2: (EIKI)XK(I),I=1,NLG (142D,15)
ABSCISSAS AND WEIGHTING FACTORS FOR GAUSS-LAGUERRE QUADRATURE
- CARD 3: (LABLIT),I=1,20 (2DA4)
PROGRAM TITLE
- CARD 4: Z1, Z2, NMAX, PMO (BF10,5)
Z1: CHARGE OF THE TARGET
Z2: CHARGE OF THE PROJECTILE
NMAX: INTERNUCLEAR DISTANCE FOR WHICH REACTION BEGINS TO OCCUR
 (FOR A-NUC CAPTURE NMAX=30)
PMO: PMO=0 IF ENERGY IS IN KEV/AMU
 PMO: PMO= MASS OF THE PROJECTILE IF ENERGY IS IN KEV
- CARD 5: NCOOE, ICCOO, JCOOE, IPNCH, IAEQ, LIMIT, RM, IPNT1,
IPNT2, NITP, NDAB, NCAB, IEL (1615)
NCOOE: NCOOE=0 NON-ITERATIVE SOLUTION OF COUPLED EQUATIONS
 IF NCOOE=0 LIMIT, RM, IPNT1, IPNT2, NITP, NCAB, NCAB
 MUST NOT BE DEFINED
 NCOOE=1 ITERATIVE SOLUTION OF COUPLED EQUATIONS
ICOOE=1 IF INTEGRATION OVER IMPACT PARAMETERS IS PERFORMED
JCOOE=1 IF UA, UB, XAB, XBA ARE PRINTED
IPNCH=1 IF MATRIX ELEMENTS ARE PUNCHED
IAEQ=1 IF MATRIX ELEMENTS ARE READ IN
LIMIT: NUMBER OF ITERATIONS NEEDED
 FOR VY=V1/2,1,21 LIMIT=6+*3
RM: IOMN=1 IS THE NUMBER OF THE INTEGRATION POINTS
 USED IN THE ITERATIVE SOLUTION
IPNT1=1 FOR EVERY NITP INTERPOLATED MATRIX ELEMENTS
 TO BE PRINTED
IPNT2=1 FOR EVERY NDAB POINTS OF EVERY ITERATIVE SOLUTION
 TO BE PRINTED
NCAB: EVERY NCAB POINTS OF THE FINAL SOLUTION ARE PRINTED IF
 NCAB IS NOT DEFINED IT IS AUTOMATICALLY SET EQUAL TO 1
IEL=1 FOR A ONE ELECTRON TARGET
- CARD 6: NI, NEV, NAO, NA, NB, NT, NP (1615)
NI: NINI=1 IS THE NUMBER OF TIME INTEGRATION POINTS
NEV: NUMBER OF ENERGIES
NAO: NUMBER OF IMPACT PARAMETERS
NA (NB): IS THE PRINCIPAL QUANTUM NUMBER FOR THE
 INITIAL (FINAL) STATE AND NEED BE DEFINED ONLY
 IF A HYDROGENIC MODEL IS USED.
NT (NP): NT=1 (NP=1) IF A NON-HYDROGENIC MODEL IS USED FOR
 THE INITIAL (FINAL) STATE. IF NT=1 (NP=1) THE 4 CARDS
 FROM PROGRAM HERMAN CONTAINING THE INFORMATION
 FOR THE INITIAL (FINAL) STATE MUST FOLLOW CARD 8
 4 FOR THE FINAL STATE THE 4 CARDS FOLLOW EITHER
 CARD 9 OR CARD 10, WHICH EVER IS LAST.
- CARD 7: (EINPT(I),I=1,NEV) (3F10,5)
ENERGY POINTS IN KEV
- CARD 8: (ED(I),I=1,NAO) (BF10,5)
IMPACT PARAMETERS IN A.U.
IF NT=1 THE INITIAL STATE INFORMATION FOLLOWS
IF NP=1 THE FINAL STATE INFORMATION FOLLOWS

WRITTEN BY LAURA TUNNELL (1978)

CC
CC

```
IMPLICIT REAL*8 (A-H,C-I)
COMPLEX*16 S5,A11,A12,A21,A22,SBA(150)
COMPLEX*16 SAB,ASB,POA,C1,PRMP
COMMON/MATR2/SAB(150),HAB(150),HBA(150),HAB(150),HBB(150)
COMMON/IMPCT/V,PHI,PH,PI,P1,NT,NP,AN,NI
COMMON/EPL/ZZR(153),F1,F5(150),L1,L2
COMMON/IMPCT/E(20),E1+PT(10),PHI,NEV,LEV,IPB
,PRB(10,20),SRP(10,20),PPAP(10,20)
COMMON/LAGU/AL(25),M(10),PLQ
COMMON/PTITL/DLNR(3),CV(53),AZ,ZZ
COMMON/FA/BALP,ZA,ACCFE(10),AFP(10),NKA(10),NA
```

```

COMMON/FB/ESTA,ZS,CCDEF(10),BXP(10),NXP(10),NB
COMMON/OPTN/LIMIT,M,IPNCH,IREG,IPN1,IPN2,NITP,NOAB,NCAB
DIMENSION LABEL(20),XXX(25),YYY(25),SGMA(10),Y(4)
100 FORMAT(14I5)
200 FORMAT(BF10,3)
300 FORMAT(20A)
400 FORMAT('1',///25X,20A4///)
249 FORMAT('E0,15)
3  FORMAT(10I1X,1P012,5)
   C1=CCP(LX10,000,1,000)
   PF1=1,000
   AZ=0,000
   BZ=0,000

   READ(5,100) NLG
   READ(5,249) (X(IX),HX(IX),IX=1,NLG)
   READ(5,300) LABDL(1),I=1,20)
   READ(5,200) Z1,Z2,RMAX,PHB
   IF(RMAX.EQ.0.000) RMAX=0,000
   IF(PHB.EQ.0.000) PHB=1,000
   READ(5,100) NCODE,ICODE,JCODE,IPNCH,IREG,
   *LIMIT,M,IPN1,IPN2,NITP,NOAB,NCAB,IEL
   IF(IEL.NE.0) PF1=0,000
   IF(NCAB.EQ.0) NCAB=5
   IF(NCAB.EQ.0) NCAB=5
   IF(NITP.EQ.0) NITP=3
   READ(5,100) NI,NEV,NRO,NA,NB,NT,NP,IFILE
   READ(5,200) (EIHPT(I),I=1,NEV)
   READ(5,200) I (SII),I=1,NRO)
   IF(NA.EQ.0) NA=1
   IF(NB.EQ.0) NB=1
   PRINT 411

411 FORMAT(' NLG, (X(IX),HX(IX),IX=1,NLG) ')
   PRINT 100, NLG
   PRINT 3, (X(IX),HX(IX),IX=1,NLG)
   PRINT 414

414 FORMAT(' Z1,Z2,RMAX,PHB ')
   PRINT 200, Z1,Z2,RMAX,PHB
   PRINT 413

413 FORMAT(' NCODE,ICODE,JCODE,IPNCH,IREG,
   *LIMIT,M,IPN1,IPN2,NITP,NOAB,NCAB ')
   PRINT 100, NCODE,ICODE,JCODE,IPNCH,IREG,
   *LIMIT,M,IPN1,IPN2,NITP,NOAB,NCAB
   PRINT 415

415 FORMAT(' NI,NEV,NRO,NA,NB,NT,NP,IFILE ')
   PRINT 100, NI,NEV,NRO,NA,NB,NT,NP,IFILE
   PRINT 416

416 FORMAT(' (EIHPT(I),I=1,NEV) ')
   PRINT 200, (EIHPT(I),I=1,NEV)
   PRINT 417

417 FORMAT(' (SII),I=1,NRC ')
   PRINT 200, (SII),I=1,NRC)
   FNA=DFLCAT(NA)
   FNB=DFLCAT(NB)
   SALP=Z1-Z2/FNA/FNA/2,000
   ESTA=Z2*Z2/FNB/FNB/2,000
   ACDEF(1)=1,000
   SCDEF(1)=1,000
   ACDEF(2)=-SQRT(3,000)
   SCDEF(2)=-SQRT(3,000)
   ACDEF(3)=SQRT(4,5000)
   SCDEF(3)=SQRT(2,5000)
   DO 20 I=1,3
   NNA(I)=1
   NNB(I)=1
   AXPI(I)=Z1/FNA
   BXP(I)=Z2/FNB
   OLVN(I)=0,000
   DO 20 J=1,3
20  CV(I,J)=0,000
   IF(IAT.EQ.0) GO TO 22
   READ(5,200) SALP,FA,OLVN(Z1,(CV(I,2),I=1,3),AZ
   NA=FA
   READ(5,100) (NNA(I),I=1,NA)
   READ(5,200) (AXP(I),I=1,NA)
   READ(5,200) (ACDEF(I),I=1,NA)
22  CONTINUE
   IF(NP.EQ.0) GO TO 24
   READ(5,200) ESTA,FB,OLVN(Z2,(CV(I,3),I=1,3),BZ
   NB=FB
   READ(5,100) (NNB(I),I=1,NB)
   READ(5,200) (BXP(I),I=1,NB)
   READ(5,200) (SCDEF(I),I=1,NB)
24  CONTINUE
   AZ=AZ+1,000

```

```

B2=81+.000
FA=QFLOAINAI
FB=QFLOATENB
PRINT 423
423 FORMAT(' EALP,NA,QLMV(2),(CV(1,2),I=1,3) ')
PRINT 200, EALP,FA,QLMV(2),(CV(1,2),I=1,3)
PRINT 425
425 FORMAT(' INXA(I),I=1,NA) ')
PRINT 100, INXA(I),I=1,NA)
PRINT 419
419 FORMAT(' (AXP(I),I=1,NA) ')
PRINT 200, (AAP(I),I=1,NA)
PRINT 421
421 FORMAT(' (ACDEF(I),I=1,NA) ')
PRINT 200, (ACDEF(I),I=1,NA)
PRINT 424
424 FORMAT(' EDTA,NB,QLMV(3),(CV(1,3),I=1,3) ')
PRINT 200, EDTA,FB,QLMV(3),(CV(1,3),I=1,3)
PRINT 418
418 FORMAT(' INXB(I),I=1,NB) ')
PRINT 100, INXB(I),I=1,NB)
PRINT 420
420 FORMAT(' (BXP(I),I=1,NB) ')
PRINT 200, (BXP(I),I=1,NB)
PRINT 422
422 FORMAT(' (BCDEF(I),I=1,NB) ')
PRINT 200, (BCDEF(I),I=1,NB)

PI=3.141592653589793238462643383279502884197169399375105820974944597408
TAP1=2.000*PI*(1.5290-08)**2
ZA=21
ZB=22
ZC=23
IF(ZB.LT.ZA) ZC=ZB
ZI=22
EALP=EALP/ZI/ZI
ESTA=ETA/ZI/ZI
NNT=3*NI
NNT1=NNT+1
NT=2*NNT+1
OD 1000 LEV=1,NEV
EKEV=EIMPT(LEV)
V=DSQRT(EKEV/F40)/5.000
SETUP TIME VECTOR
TIME(NT)=0.0
IF(NE.EQ.0) GO TO 1005
TIME(NT)=RMAX/IZC-201/V
NT=TIME(NT)/7.000/QFLCAT(NI)
DO 10 J=1,3
J1=J-11*NI
DO 12 I=1,NI
J11=1
IF(I.GT.1) J11=(I2**J-1)
TIME(NT1+J1+1)=TIME(NT1+J1+J11*NT
12 CONTINUE
10 CONTINUE
DO 14 I=1,NNT
TIME(NT1-I)=-TIME(NNT-I)
14 CONTINUE
1005 CONTINUE
DO 1001 IPB=1,NRO
RND=811*PI
R(NT1)=R*0
IF(NE.EQ.0) GO TO 1006
DO 15 I=1,NNT
R(NT1+I)=DSQR(RND*RND+V*V*TIME(NT1+I)*TIME(NT1+I)
R(NT1-I)=R(NT1+I)
15 CONTINUE
IF(IREQ.EQ.1) GO TO 50
1006 CONTINUE
CALL CMATX
DO TO 60
CONTINUE
50 DO 51 I=1,NNT1
READ(5,52) TIME(I),HAI(I),HBI(I)
READ(5,52) SABI(I),HBI(I),HBA(I)
52 FORMAT(6 (IPD12.53))
51 CONTINUE
60 CONTINUE
IF(IPNC=NE-1) GO TO 61
DO 62 I=1,NNT1
PUNCH 52, TIME(I),HAI(I),HBI(I)
62 PUNCH 52, SABI(I),HBI(I),HBA(I)

```



```

81 CONTINUE
DO 55 I=1,NNT1
I1=NT-I-1
TIME(I)=TIME(I1)*2*Z2
TIME(I1)=TIME(I)
R(I)=R(I1)*Z
R(I1)=R(I)
SAB(I1)=DCNJG(SAB(I))
HBA(I1)=DCNJG(HBA(I))
HSA(I1)=DCNJG(HSA(I))
HAA(I1)=HAA(I)
HBB(I1)=HBB(I)
55 CONTINUE
EKEV=EKEV/Z2/Z2
V=V/Z2
RHO=RHO*Z2
VR=DSQRT(EKEV/EALP/PM5/27.21060-03/1836.0)
PRINT 40,ELASB(I),I=1,Z0)
PRINT 41
91 FORMAT(' TIME...R SAB...HAB...HBA HAA...HBB '/')
DO 92 IT=1,NNT1
92 PRINT 93, TIME(IT),R(IT),SAB(IT),HAB(IT),HBA(IT),HAA(IT),HBB(IT)
93 FORMAT(21X,F10.51,5X,3(IPO11,4,1X,IPO11,4,2X),3X,2(IPO11,4,1X))
PRINT 94, Z2,EKEV,V,VR,RHO
94 FORMAT('/', SCALING FACTOR =',F6.2,' SCALING QUANTITIES ) E(KEV)=',
,IPO11,4,1X,V',IPO2,2,' V(VK =',IPO2,2,' RHO =',IPO2,2//)
IF(NGCODE.EQ.1) CALL COUPEQ(NT)
IF(NGCODE.NE.0) GO TO 96
PRINT 97
97 FORMAT('1',///' TIME...R CA...CB...PRCB...UNIT '/')
Y(1)=1.000
Y(2)=0.000
Y(3)=0.300
Y(4)=0.300
CALL DIFDCI(TIME(I),(TIME(I)+TIME(I2))/2.00C,Y,0.2000,4,1.0=)
DO 90 IT=2,NT
CALL DCI(TIME(I),TIME(I2),Y,HR,4,1.0=6)
PRDB=Y(1)*Y(3)+Y(4)*Y(4)
UNIT=PRDB*Y(1)*Y(1)+Y(2)*Y(2)+1.000
UNIT=UNIT*2.000/SAB(IT)*DCPLX(Y(1),-Y(2))/DCPLX(Y(3),Y(4))
/DCI(TIME(I),TIME(I2),E,C,STAI)
90 PRINT 98, TIME(IT),R(IT),(Y(I),I=1,4),PRDB,UNIT
98 FORMAT(21X,F10.51,6X,2(IPO10,3,1X,IPO10,3,2X),2X,2(IPO10,3,1X))
PRB(LEV,IPB)=PRDB
SRPB(LEV,IPB)=SRPB(LEV,IPB)
PRMP(LEV,IPB)=DCPLX(Y(3),Y(4))
PRINT 99, PRB(LEV,IPB),SRPB(LEV,IPB),I(MPT(LEV),E(I,IPB)
99 FORMAT('/', PRB =',IPO2,2,' PRDB A RHC =',IPO2,2,' AT E(KEV) =',
,F10.2,' RHO =',F6.2//)
96 CONTINUE
IF(JCODE.EQ.0) GO TO 83
PRINT 81
81 FORMAT('1',///' TIME.....R A11.....A12.....A21.....A22')
DO 82 I=1,NNT1,NT
SBA(I1)=DCNJG(SAB(I))
SS=1.000-SAB(I1)*SBA(I1)
A11=(HAB(I1)-SAB(I1)*HBA(I1))/SS
A12=(HAB(I1)-SAB(I1)*HBA(I1))/SS
A21=(HBA(I1)-SBA(I1)*HBA(I1))/SS
A22=(HBA(I1)-SBA(I1)*HBA(I1))/SS
PRINT 3, TIME(I),R(I),A11,A12,A21,A22
82 CONTINUE
83 CONTINUE
EKEV=EKEV*2*Z2
V=V*Z2
RHO=RHO/Z2
DO 56 I=1,NNT1
I1=NT-I-1
TIME(I)=TIME(I1)/Z2/Z2
TIME(I1)=TIME(I)
R(I1)=R(I)/Z2
R(I)=R(I)
56 CONTINUE
1001 CONTINUE
IF(JCODE.EQ.0) GO TO 1000
DO 85 I=1,NAD
XXX(I)=EBC(I)
DFZ(I)=DO=PMI*PRB(LEV,I)
85 Y(I)=SAB(LEV,I)*P2
CALL AREA(XXX,YYY,NRC,AAA)
SGNA(LEV)=TDCPI*AAA
1000 CONTINUE
101 FORMAT(10X,I6I5)
201 FORMAT(10X,8F13.5)
333 FORMAT(10X,9I1X,IPO(2,5))

```

```

DO 402 I,J=1,4
PRINT 301, (LABEL(I), I=1,20), IFILE
PRINT 411
PRINT 101, NLG
PRINT 333, (X(I),X(X(I)), I=1,NLG)
PRINT 414
PRINT 201, ZA,ZB,AMAX,PHB
PRINT 413
PRINT 101, NCODE,ICODE,JCCOE,IPNCH,IREO,
+LIMIT,MM,IPNT1,IPNT2,NITP,NGAU,NCAS
PRINT 415
PRINT 101, NI,NEV,NRO,NA,NB,NT,NP,(FILE
PRINT 416
PRINT 201, (EIMPT(I), I=1,NEV)
PRINT 417
PRINT 201, (EBI(I), I=1,NRC)
301 FORMAT(' ',10X,20A9,' FILE NO. ',I6)
PRINT 401, (LABEL(I), I=1,20)
401 FORMAT(' ',///25X,20A4///)
DO 1000 LEV=1,NEV
PRINT 1001
1001 FORMAT:10X,' RND PROS.AMP....PROB....PROB X RHO'///
DO 10002 IPB=1,NRO
10002 PRINT 10003, EB(IPB),PRMP(LEV,IPB),PRBI(LEV,IPB),BRPS(LEV,IPB)
10003 FORMAT(10X,F10.5,X2(1P011.4,1X),2(2X,1P011.4)
PRINT 10004, SGMA(LEV),EIMPT(LEV)
10004 FORMAT(1/20X,' TOTAL CROSS SECTION/ELECTRONIC**2) ',I09.2,
' AT E(KEV) =',DPP12.5///)
10000 CONTINUE
402 CONTINUE
STOP
END
SUBROUTINE CMATRX
IMPLICIT REAL*(A-H,O-Z)
COMPLEX*16 C,C1,C2,C3,COSX,TSINX
COMPLEX*16 SABI,MABI,MBAI, SABI,MBAI,MBAI, SABI,MBAI,MBAI, SABI,MBAI,MBAI
COMPLEX*16 SABI,MBAI,MBAI, SABI,MBAI,MBAI, SABI,MBAI,MBAI
COMPLEX*16 SABI,MBAI,MBAI, SABI,MBAI,MBAI, SABI,MBAI,MBAI
COMPLEX*16 SABI,MBAI,MBAI, SABI,MBAI,MBAI, SABI,MBAI,MBAI
COMMON/IMPCT1/V,RHO,RN,T1,PE,NT,NNT,NNT1
COMMON/IMPCT2/R1(150),T1HE(150),Z1,Z2
COMMON/IMPCT3/EI(20),EIMPT(10),NRO,NEV,LEV,IPB
COMMON/MATRX/SABI(150),MABI(150),MBAI(150),HAA(150),HAB(150),HBI(150)
COMMON/LAGU/XX(32),XXI(32),NAG
COMMON/PNTL/OLY(43),CV(3,3),AZ,BZ,Z13
COMMON/HFA/EALP,ZA,ACDFP(10),AXP(10),NKA(10),NA
COMMON/HFB/EFTA,ZB,OCDFP(10),BXP(10),NKB(10),NB
COMMON/CNST/A(13,15),DP(20),DG(20)
DIMENSION VV(5,3),P(3),DPCS(3),DNEG(3),CLP(3),OPX(3),MH(3)

NAI=NXA*(NA)+1
NBI=NXB*(NB)+1
NMX=NAI+NB1
NRO=NRO+3
C=OC*PLX(0.000,0.000)
C1=OC*PLX(0.000,1.000)
C2=OC*PLX(1.000,0.000)
PL(1)=CR
GMA2=V*MG/Z.000
P(1)=0.000
P(2)=1.000
P(3)=1.000
Z(1)=0.000
Z(2)=ZA-AZ
Z(3)=ZB-BZ
OLYV(1)=0.000
DO I=1,3
14 CV(I,1)=0.000
IF(IPB,GT,1) GO TO 499
IF(LEV,GT,1) GO TO 499

OP(1)=0.000
OP(2)=1.000
OG(1)=1.000
OG(2)=1.000
DO IS=1,19
OP(1+IS)=OP(1+IS)+1.000
15 OG(1+IS)=OG(1+IS)+OG(1)
DO I=1,NA
NI=2*NXA(I)+1
AI=(2.000*AXP(I))+NI/OG(1)
16 ACDFP(I)=ACDFP(I)*NSQRT(DABS(AI))
DO J=1,NB

```

```

NJ=2*NR2/JJ+1
S1=(2.000*BXP(J))*NJ/DG(NJ)
17 RCDEF(J)=BCDEF(J)*DSQR(1/DABS(B1))

A(L,1)=1.000
A(2,2)=1.000/3.000
DO 20 K=2,NM,2
AK=DF(K+1)
A(K+1,1)=1.000/(AK+1.000)
KX=K+1
AKK=DF(KK+1)
A(KK+1,2)=1.000/(AKK+2.000)
DO 20 L=2,KK,2
AL=DF(L+1)
A(K+1,L+1)=(2.000+AK-AL)*A(K+1,L-1)/(1.000+AK+AL)
LL=L+1
ALL=DF(LL+1)
A(KK+1,LL+1)=(2.000+AKK-ALL)*A(KK+1,LL-1)/(1.000+AKK+ALL)
20 CONTINUE

```

```

499 CONTINUE
DO 500 I=1,NNT1
GMAI=Y*V*TIME(I)/Z.000
RZ=R1/I/I/Z.000
SAB1=C
HAB1=C
HMA1=C
DO 510 I=1,NA
NP=NXA(I)+1
SABJ=C
HABJ=C
HMAJ=C
DO 520 J=1,NB
NM=NXS(J)+1
NMM=N*PC+1
OPDS1=(A*P(I))+BXP(J)*RZ
ONEG1=(A*P(I))-BXP(J)*RZ
SABX=C
HABX=C
HMAX=C
DO 530 IX=1,NLS
DO 9 M=1,3
DPOS(M)=OPDS1+DLV(M)*RZ
DNEG(M)=ONEG1+DLV(M)*RZ*P(M)
DLN(M)=1.000+XX(I)/OPDS1(M)
DX=0.000
IF(DPOS(M),LT,1.30+GZ) DX=DEXP(-DPOS(M))
DPE(M)=DX/OPDS1(M)
ON=0.000
IF(DABS(DNEG(M)),LT,1.30+GZ) ON=DNEG(M)
TGS=DC*PLX(GMAI)*GLN(M),CNZ
TSLN=DC*PLX(DSQR(TOLN1))*GLN(M-1.000)*GRAZ,0.000)
RD=RZ*DLN(M)
ZZ=Z(M)
YV(2,M)=ZZ*(1.000+RD*(C*(1,M)+RD*(C*(2,M)+RD*(C*(3,M)+1))
YV(3,M)=P(M)*Z*(C*(1,M)+RD*(2.000*(C*(2,M)+RD*(3.000*(C*(3,M)+1))
YV(4,M)=Z*(RZ*(C*(1,M)+RD*(3.000*(C*(3,M)+1))
YV(5,M)=PE(M)*Z*(RZ*(C*(1,M)+RD*(3.000*(C*(3,M)+1))
IF(N,GT,1).AND.(DLV(M),LT,1.00-08)) GO TO 91
T=CDSCR(TS1+NK*TS2+NK*TCOSX)
X=TCOSX/T
JL(1)=COSR(1)/T
JL(2)=JL(1)-COSC(1)/T
PL(2)=X
PL(M,1)=M(1,1)*JL(1)*PL(1)
PL(M,2)=M(2,2)*JL(2)*PL(2)*3.000*C1
DO 10 N=2,NM,2
FAN=DF(N+1)
JL(N+1)=(2.000*FN-1.000)*JL(N)/T-JL(N-1)
PL(N+1)=(2.000*FN-1.000)*PL(N)-FN-1.000)*PL(N-1)/FN
PL(N,N+1)=A(N+1,1)*JL(1)*PL(1)
NN=N+1
FNN=DF(N+1)
JL(NN+1)=(2.000*FNN-1.000)*JL(NN)/T-JL(NN-1)
PL(NN+1)=(2.000*FNN-1.000)*PL(NN)-FNN-1.000)*PL(NN-1)/FNN
PL(N,N+1)*C1*3.000*(N+1,2)*JL(2)*PL(2)
DO 10 L=2,NN,2
AL=DF(L+1)
PL(N,N+1)=PL(N,N+1)+(2.000*AL+1.000)
* A(N+1,L+1)*JL(L+1)*PL(L+1)
LL=L+1
ALL=DF(LL+1)
PL(N,N+1)=PL(N,N+1)+C1*(2.000*ALL+1.000)

```

```

*      *(N+1,LL+1)*JL(LL+1)*PL(LL+1)
10 CONTINUE
DO TO 9
91 CONTINUE
NL=NX+1
DO 92 N=1,NL
92 FL(N,N)=FL(1,N)
9 CONTINUE
100 CONTINUE

NX=NP+NC-2
DO 35 K=1,NX
DO 36 L=1,NX
GSAB(K,L)=DPX(1)*FL(1,L)
GHAB(K,L)=A2*GSAB(K,L)+DPX(2)*(VV(2,2)*FLM(2,L)+VV(3,2)*FLM(2,L+1)
+VV(4,2)*FLN(2,L+2)+VV(5,2)*FLM(2,L+3))
* GHAB(K,L)=B2*GSAB(K,L)+DPX(3)*(VV(2,3)*FLM(3,L)+VV(3,3)*FLM(3,L+1)
+VV(4,3)*FLN(3,L+2)+VV(5,3)*FLM(3,L+3))
36 CONTINUE
GSAB(K,NX+1)=DPX(1)*FL(1,NX+1)
DO 37 L=1,3
37 DPX(L)=DLM(L)*DPX(L)
35 CONTINUE
NX=NX+1
DO 38 L=1,NX
38 GSAB(NX,L)=DPX(1)*FL(1,L)

SABP=C
HABP=C
HSABP=C
DO 540 IP=1,NP
SABQ=C
HABQ=C
HSABQ=C
CI=1.000
DO 550 IC=1,NQ
NI=NXA(1)+NXB(J)-IP-1Q
N2=IP+1Q
CCQ=OG(NC)/OG(IQ)/OG(NQ-1Q+1)*CI
SABQ=SABQ*GSAI(1)+2I+(1Q-2I+1)*CCQ
IF(NI.EQ.-2) GO TO 551
HABQ=HABQ*GHAB((NI+1)+1,(N2-2I+1)*CCQ
HBAQ=HBAQ*GHAH((NI+1)+1,(N2-2I+1)*CCQ*(OF(NQ)-OF(IQ))/OF(NP))
551 CONTINUE
550 QI=QI
CCP=OG(NP)/OG(1P)/OG(NP-1P+1)
SABP=SABP*SABQ*CCP
HABP=HABP*HABQ*CCP*(OF(NP)-OF(1P))/OF(NP)
HSABP=HSABP*HSABQ*CCP
540 CONTINUE
SABX=SABX+SABP*NX(IX)
HABX=HABX+HABP*HX(IX)
HBAJ=HBAJ+HBAJ*NX(IX)
530 CONTINUE
CCJ=BCDF(IJ)*CRJ*(HXA(1)+NXB(J))
SABJ=SABJ+SABX*CCJ
HABJ=HABJ+HABX*CCJ
HSAJ=HBAJ+HBAJ*CCJ
520 CONTINUE
CCI=ACDEF(IJ)
SABI=SABI+SABJ*CCI
HABI=HABI+HABJ*CCI
HSAI=HBAI+HSAJ*CCI
510 CONTINUE
SAB(IT)=SABI*E2
HAB(IT)=HABI/E2/E2
HSA(IT)=DCONJ(I-HSAI)/E2/E2
500 CONTINUE

CALL DIAGACDEF,AXP,NXA,NA,3,HAA)
CALL DIAGBCDEF,AXP,NXB,NB,2,HBB)

RETURN
END

SUBROUTINE DIAGICDEF,AXP,NXC,NC,NV,HH)
IMPLICIT REAL*8(A-H,C-Z)
COMMON/IRCF1/V,ANG,RR,T1,P1,NT,NVE,INT1
COMMON/IRCF2/R1(150),TIME(150),Z1,Z2
COMMON/PTNTL/OL TV(3),VC(3,3),A2+G,2(3)

```

```

COMMON/CNST/MI(15,15),OF(20),GG(20)
DIMENSION CUBF(1),CYP(1),MKC(1)
DIMENSION F(20),FF(20),G(20),GG(20)
DIMENSION CV(3),MH(150)

C=0.000
ZZ1=8Z
IF(IV.EQ.2) ZZ1=AZ
ZZ2=Z(NV)
OLH=OLHV(INV)
CV(1)=VC(1,NV)
CV(2)=VC(2,NV)
CV(3)=VC(3,NV)
DO 100 IT=1,NMT1
RZ=RL(IT)/Z.000
NI=C
DO 200 I=1,NC
MJ=C
NI=MKC(I)
MI=MI+1
DO 300 J=1,NC
MPC
NJ=MKC(J)
MH=MH+J
NM3=NM3+J+1
A=(CXP(I)+CXP(J))*RZ
B=A
AA=A+OLH*RZ
BB=B-OLH*RZ
GX=C
GGX=C
FFX=C
IF(12.000*B).LE.1.200+0Z) GX=DEXP(-2.000*B)
IF(12.000*B).LE.1.200+0Z) GXA=DEXP(-2.000*BB)
IF(BB-AA).LE.1.00+0Z) FFX=DEXP(BB-AA)
F(I)=1.000/A
FF(I)=F/AA
G(I)=(1.000-GX)/B
GG(I)=(1.000-GGX)/BB
GM=-1.000
NM3=NM3+2
DO 13 K=2,NM3
FK(K)=(OF(K)*FK(I)+1.000)/A
FF(K)=(OF(K)+FK(I)+FF(I))/A
GK(K)=(OF(K)*G(K)+1+GM)/B
GG(K)=(OF(K)*GG(K)+1+GM-GGX)/BB
13 GM=GM
DO 400 IP=1,NII
HQ=C
DO 500 IQ=1,NJ
MH=MH+2-IP+IQ
MH=IP+IQ-1
QO=FF(I)*GG(I)
Q1=CV(1)*FF(I+1)*GG(I)-FF(I)*GG(I+1)
Q2=CV(2)*FF(I+2)*GG(I)-2.000*FF(I+1)*G(I+1)+FF(I)*GG(I+2)
Q3=CV(3)*FF(I+3)*GG(I)-3.000*FF(I+2)*GG(I+1)
-Q3=FF(I+1)*GG(I+2)+FF(I)*GG(I+3)
Q=ZZ1*F(I)*G(I)+ZZ2*(Q+Q2+Q3+Q3)
CO=GG(I)/OSI(I)/OSIN(I-10+1)
HQ=HQ+Q*CO
500 CONTINUE
CP=GG(I)/GG(I)/GG(I)-IP+2)
MH=MH+HQ*CP
400 CONTINUE
CJ=CDEF(I)+RZ*MM)
MH=MH+M*CMJ
300 CONTINUE
CI=CDEF(I)
MI=MI+M*CI
200 CONTINUE
MH(IT)=-P/2.000/Z/Z
100 CONTINUE

RETURN
END

SUBROUTINE AFEA(X,Y,N,AA)
IMPLICIT REAL*8 (A-H,O-Z)
DIMENSION X(25),Y(25)
INDEX=0
AA=0.
NM=N+1
Y(NM)=0.
X(NM)=2*X(N)-X(N-1)
X1=0.

```

```

Y1=0.
I=0
70 CONTINUE
X2=X1(I+1)
Y2=Y1(I+1)
X3=X1(I+2)
Y3=Y1(I+2)
O1=(Y1-Y2)/(X1-X2)
O2=(Y2-Y3)/(X2-X3)
A=(O1-O2)/(X1-X3)
B=O1-A*(X1+X2)
C=Y1-A*X1+B*X1
IF(INDEX(.NE.,O)) X1=X2
A=AA+A*(X3**3-X1**3)/3+B*(X3*X3-X1*X1)/2+C*(X3-X1)
IF(I+2).GE.NN) RETURN
X1=X3
Y1=Y3
I=I+2
IF(I+2).GT.NN) GO TO 80
GO TO 70
80 I=1
X1=X2
Y1=Y2
INDEX=.1
GO TO 70
END
SUBROUTINE DERIV,Y,YP1
IMPLICIT REAL*8 (A-H,O-Z)
COMPLEX*16 SS,A,B,ACCT,BDOT,ENT,CHI
COMPLEX*16 S12,S21,H12,H21,SAB,SBA,HAB,HBA
COMMON/MATRX/S12(150),H12(150),H21(150),H11(150),H22(150)
COMMON/IMPCT/V,ABC,RM,TZ,P1,NT,NHT,NNT1
COMMON/HFA/EALP,ZA
COMMON/HFB/ESTA,ZB
COMMON/IMPCT2/R(150),TIME(150)
DIMENSION Z(150),ARG( 5),VAL( 5),Y(4),YP(4)
CHI=OCMPLEX(0.000,-1.000)
DO 301 I=1,NT
301 Z(I)=S12(I)
CALL DATSMI T,TIME,Z,NT,1,ARG,VAL,5)
CALL DALIT,ARG,VAL,Z1,5,1.E-5,IER)
DO 302 I=1,NT
302 Z(I)=S12(I)*CHI
CALL DATSMI T,TIME,Z,NT,1,ARG,VAL,5)
CALL DALIT,ARG,VAL,Z2,5,1.E-5,IER)
SAB=OCMPLEX(Z1,Z2)
DO 303 I=1,NT
303 Z(I)=H12(I)
CALL DATSMI T,TIME,Z,NT,1,ARG,VAL,5)
CALL DALIT,ARG,VAL,Z1,5,1.E-5,IER)
DO 304 I=1,NT
304 Z(I)=H12(I)*CHI
CALL DATSMI T,TIME,Z,NT,1,ARG,VAL,5)
CALL DALIT,ARG,VAL,Z2,5,1.E-5,IER)
HAB=OCMPLEX(Z1,Z2)
DO 305 I=1,NT
305 Z(I)=H21(I)
CALL DATSMI T,TIME,Z,NT,1,ARG,VAL,5)
CALL DALIT,ARG,VAL,Z1,5,1.E-5,IER)
DO 306 I=1,NT
306 Z(I)=H21(I)*CHI
CALL DATSMI T,TIME,Z,NT,1,ARG,VAL,5)
CALL DALIT,ARG,VAL,Z2,5,1.E-5,IER)
HBA=OCMPLEX(Z1,Z2)
DO 307 I=1,NT
307 Z(I)=H11(I)
CALL DATSMI T,TIME,Z,NT,1,ARG,VAL,5)
CALL DALIT,ARG,VAL,Z1,5,1.E-5,IER)
HAA=Z1
DO 308 I=1,NT
308 Z(I)=H22(I)
CALL DATSMI T,TIME,Z,NT,1,ARG,VAL,5)
CALL DALIT,ARG,VAL,Z2,5,1.E-5,IER)
HBB=Z2
SBA=OCNJG(SAB)
ENT=OCMPLEX(0.000,T*(ESTA-EALP))
SS=(1.000-SAB*SBA)*0.000(1.000)
SP=1.000/SS
A=OCMPLEX(Y(1),Y(2))
B=OCMPLEX(Y(3),Y(4))
ADDT=SS*(A*(HAA-SAB*HBA)+B*(HBB-SAB*HBB))*CDEXPI(ENT)
BDOT=SS*(A*(HBB-SBA*HAB)+B*(HBA-SBA*HAA))*CDEXPI(-ENT)
YP(1)=ADCT
YP(2)=ADCT*CHI

```

```

YPI3)=BOOT
YPI4)=DCC1*CHI
RETURN
END
SUBROUTINE COUPEQIN)
IMPLICIT REAL*8 (A-H,O-Z)
COMPLEX*16 GG,SUM,A,3,ENT,U,CHI,PRHP
COMPLEX*16 XAB(600),XBA(600)
COMPLEX*16 DAI(600),DBI(600),DELTA(600)
COMPLEX*16 SL2,Z1,Z1,Z1,Z1,Z1
COMPLEX*16 SBA(600),SBA(600),HAB(600),HBA(600)
COMPLEX*16 ALP(600),BTA(600),AA(600),BB(600),CA(600),CB(600)
COMPLEX*16 Y1,Y2,Y3
COMMON/MATXS/5,2(1:50),H12(1:50),H21(1:50),H11(1:50),H22(1:50)
COMMON/OPTV/LNIT,MM,IPNCH,IRED,IPNT1,IPNT2,NITP,NDAB,HCAB
DIMENSION A(1:600),B(1:600)
DIMENSION A(1:50),VAL(1:50),TIME(600),R(600),Z(1:50)
COMMON/IMPCT1/V,RHD
COMMON/IMPCT2/RA(1:50),T(1:50)
COMMON/IMPCT3/E(1:20),EIMPT(1:10),NAC,NEV,LEV,IPB
,P(1:10,20),B(1:10,20),P(1:10,20)
COMMON/WFA/EALP,ZA
COMMON/WFB/EBA,ZB

CHI=DCPLX(0.000,-1.000)
SET UP TIME VECTOR
T1=T(1)
H=16.000*TI/(51.000*MM)
K=0
H=H+1
92 CONTINUE
DO 91 I=1,MM
91 TIME(K*MM)=T1+(I-1)*H
K=K+1
IF(K-GT.4) GO TO 93
T1=TIME(K*MM+1)
H=H/2.000
GO TO 92
93 CONTINUE
NNT=5*MM
NNT1=NNT+1
NT=2*NNT+1
DO 98 I=1,NNT1
I1=NT-I-1
TIME(I1)=TIME(I)
R(I1)=SQRT(SINC**2+(V*TIME(I1))**2)
R(I1)=R(I1)
98 CONTINUE
EKEV=25*V*V

DO 500 K=1,NNT1
DO 301 I=1,N
301 Z(I)=SL2(I)*CHI
CALL DATSM(TIME(K),T,Z,N,1,ARG,VAL,5)
CALL DAL I (TIME(K),ARG,VAL,Z1,S,1,E=5,IER)
DO 302 I=1,N
302 Z(I)=SL2(I)*CHI
CALL DATSM(TIME(K),T,Z,N,1,ARG,VAL,5)
CALL DAL I (TIME(K),ARG,VAL,Z2,S,1,E=5,IER)
SAB(K)=DCPLX(Z1,Z2)
DO 303 I=1,N
303 Z(I)=H12(I)
CALL DATSM(TIME(K),T,Z,N,1,ARG,VAL,5)
CALL DAL I (TIME(K),ARG,VAL,Z1,S,1,E=5,IER)
DO 304 I=1,N
304 Z(I)=H12(I)*CHI
CALL DATSM(TIME(K),T,Z,N,1,ARG,VAL,5)
CALL DAL I (TIME(K),ARG,VAL,Z2,S,1,E=5,IER)
HAB(K)=DCPLX(Z1,Z2)
DO 305 I=1,N
305 Z(I)=H21(I)
CALL DATSM(TIME(K),T,Z,N,1,ARG,VAL,5)
CALL DAL I (TIME(K),ARG,VAL,Z1,S,1,E=5,IER)
DO 306 I=1,N
306 Z(I)=H21(I)*CHI
CALL DATSM(TIME(K),T,Z,N,1,ARG,VAL,5)
CALL DAL I (TIME(K),ARG,VAL,Z2,S,1,E=5,IER)
HBA(K)=DCPLX(Z1,Z2)
DO 307 I=1,N
307 Z(I)=H11(I)
CALL DATSM(TIME(K),T,Z,N,1,ARG,VAL,5)
CALL DAL I (TIME(K),ARG,VAL,Z1,S,1,E=5,IER)
HAA(K)=Z1
DO 308 I=1,N

```

```

308 I(1)=H2(I)
CALL DATSH(TIME(K),T,2,N,1,ARG,VAL,5)
CALL DAL1(TIME(K),ARG,VAL,2,5,1,E=5,IER)
HDB(K)=Z2
500 CONTINUE

IF(IPNT1.EQ.0) GO TO 11
PRINT 520
520 FCRMAT(' ',///'SOX','INTERPOLATED MATRIX ELEMENTS'///)
PRINT 521
521 FORMAT(' TIME...R SAB...HAB...HBA...HAA...HBB '///)
DO 507 I=1,NT1,NTIP
507 PRINT 508,TIME(I),R(I),SAB(I),HAB(I),HBA(I),HAA(I),HBB(I)
508 FCRMAT(2(I),F10.5),D4,4(IPO11-4,IX,IP011-4,2X))
11 CONTINUE

DO 600 I=1,NT1
I=NT-I-1
SAB(I)=CCNJG(SAB(I))
SBA(I)=CCNJG(SBA(I))
SBI(I)=CCNJG(SBI(I))
HAB(I)=CCNJG(HAB(I))
HBA(I)=CCNJG(HBA(I))
HAA(I)=HAA(I)
HBB(I)=HBB(I)

SS=L,DD=0-SAB(I)*SBA(I)
AA(I)=(HBA(I)-SAB(I))*HBA(I)/SS
AA(I)=CCNJG(AA(I))
BB(I)=(HBB(I)-SBA(I))*HBB(I)/SS
600 BB(I)=CCNJG(BB(I))

NT1=NT-1
DELTA(I)=(0.000,0.000)
ALP(I)=(0.000,0.000)
BTA(I)=(0.000,0.000)
DO 700 J=2,NT1
X1=TIME(J-1)
X2=TIME(J)
X3=TIME(J+1)
Y1=AA(J-1)
Y2=AA(J)
Y3=AA(J+1)
ALP(J)=ALP(J-1)+SUM(X1,X2,X3,Y1,Y2,Y3)
Y1=BB(J-1)
Y2=BB(J)
Y3=BB(J+1)
BTA(J)=BTA(J-1)+SUM(Y1,Y2,Y3)
700 DELTA(J)=ALP(J)-BTA(J)
X1=TIME(NT)
X2=TIME(NT1)
X3=TIME(NT1-1)
Y1=AA(NT)
Y2=AA(NT1)
Y3=AA(NT1-1)
ALP(NT)=ALP(NT1)+SUM(X1,X2,X3,Y1,Y2,Y3)
Y1=BB(NT)
Y2=BB(NT1)
Y3=BB(NT1-1)
BTA(NT)=BTA(NT1)+SUM(X1,X2,X3,Y1,Y2,Y3)
DELTA(NT)=ALP(NT)-BTA(NT)

DO 800 K=1,NT
DELTA(K)=DELTA(K)-TIME(K)*REAL(DDTA)
SS=L,DD=0-SAB(K)*SBA(K)
Y3=COEXP(DELTA(K)/CH1)
XAB(K)=(HAB(K)-SAB(K))*HDB(K)*CH1*Y3/SS
XBA(K)=(HBA(K)-SBA(K))*HAA(K)*CH1*Y3/SS
DAE(K)=L,DD=0,DD001
800 DB(K)=(0.000,0.000)

SS=0.000
DO 1000 K=1,LIMIT
DAE(K)=(0.000,0.000)
DB(K)=(0.000,0.000)
DO 900 J=2,NT1
X1=TIME(J-1)
X2=TIME(J)
X3=TIME(J+1)
Y1=XBA(J-1)*DAE(J-1)
Y2=XBA(J)*DAE(J)
Y3=XBA(J+1)*DAE(J+1)
900 DB(J)=DB(J-1)+SUM(Y1,Y2,Y3)

```



```

X3=TIME(NT)
X2=TIME(NTL)
X1=TIME(NTL-1)
Y1=XBA(NT)*DA(NT)
Y2=XBA(NTL)*DA(NTL)
Y3=XBA(NTL-1)*DA(NTL-1)
DA(NT)=DA(NTL)+SUM(X1,X2,X3,Y1,Y2,Y3)
DO 950 J=2,NTL
X1=TIME(J-1)
X2=TIME(J)
X3=TIME(J+1)
Y1=XBA(J-1)*DA(J-1)
Y2=XBA(J)*DA(J)
Y3=XBA(J+1)*DA(J+1)
950 DA(J)=DA(J-1)+SUM(X1,X2,X3,Y1,Y2,Y3)
X3=TIME(NT)
X2=TIME(NTL)
X1=TIME(NTL-1)
Y1=XBA(NT)*DA(NT)
Y2=XBA(NTL)*DA(NTL)
Y3=XBA(NTL-1)*DA(NTL-1)
DA(NT)=DA(NTL)+SUM(X1,X2,X3,Y1,Y2,Y3)
IF(IPNT 2,EQ,0) GO TO 13
PRINT 21, K1
21 FORMAT('1 ITERATION=',I3/1)
PRINT 125
125 FORMAT('4X,4X,TIME',25X,'DA',30X,'CB'//)
DO 22 I=1,NCAS
22 PRINT 23, TIME(I),DA(I),DB(I)
23 FORMAT(2X,F12.6,4X,E16.7)
13 CONTINUE

SS1=0.000
SS2=0.000
DO 960 I=1,NT
SS1=SS1+CBAS(DA(I)-DB(I))
960 SS2=SS2+CBAS(DB(I))
SS3=SS1/SS2
1000 CONTINUE

2000 CONTINUE
PRINT 3
3 FORMAT('/// R UA..UB XBA..XBA CA..CB..PRDB..UNITARITY'//)
DO 50 I=1,NT,NCAS
CA(I)=DA(I)*CDEXP(EO,DOO,-1.000)*ALP(I)
CB(I)=DB(I)*CDEXP(EO,DOO,-1.000)*BTA(I)
PRDB=CB(I)*OCNJG(CB(I))
ENN=TIME(I)*EALP-EST4
ENT=CDEXP(L,DOO,-ENN)
UNIT=PRDB*CA(I)*OCNJG(CA(I))
U=OCNJG(CA(I))*CB(I)*AB(I)*CDEXP(ENT)
UNIT=UNIT+OCNJG(U)
UNIT=L,CO=UNIT
S3=L,CO=SAB(I)*SEA(I)
X1=(MBA(I)-SAB(I)*MBA(I))/SS-EALP
X2=(HBB(I)-SBA(I)*HBB(I))/SS-ESTA
Y1=(MAB(I)-SAB(I)*MAB(I))/SS
Y2=(HBA(I)-SAB(I)*HBA(I))/SS
50 PRINT 40, R(I),X1,X2,Y1,Y2,CA(I),CB(I),PRDB,UNIT
60 FORMAT(1X,F9.3,12(1X,1P09.2))

SP=PRDB*BC(IPB)
PRINT 225,SP,ED(IPB),EHP(LEV)
225 FC=NT*F, PRDB*BB*G,EL2,S, AT RPO,FB,4, EKEV,F10.3/1
FMP(LEV,IPB)*CB(NT)
PRB(LEV,IPB)*PRB
BRP(LEV,IPB)*BP
RETURN
END
SUBROUTINE DATSM
..... OTSM 10
SUBROUTINE DATSM OTSM 20
OTSM 30
PURPOSE OTSM 50
NOIM POINTS OF A GIVEN TABLE WITH MONOTONIC ARGUMENTS ARE OTSM 60
SELECTED AND ORDERED SUCH THAT OTSM 70
ABS(ARG(I)-X).GE.ABS(ARG(J)-X) IF I.GT.J. OTSM 80
OTSM 90
USAGE OTSM 100
CALL DATSM (X,Z,F,IRG,ICOL,ARG,VAL,NOIM) OTSM 110
OTSM 120

```

		OTS# 130
DESCRIPTION OF PARAMETERS		OTS# 140
X	- DOUBLE PRECISION SEARCH ARGUMENT.	OTS# 150
Z	- DOUBLE PRECISION VECTOR OF ARGUMENT VALUES (DIMENSION IRDOW), THE ARGUMENT VALUES MUST BE STORED IN INCREASING OR DECREASING SEQUENCE.	OTS# 160
		OTS# 170
F	- IN CASE ICOL=1, F IS THE DOUBLE PRECISION VECTOR OF FUNCTION VALUES (DIMENSION IRDOW).	OTS# 180
		OTS# 190
	IN CASE ICOL=2, F IS A DOUBLE PRECISION IRDOW BY 2 MATRIX, THE FIRST COLUMN SPECIFIES VECTOR OF FUNCTION VALUES AND THE SECOND VECTOR OF DERIVATIVES.	OTS# 200
		OTS# 210
IRDOW	- THE DIMENSION OF VECTOR Z AND OF EACH COLUMN IN MATRIX F.	OTS# 220
		OTS# 230
ICOL	- THE NUMBER OF COLUMNS IN F (1,0, 1 OR 2).	OTS# 240
ARG	- RESULTING DOUBLE PRECISION VECTOR OF SELECTED AND ORDERED ARGUMENT VALUES (DIMENSION NDIM).	OTS# 250
		OTS# 260
VAL	- RESULTING DOUBLE PRECISION VECTOR OF SELECTED FUNCTION VALUES (DIMENSION NDIM) IN CASE (COL=1).	OTS# 270
		OTS# 280
	IN CASE ICOL=2, VAL IS THE DOUBLE PRECISION VECTOR OF FUNCTION AND DERIVATIVE VALUES (DIMENSION 2*NDIM) WHICH ARE STORED IN PAIRS (I.E. EACH FUNCTION VALUE IS FOLLOWED BY ITS DERIVATIVE VALUE).	OTS# 290
		OTS# 300
NDIM	- THE NUMBER OF POINTS WHICH MUST BE SELECTED OUT OF THE GIVEN TABLE (Z,F).	OTS# 310
		OTS# 320
		OTS# 330
		OTS# 340
		OTS# 350
		OTS# 360
		OTS# 370
REMARKS		OTS# 380
	NO ACTION IN CASE IRDOW LESS THAN 1.	OTS# 390
	IF INPUT VALUE NDIM IS GREATER THAN IRDOW, THE PROGRAM SELECTS ONLY A MAXIMUM TABLE OF IRDOW POINTS. THEREFORE THE USER OUGHT TO CHECK CORRESPONDENCE BETWEEN TABLE (ARG,VAL) AND ITS DIMENSION BY COMPARISON OF NDIM AND IRDOW, IN ORDER TO GET CORRECT RESULTS IN FURTHER WORK WITH TABLE (ARG,VAL). THIS TEST MAY BE DONE BEFORE OR AFTER CALLING SUBROUTINE CATSM.	OTS# 400
		OTS# 410
	SUBROUTINE CATSM ESPECIALLY CAN BE USED FOR GENERATING THE TABLE (ARG,VAL) NEEDED IN SUBROUTINES DALLI, DASHI, AND DACFI.	OTS# 420
		OTS# 430
		OTS# 440
		OTS# 450
		OTS# 460
		OTS# 470
		OTS# 480
		OTS# 490
		OTS# 500
		OTS# 510
		OTS# 520
		OTS# 530
		OTS# 540
		OTS# 550
		OTS# 560
		OTS# 570
		OTS# 580
		OTS# 590
		OTS# 600
		OTS# 620
		OTS# 630
		OTS# 640
		OTS# 650
		OTS# 660
		OTS# 670
		OTS# 680
		OTS# 690
		OTS# 700
		OTS# 710
		OTS# 720
		OTS# 730
		OTS# 740
		OTS# 750
		OTS# 760
		OTS# 770
		OTS# 780
		OTS# 790
		OTS# 800
		OTS# 810
		OTS# 820
		OTS# 830
		OTS# 840
		OTS# 850
		OTS# 860
		OTS# 870
		OTS# 880
		OTS# 890
		OTS# 900
		OTS# 910
		OTS# 920
		OTS# 930
		OTS# 940
		OTS# 950
		OTS# 960
		OTS# 970
		OTS# 980
		OTS# 990

IF1 ICOL=114,14,13	DTSM 980
13 VAL(2)=1-F(K)	DTSM 990
KK=K+IRD	DTSM1000
VAL(2)=FEKK	DTSM1010
GDTO 15	DTSM1020
14 VAL(1)=F(K)	DTSM1030
15 JJR=J+JR	DTSM1040
IF1 JJR=10H)16,18,18	DTSM1050
16 JLL=J-JL	DTSM1060
IF1 JLL=1)19,19,17	DTSM1070
17 IF1 CABS(21JJR+1)-X)-CABS(21JLL-1)-X)1)19,19,18	DTSM1080
18 JLL=JL+1	DTSM1090
K=J-JL	DTSM1100
GDTO 20	DTSM1110
19 JJR=JR+1	DTSM1120
K=J+JR	DTSM1130
20 CONTINUE	DTSM1140
RETURN	DTSM1150
CASE IRD=1	DTSM1160
21 ARG(1)=Z(1)	DTSM1170
VAL(1)=F(1)	DTSM1180
IF1 ICOL=2)23,22,23	DTSM1190
22 VAL(2)=F(2)	DTSM1200
23 RETURN	DTSM1210
END	DTSM1230
.....	CALL 10
.....	CALL 20
.....	CALL 30
.....	CALL 40
.....	CALL 50
.....	CALL 60
.....	CALL 70
.....	CALL 80
.....	CALL 90
.....	CALL 100
.....	CALL 110
.....	CALL 120
.....	CALL 130
.....	CALL 140
.....	CALL 150
.....	CALL 160
.....	CALL 170
.....	CALL 180
.....	CALL 190
.....	CALL 200
.....	CALL 210
.....	CALL 220
.....	CALL 230
.....	CALL 240
.....	CALL 250
.....	CALL 260
.....	CALL 270
.....	CALL 280
.....	CALL 290
.....	CALL 300
.....	CALL 310
.....	CALL 320
.....	CALL 330
.....	CALL 340
.....	CALL 350
.....	CALL 360
.....	CALL 370
.....	CALL 380
.....	CALL 390
.....	CALL 400
.....	CALL 410
.....	CALL 420
.....	CALL 430
.....	CALL 440
.....	CALL 450
.....	CALL 460
.....	CALL 470
.....	CALL 480
.....	CALL 490
.....	CALL 500
.....	CALL 510
.....	CALL 520
.....	CALL 530
.....	CALL 540
.....	CALL 550
.....	CALL 560
.....	CALL 570
.....	CALL 580
.....	CALL 590

SUBROUTINE DALI

PURPOSE

TO INTERPOLATE FUNCTION VALUE Y FOR A GIVEN ARGUMENT VALUE X USING A GIVEN TABLE (ARG,VAL) OF ARGUMENT AND FUNCTION VALUES.

USAGE

CALL DALI (X,ARG,VAL,Y,NDIM,EPS,IER)

DESCRIPTION OF PARAMETERS

X - DOUBLE PRECISION ARGUMENT VALUE SPECIFIED BY INPUT

ARG - DOUBLE PRECISION INPUT VECTOR (DIMENSION NDIM) OF ARGUMENT VALUES OF THE TABLE (NOT DESTROYED).

VAL - DOUBLE PRECISION INPUT VECTOR (DIMENSION NDIM) OF FUNCTION VALUES OF THE TABLE (DESTROYED).

Y - RESULTING INTERPOLATED DOUBLE PRECISION FUNCTION VALUE.

NDIM - AN INPUT VALUE WHICH SPECIFIES THE NUMBER OF POINTS IN TABLE (ARG,VAL).

EPS - SINGLE PRECISION INPUT CONSTANT WHICH IS USED AS UPPER BOUND FOR THE ABSOLUTE ERROR.

IER - A RESULTING ERROR PARAMETER.

REMARKS

(1) TABLE (ARG,VAL) SHOULD REPRESENT A SINGLE-VALUED FUNCTION AND SHOULD BE STORED IN SUCH A WAY, THAT THE DISTANCES ABS(ARG(I)-X) INCREASE WITH INCREASING SUBSCRIPT I. TO GENERATE THIS ORDER IN TABLE (ARG,VAL), SUBROUTINES DATSG, DATSM OR DATSE COULD BE USED IN A PREVIOUS STAGE.

(2) NO ACTION BECOMES ERROR MESSAGE IN CASE NDIM LESS THAN 1.

(3) INTERPOLATION IS TERMINATED EITHER IF THE DIFFERENCE BETWEEN TWO SUCCESSIVE INTERPOLATED VALUES IS ABSOLUTELY LESS THAN TOLERANCE EPS, OR IF THE ABSOLUTE VALUE OF THIS DIFFERENCE STOPS DIMINISHING, OR AFTER (NDIM-1) STEPS. FURTHER IT IS TERMINATED IF THE PROCEDURE DISCOVERS TWO ARGUMENT VALUES IN VECTOR ARG WHICH ARE IDENTICAL. DEPENDENT ON THESE FOUR CASES, ERROR PARAMETER IER IS CODED IN THE FOLLOWING FORM

IER=0 - IT WAS POSSIBLE TO REACH THE REQUIRED ACCURACY (END ERROR).

IER=1 - IT WAS IMPOSSIBLE TO REACH THE REQUIRED ACCURACY BECAUSE OF ROUNDING ERRORS.

IER=2 - IT WAS IMPOSSIBLE TO CHECK ACCURACY BECAUSE NDIM IS LESS THAN 3, OR THE REQUIRED ACCURACY COULD NOT BE REACHED BY MEANS OF THE GIVEN TABLE. NDIM SHOULD BE INCREASED.

IER=3 - THE PROCEDURE DISCOVERED TWO ARGUMENT VALUES IN VECTOR ARG WHICH ARE IDENTICAL.

SUBROUTINES AND FUNCTION SUBPROGRAMS REQUIRED

NDIM

```

METHOD                                     DALL 600
INTERPOLATION IS DONE BY MEANS OF AITKEN'S SCHEME OF          DALL 610
LAGRANGE INTERPOLATION, ON RETURN Y CONTAINS AN INTERPOLATED DALL 620
FUNCTION VALUE AT POINT X, WHICH IS IN THE SENSE OF REMARK DALL 630
(3) OPTIMAL WITH RESPECT TO GIVEN TABLE. FOR REFERENCE, SEE DALL 640
F. S. MILDEBRAND, INTRODUCTION TO NUMERICAL ANALYSIS,       DALL 650
MCGRAW-HILL, NEW YORK/TORONTO/LONDON, 1956, PP.49-50.     DALL 660
.....DALL 670
.....DALL 680
SUBROUTINE DALL(X,ARG,VAL,Y,NDIM,EPS,IER)
*
*
DALL 710
DALL 720
DOUBLE PRECISION ARG,VAL,X,Y,H
DIMENSION ARG(NDIM),VAL(NDIM)
IER=2
DELT2=0.
IF(NDIM-1)9,7,1
START OF AITKEN-LOOP
DALL 750
1 DD & J=2,NDIM
DELT1=DELT2
DALL 760
IEND=J-1
DALL 770
DO 2 I=I,IEND
DALL 780
H=ARG(I)-ARG(J)
DALL 790
IF(OABS(H).LT.1.0D-6) GO TO 13
DALL 800
2 VAL1J=(VAL1J)-(X-ARG(J))*(VAL1J)-(X-ARG(I)))/H
DALL 810
DELT2=DAESI(VAL1J)-VAL1(NDIM)
DALL 820
IF(J-2)4,4,3
DALL 830
3 IF(ODELT2-EPS)10,10,4
DALL 840
4 IF(J=NDIM,5,5)
DALL 850
5 IF(ODELT2-DELT1)6,11,11
DALL 860
6 CONTINUE
DALL 870
END OF AITKEN-LOOP
DALL 880
7 J=NDIM
DALL 890
8 Y=VAL(J)
DALL 900
9 RETURN
DALL 910
DALL 920
DALL 930
DALL 940
DALL 950
DALL 960
DALL 970
DALL 980
DALL 990
DALL1000
DALL1010
DALL1020
DALL1030
DALL1040
DALL1050
DALL1060
DALL1070
DALL1080
DALL1090
DALL1100
DALL1110
THERE IS SUFFICIENT ACCURACY WITHIN NDIM-1 ITERATION STEPS
10 IER=0
GOTO 8
TEST VALUE DELT2 STARTS OSCILLATING
11 IER=1
12 J=IEND
GOTO 8
THERE ARE TWO IDENTICAL ARGUMENT VALUES IN VECTOR ARG
13 IER=3
GOTO 12
END
COMPLEX FUNCTION SUM*(X1,X2,X3,Y1,Y2,Y3)
IMPLICIT REAL*8 (A-H,O-Z)
COMPLEX*16 Y1,Y2,Y3,A,B,C,D,H,P
IF(OABS(X3-X2)-(X2-X1)).LT.1.0E-8) GO TO 10
A=Y1/(X3-X2)*(X1-X3)
B=Y2/(X2-X3)*(X2-X1)
C=Y3/(X3-X1)*(X3-X2)
D=A+B+C
E=A*(X2+X3)-B*(X1+X3)-C*(X2+X1)
F=A*X2*B+D*X1*B3+C*X1*F2
SUM=10*(A2**2+X1*(X2+X1))/3.00D+*(X2+X1)/2.00D+F*(X2-X1)
RETURN
10 D=X2-X1
SUM=D*(5*Y1+B*Y2-Y3)/12.00D
RETURN
END
SUBROUTINE DIFEQ(LX,RND,YO,HH,NN,EE)
.....
*WRITTEN BY L. AUER, 11/14/67. MODIFIED FOR IBM 370 BY A. ERGAL
*3/13/74.
*
*PURPOSE
*
* SIMULTANEOUS SOLUTION OF NN FIRST ORDER DIFFERENTIAL
* EQUATIONS IN ONE INDEPENDENT VARIABLE AND NN DEPENDENT
* VARIABLES. NN MAY BE UP TO 100.
*
*ARGUMENTS
*
* X0 = STARTING VALUE FOR INDEPENDENT VARIABLE
* XND = VALUE OF INDEPENDENT VARIABLE AT WHICH VALUES FOR
* DEPENDENT VARIABLES ARE TO BE RETURNED
* YO = ARRAY OF DIMENSION NN WHICH WILL CONTAIN INITIAL
* VALUES OF DEPENDENT VARIABLES UPON ENTRY
* = ARRAY OF FINAL VALUES OF DEPENDENT VARIABLES UPON

```

```

      * RETURN
      * NH = INITIAL STEP SIZE TO BE USED. STEP SIZE IS NORMALLY
      * MODIFIED TO PRESERVE ACCURACY AND INCREASE SPEED
      * EE = MAX. PERMISSIBLE TRUNCATION ERROR (SHOULD BE 1-E-5 TO
      * 1-E-6), OR
      * RELATIVE ERROR IF NEGATIVE
      *
      *-----*
      * IMPLICIT REAL*8 (A-H,O-Z)
      * REAL*8 N
      * COMMON/INTEG/X,N,NH,I1,I2,I3,I4
      *-----*
      * COMMON/INTEG/ IS A COMMON AREA USED TO COMMUNICATE WITH OTHER
      * SUBROUTINES IN THIS PACKAGE.
      *-----*
      * COMMON/SCRATCH/H(100),T(100),TP(100),CE(100),DE(100)
      *-----*
      * COMMON/SCRATCH/ IS A SCRATCH AREA WHICH MAY BE REUSED ELSEWHERE.
      * NOTE THAT N IS OF TYPE REAL*8
      *-----*
      * COMMON/YS/Y(100,4),YP(100,4),A(4)
      *-----*
      * COMMON/YS/ IS A SCRATCH AREA WHICH MAY BE REUSED ELSEWHERE. THE
      * SIZE OF THESE ARRAYS AND THOSE IN COMMON/SCRATCH/ SET THE
      * UPPER LIMIT ON NN.
      *-----*
      * DIMENSION Y0(I)
      *-----*
      * SUBPROGRAMS NEEDED
      * SUBROUTINE HERMIT - SUPPLIED IN THE PACKAGE
      * SUBROUTINE SUP - SUPPLIED IN THE PACKAGE
      * SUBROUTINE GILL - SUPPLIED IN THE PACKAGE
      * CONTAINS ENTRY POINT GILL2
      * SUBROUTINE DER (X,Y,YP) - SUBROUTINE WHICH GENERATES THE NN
      * DERIVATIVES OF THE DEPENDENT
      * VARIABLES WITH RESPECT TO THE
      * INDEPENDENT VARIABLE. IT MUST BE
      * SUPPLIED WITH THE VALUE OF NN
      * WHEN WRITTEN BY THE USER.
      *
      * ARGUMENTS FOR DER
      * X = VALUE OF INDEPENDENT VARIABLE
      * Y = ARRAY OF VALUES OF DEPENDENT VARIABLES
      * YP = ARRAY OF VALUES OF DERIVATIVES. Y AND YP MUST BE
      * OF DIMENSION NN
      *
      * ENTRY DER (X0,XND,Y0,HH,NN,EE)
      * THIS IS PROVIDED TO CONTINUE THE INTEGRATION FROM THE POINT
      * WHERE THE PREVIOUS CALL TO DIFEC LEFT OFF, WHICH IN
      * GENERAL MAY NOT BE THE LAST XND.
      * THE MEANING OF THE ARGUMENTS ARE THE SAME AS IN THE MAIN
      * ENTRY, THOUGH X0, Y0, AND HH ARE NOT USED AND NEED NOT BE
      * DEFINED
      *-----*
9999 CONTINUE
      *-----*
      * METHOD
      * HANNING'S METHOD PREDICTOR-CORRECTOR STARTED BY THREE GILL-
      * RUNGE-KUTTA STEPS AND INTERNAL HALVING AND DOUBLING OF STEP
      * SIZE TO PRESERVE ACCURACY AND INCREASE SPEED
      * THE STEP-HALVING IS DONE BY 4-POINT HERMITE INTERPOLATION
      *
      * ADDITIONAL DOCUMENTATION AVAILABLE
      *-----*
      *
      * N = NN
      * H = HH
      * HMIN = CABS (HH) / 4056.
      * R = X0
      * I1 = 1
      * I2 = 2
      * I3 = 3
      * I4 = 4
      * DO I = 1, N
      * Y(I,I) = Y0(I)
      * CALL DER (X, Y0, YP(I,I))
      * CALL GILL (Y(I,I), Y(I,2), YP(I,2))
      *-----*
      * X IS UPDATED WITHIN GILL
      *-----*
      * CALL GILL2 (Y(I,2), Y(I,3), YP(I,3))
      * CALL GILL2 (Y(I,3), Y(I,4), YP(I,4))
      *-----*
      * WE NOW HAVE THE VALUES AND THE DERIVATIVES AT THE FIRST 4 POINTS
      * AND ARE READY TO USE THE HANNING'S PREDICTOR-CORRECTOR. THESE
      * RUNGE-KUTTA STEPS ARE ALWAYS COMPUTED TO RESTART THE SOLUTION
      *-----*

```

```

.....
2 DO 3 I = 1, N
3   M11 = 0.
   ENTRY DER (X0, XND, Y0, HN, NN, EE)
   EPS = DABS (EE)
   IF (X .GE. XND) GO TO 14
4 DO 5 I = 1, N
   T(I) = Y(I,11) + 4. * H * (2. * YP(I,14) - YP(I,13)) + 2. *
   * YP(I,12) / 3.
   .....
   .D2 IS THE MODIFIED PREDICTOR
   .....
5   D2(I) = T(I) + .92581983 * M11
   CALL DER (X+H, D2, TP)
   DO 6 I = 1, N
   D1(I) = (19. * Y(I,14) - Y(I,12)) + 3. * H * (TP(I) + 2. *
   * YP(I,14) - YP(I,13)) / 8.
6   M11 = D1(I) - T(I)
   .....
   .CHECK WHETHER THE STEP SIZE SHOULD BE HALVED OR DOUBLED
   .....
   EMIN = 0.
   DO 7 I = 1, N
   .....
   .CHECK THAT THE RELATIVE ACCURACY CRITERION IS BEING
   .SATISFIED
   .....
   E = H * DABS (M11) / D2(I)
   IF (E .LT. 0.) E = 2. * E / DABS (D1(I) + T(I) + 1.e-05)
   IF (E .GT. EPS) GO TO 9
7   ENIN = DMAX (E, ENIN)
   .....
   .THE LAST STEP WAS OF SATISFACTORY ACCURACY SO THE SOLUTION MAY
   .BE UPDATED
   .....
8 DO 8 I = 1, N
   Y(I,11) = D1(I) - .07438016 * M11
   .....
   .MODIFY THE FINAL SOLUTION INSTEAD OF ITERATING
   .....
   X = X + H
   CALL DER (X, Y(I,11), YP(I,11))
   CALL IUP
   IF (X .GE. XND) GO TO 14
   IF (ENIN .GT. 0.001 * EPS) GO TO 4
   GO TO 11
   .....
   .STEP HALVING
   .....
9 CALL HERMIT (X-0.5*H, D2)
   CALL HERMIT (X-1.5*H, D1)
   DO 10 I = 1, N
   M11 = M11 / 32.
   Y(I,12) = Y(I,11)
   .....
   YP(I,12) = YP(I,11)
   .....
   Y(I,13) = D1(I)
10  Y(I,14) = D2(I)
   CALL DER (X-0.5*H, D2, YP(I,13))
   CALL DER (X-1.5*H, D1, YP(I,14))
   H = H / 2.
   IF (DABS (H) .GT. HMIN) GO TO 4
   PRINT LOG,X,H
100 FORMAT (' STEP SIZE H HAS BEEN HALVED TOO OFTEN AT X=',I10D15.5,/,
$ ' PRESENT STEP SIZE IS H=',D12.5)
   PRINT 101
101 FORMAT (10X,'N',9X,'Y(11)',8X,'YP(11)',9X,'Y(12)',8X,'YP(12)',
$ ' 5X,'Y(13)',8X,'YP(13)',9X,'Y(14)',8X,'YP(14)')
   PRINT LOG,(X(1),Y(1,11),YP(1,11),Y(1,12),YP(1,12),Y(1,13),YP(1,13))
$ ' Y(1,14),YP(1,14),I=1,N)
102 FORMAT (I10D14.6)
   GO TO 4
   .....
   .STEP DOUBLING
   .....
11 DO 12 I = 1, N
   Y(I,13) = Y(I,12)
12  YP(I,13) = YP(I,12)
   H = 2. * H
   CALL GILL (Y(I,14), Y(I,11), YP(I,11))

```

```

CALL IUP
CALL GILL2 (YI,I4) , Y(I,I1) , YP(I,I1)
CALL IUP
DO 13 I = 1 , N
13  H(I) = 0.
.....
DUNCE MORE CHECK THE TERMINATION CONDITION
.....

14 CALL HERMIT (XND , YD)
IF (X .LT. XND) GO TO 2

RETURN
END
SUBROUTINE HERMIT (XND , YD)
.....
THIS ROUTINE PERFORMS THE HERMITE INTERPOLATION FOR STEP HALVING.
IN DIFEQ. SEE DIFEQ FOR ADDITIONAL DOCUMENTATION.
.....
IMPLICIT REAL*8 (A-H,O-Z)
REAL*8 L,LP
COMMON/INTEG/X,H,N,I1,I2,I3,I4
COMMON/Y/S/Y(100,4),YP(100,4),A(4)
DIMENSION YD(I)

A(I1) = X
A(I2) = X - H
A(I3) = A(I2) - H
A(I4) = A(I3) - H
DO 1 I = 1 , N
1  YD(I) = 0.
DO 4 I = 1 , 4
  L = 1.
  LP = 0.
  DO 2 J = 1 , 4
    IF (I .EQ. J) GO TO 2
    L = L * (XND - A(J)) / (A(I) - A(J))
    LP = LP * 1. / (A(I) - A(J))
  2
  DO 3 K = 1 , N
    YD(K) = YD(K) + ((1. - 2. * (XND - A(I)) * LP) * Y(K,I)
      3 + (XND - A(I)) * YP(K,I)) * L * L
  4
CONTINUE
RETURN
END
SUBROUTINE IUP
.....
THIS SUBROUTINE UPDATES THE INDICES IN COMMON/INTEG/ WHEN CALLED.
BY DIFEQ. SEE DIFEQ FOR ADDITIONAL DOCUMENTATION.
.....
REAL*8 S , H
COMMON/INTEG/X,H,N,I1,I2,I3,I4

I1 = MOD (I1 , 4) + 1
I2 = MOD (I2 , 4) + 1
I3 = MOD (I3 , 4) + 1
I4 = MOD (I4 , 4) + 1

RETURN
END
SUBROUTINE GILL (YD , YI , YP)
.....
THIS ROUTINE PERFORMS THE GILL-RUNGA-KUTTA STEPS WHEN CALLED BY
DIFEQ. SEE DIFEQ FOR ADDITIONAL DOCUMENTATION.
.....
IMPLICIT REAL*8 (A-H,O-Z)
COMMON/INTEG/X,H,N,I1,I2,I3,I4
DATA CONS/D,T010678116054700/
DIMENSION YD(I),Y(I1),Y(I2),Y(I3),Y(I4)
COMMON/SCATG/T1(100),T2(100),T3(100),T4(100),S(100)
.....
THIS IS A GILL'S METHOD OF INTEGRATION.
.....
CALL DER (X , YD + T1)

ENTRY GILL2 (YD , YI , YP)
DO 1 I = 1 , N
  T1(I) = H * T1(I)
  S(I) = YD(I) + 0.5 * T1(I)
1 CALL DER (X+0.5*H , S , T2)
DO 2 I = 1 , N

```

```

      T2(I) = H * T2(I)
2     S(I) = YD(I) + (CCNS - 0.5) * T1(I) + (1.0 - CCNS) * T2(I)
      CALL DER (X+D.5*M , S , T3)
      DO 3 I = 1 , N
          T3(I) = H * T3(I)
3     S(I) = YD(I) - CCNS * T2(I) + (1.0 + CCNS) * T3(I)
      X = X + H
      CALL DER (X , S , T4)
      DO 4 I = 1 , N
          Y1(I) = YD(I) + (T1(I) + 2. * (1. - CCNS) * T2(I) + 2. *
4         (1. + CCNS) * T3(I) + H * T4(I)) / 6.
      CONTINUE
      CALL DER (X , Y1 , YP)
      DO 5 I = 1 , N
5     T1(I) = YP(I)

      RETURN
      END

```



```

*,PRB(2,10,20),GRPS(2,10,20),PRHP(2,10,20)
COMMON/ALU/AL(21),N(132),NLG
COMMON/PNT/L/UL(41),CVI(3),AZ,GE
COMMON/FA/EALP,ZA,ALLEF(10),ASP(10),NKA(10),NA
COMMON/FA/ESTA,ZB,ACCPE(10),BXP(10),NYD(10),NB
COMMON/OPTV/LIMIT,MH,LPNCH,LRED,IPNT1,LPNT2,NITP,NCAB,NCAB
DIMENSIONA LABEL(20),XXX(25),YYY(25),SOMA(2,10),Y(4)
3 FORMAT(10IX,IP2I2,5)
81 FORMAT(11,////TIME,....R A11.....A12.....A21.....A22*/)
100 FORMAT(11,5)
200 FORMAT(4P10,4)
300 FORMAT(20A4)
400 FORMAT(11,////25K,20A6)
249 FORMAT(4E20,15)
AZ=0.000
ZB=0.000
PF1=1.000

READ(5,1CG) NLG
READ(5,249) (X(IX),X(IX),IX=1,NLG)
READ(5,300) (LABEL(I),I=1,20)
READ(5,200) Z1,Z2,FMAX,FMS
IF(FMAX.EQ.0.000) FMAX=40.000
IF(FMS.EQ.0.000) FMS=1.000
READ(5,100) NCCDE,ICODE,ACCDE,LPNCH,LRED,
*LIMIT,MH,IPNT1,IPNT2,NITP,NCAB,NCAB,IEL
IF(IEL.NE.0) PF1=0.000
IF(NCAB.EQ.0) NCAB=5
IF(NDAB.EQ.0) NDAB=5
IF(NITP.EQ.0) NITP=5
READ(5,1CG) NI,NEV,NRO,NA,NB,NT,NP,IFILE
READ(5,200) (EIMPT(I),I=1,NEV)
READ(5,200) (EB(I),I=1,NRO)
IF(NA.EQ.0) NA=1
IF(NB.EQ.0) NB=2
PRINT 411
411 FORMAT(11 NLG, (X(IX),X(IX),IX=1,NLG) *)
PRINT 100, NLG
PRINT 3, (X(IX),X(IX),IX=1,NLG)
PRINT 414
414 FORMAT(11 Z1,Z2,FMAX,FMS *)
PRINT 200, Z1,Z2,FMAX,FMS
PRINT 413
413 FORMAT(11 NCCDE,ICODE,ACCDE,LPNCH,LRED,
*LIMIT,MH,IPNT1,IPNT2,NITP,NCAB,NCAB *)
PRINT 100, NCCDE,ICODE,ACCDE,IPNCH,LRED,
*LIMIT,MH,IPNT1,IPNT2,NITP,NCAB,NCAB
PRINT 415
415 FORMAT(11 NI,NEV,NRO,NA,NB,NT,NP,IFILE *)
PRINT 100, NI,NEV,NRO,NA,NB,NT,NP,IFILE
PRINT 416
416 FORMAT(11 (EIMPT(I),I=1,NEV) *)
PRINT 200, (EIMPT(I),I=1,NEV)
PRINT 417
417 FORMAT(11 (EB(I),I=1,NRC) *)
PRINT 200, (EB(I),I=1,NRC)
FNA=OFLCAT(NA)
FNB=OFLCAT(NB)
EALP=Z1*Z2/FNA/FNA/2.000
ESTA=Z2*Z2/FNB/FNB/2.000
ACDEF(1)=1.000
ACDEF(2)=OSQRT(3.000)
ACDEF(3)=OSQRT(2.5000)
BCDEF(1)=OSQRT(24.000)
BCDEF(2)=OSQRT(45.000)
IF(NB.EQ.2) BCDEF(1)=1.000
DO 20 J=1,3
NKA(J)=1
NBI(J)=41
ASP(J)=Z1/FNA
BAP(J)=Z2/FNB
OLMW(J)=0.000
DO 20 J=1,3
20 CVI(J)=0.000
NGB=NB-1
IF(NB.EQ.0) GO TO 22
READ(5,200) EALP,FA,OLMW(2),(CVI(J),J=1,3),AZ
NA=FA
READ(5,100) (NKA(I),I=1,NA)
READ(5,200) (NBI(I),I=1,NA)
READ(5,200) (ACDEF(I),I=1,3)
22 CONTINUE
IF(NP.EQ.0) GO TO 24
READ(5,200) ESTA,FNB,OLMW(3),(CVI(J),J=1,3),BZ
NB=FB

```

```

READ(5,100) (NTB(I),I=1,NS)
READ(5,200) (GXP(I),I=1,NG)
READ(5,200) (GCOEF(I),I=1,NG)
24 CONTINUE
FA=DFLOAT(NA)
FB=DFLOAT(NB)
PRINT *23
FORMAT I' EALP,NA,OLMV(2),ICV(1,2),I=1,3)'
PRINT 200, EALP,FA,OLMV(2),ICV(1,2),I=1,3)
PRINT *25
245 FORMAT I' (NXA(I),I=1,NA)'
PRINT 100, (NXA(I),I=1,NA)
PRINT *19
249 FORMAT I' (LXP(I),I=1,NA)'
PRINT 200, (LXP(I),I=1,NA)
PRINT *21
241 FORMAT I' (ACCEP(I),I=1,NA)'
PRINT 200, (ACCEP(I),I=1,NA)
PRINT *24
244 FORMAT I' (BTA,NG,OLMV(3),ICV(1,3),I=1,3)'
PRINT 200, (BTA,FB,OLMV(3),ICV(1,3),I=1,3)
PRINT *18
248 FORMAT I' (NXB(I),I=1,NB)'
PRINT 100, (NXB(I),I=1,NB)
PRINT *20
240 FORMAT I' (GXP(I),I=1,NG)'
PRINT 200, (GXP(I),I=1,NG)
PRINT *22
242 FORMAT I' (GCOEF(I),I=1,NG)'
PRINT 200, (GCOEF(I),I=1,NG)

AZ=AZ+1.000
BZ=BZ+1.000
C1=DCNPLX(0.000,1.000)
P1=DARCOSS(-1.000)
TKOP1=2.000*PI*(1.5290-08)**2)
ZA=Z1
ZB=Z2
ZC=ZA
IF(ZB-LT,ZA) Z2=ZB
Z1=Z2
EALP=EALP/Z2/Z2
EBTA=EBTA/Z2/Z2
NNT=3*N1
NNT1=NNT+1
NT=2*NNT+1
DO 1000 LEF=1,NEV
EKEV=EKEPTILEV)
V=DSQRT(EKEV/FMB)/5.000
SETUP TIME VECTOR
TIME(NNT1)=0.0
IF(NE.EQ.9) GO TO 1005
TIME(NT1)=CMAJ(I ZA+23)/V
TIME(NNT1)=0.000
HT=TIME(NT1)/3.000/DFLCAT(N1)
DO 10 J=1,3
J1=(J-1)*N1
DO I2 I=1,N1
J11=I
IF(J.GT.1) J11=I+(2**J-1)
TIME(NNT1+J11)=TIME(NNT1+J1)+J11*HT
12 CONTINUE
10 CONTINUE
DO 14 I=1,NNT
14 TIME(NNT1+I)=TIME(NNT1+1)
1005 CONTINUE
DO 1001 I=1,NG
RHO=EB(I*G)
RHNNT1=RHO
IF(NE.EQ.0) GO TO 1004
DO 15 I=1,NNT
RHNNT1+I)=DSQRT(RHO*RHO+V*V*TIME(NNT1+I)*TIME(NNT1+1))
RHNNT1+I)=RHNNT1+1
15 CONTINUE

IF(IREQ.EQ.1) GO TO 90
1006 CONTINUE
CALL CMA TRX
GO TO 95
90 CONTINUE
EKL=LKEV/Z2/Z2
V=V/Z2
R1C=SNO=Z2
VA=DSQR TICKEV/EALP/FMB/27+2100-D3/(936*0)
DO 99 I=1,4,2

```

```

DO 51 I=1,NT
READ(5,52) TIME(I),HAA(I),HBB(I)
READ(5,52) SAA(I),HAB(I),HBA(I)
TIME(I)=TIME(I)*22*Z2
51 CONTINUE
52 FORMAT(7E11.5)
IF(III.EC.1) PRINT 91
IF(III.EC.2) PRINT 61
DD 75 I7=1,NN11
75 PRINT 93, TIME(I),R(I),SAB(I),HAB(I),HBA(I),HAA(I),HBB(I)
93 FORMAT(2X,F10.8,5X,3(IPD11.4,1X,1P011.4,2X),3X,2(IPD11.4,1X))
PRINT 94, Z2,EKEV,V,VR,RHD
IF(INCDE.E2.1) CALL C03:EQN(7,III)
IF(INCDE.NE.0) GO TO 76
IF(III.EC.1) PRINT 97
IF(III.EC.2) PRINT 67
Y(1)=1.000
Y(2)=0.000
Y(3)=0.000
Y(4)=0.000
CALL DIFEQ(TIME(I),TIME(I2)/2.000,Y,0.2000,4,1.0-6)
DD 78 I7=2,NT
CALL DEQ(TIME(I),TIME(I2),Y,HH,4,1.0-6)
PRB=Y(3)*Y(1)+Y(4)*Y(1)
UNIT=PRB*Y(1)*Y(1)+Y(2)*Y(2)+Y(3)+Y(4)
UNIT=UNIT+2.000*SAB(I)*DCMPLX(Y(1),-Y(2))*DCMPLX(Y(3),Y(4))
/CDXPIC(TIME(I)*EALP-EBAI)
78 PRINT 95, TIME(I),R(I),Y(1),Y(1),Y(4),PRB,UNIT
PRB(III,LEV,IPB)=PRB
BAP(III,LEV,IPB)=PRB*EB(IPB)
PRMP(III,LEV,IPB)=DCMPLX(Y(1),Y(4))
PRINT 95, PRB(III,LEV,IPB),BAP(III,LEV,IPB),EINPT(LEV),EB(IPB)
79 CONTINUE
59 CONTINUE
GO TO 53
85 CONTINUE
EKEV=EKEV/Z2/Z2
V=V/Z2
RHD=RHD/Z2
V=DSQRT(EKEV/EALP/PRB/27.21360-03/1836.0)
DO 86 I=1,NT1
I=NT-I-1
TIME(I)=TIME(I)*22*Z2
TIME(I)=-TIME(I)
SAB(I)=SABPX(I)
HAB(I)=HABPX(I)
HBA(I)=HBAPIX(I)
HBB(I)=HBBPX(I)
SAA(I)=SABPX(I)
HAB(I)=HABPX(I)
HBA(I)=HBAPIX(I)
HBB(I)=HBBPX(I)
56 CONTINUE
IF(IPNH.EQ.0) GO TO 70
DO 71 I=1,NT1
PUNCH 82, TIME(I),HAA(I),HBB(I)
71 PUNCH 52, SAB(I),HAB(I),HBA(I)
70 CONTINUE
PRINT 40C, (LABEL(I),I=1,20)
PRINT 91
91 FORMAT(1' NPX TIME...R SAB...HAB...HBA HAA...HBB '///)
DD 92 I7=1,NN11
92 PRINT 93, TIME(I),R(I),SAB(I),HAB(I),HBA(I),HAA(I),HBB(I)
PRINT 94, Z2,EKEV,V,VR,RHD
94 FORMAT(// SCALING FACTOR *'F0.2, SCALED QUANTITIES ; EKEV) **,
1P011.4, * Y *',1P09.2, * V/VK *',1P09.2, * RHD *',1P09.2//)
IF(INCDE.EQ.1) CALL C03:EQN(7,III)
IF(INCDE.NE.0) GO TO 96
PRINT 97
97 FORMAT(1' /// NPX TIME...R CA...C0...PRB...UNIT '///)
Y(1)=1.000
Y(2)=0.000
Y(3)=0.000
Y(4)=0.000
CALL DIFEQ(TIME(I),TIME(I2)/2.000,Y,0.2000,4,1.0-6)
DD 98 I7=2,NT
CALL DEQ(TIME(I),TIME(I2),Y,HH,4,1.0-6)
PRB=Y(3)*Y(1)+Y(4)*Y(1)
UNIT=PRB*Y(1)*Y(1)+Y(2)*Y(2)+Y(3)+Y(4)
UNIT=UNIT+2.000*SAB(I)*DCMPLX(Y(1),-Y(2))*DCMPLX(Y(3),Y(4))
/CDXPIC(TIME(I)*EALP-EBAI)
98 PRINT 95, TIME(I),R(I),Y(1),Y(1),Y(4),PRB,UNIT
95 FORMAT(2X,F10.8,5X,2(IPD10.3,1X,1P010.3,2X),3X,2(IPD10.3,1X))
PRB(III,LEV,IPB)=PRB
BAP(III,LEV,IPB)=PRB*EB(IPB)

```

```

PRMP(1,LEV,IP0)=DCPLX(Y(3),Y(4))
PRIN 99, PRB(1,LEV,IP0),BRP01,LEV,IP0,EIMPT(LEV),EB(IP0)
99 FORMAT(' PRG0 =',IP0,2,' PRG0 X RHO =',IP0,2,' AT E(KEV) =',
' FID,2,' RHO =',F8.0//)
96 CONTINUE
IF IJCODE.EQ.0) GO TO 84
PRINT 81
DO 82 I=NT1,NT
SBA(I)=DCNJ(SAB(I))
SS=1.000-SAB(I)*SBA(I)
A11=-EALP*(HAA(I)-SAB(I))*HBA(I)/SS
A12=HAB(I)-SAB(I)*HBB(I)/SS
A21=HBA(I)-SBA(I)*HAA(I)/SS
A22=-EBA*(HBB(I)-SBA(I)*HAB(I))/SS
PRINT 3, TIME(I),R(I),A11,A12,A21,A22
82 CONTINUE
84 CONTINUE
DO 57 I=1,NTI
II=NT-I-1)
SAB(I)=SABP(II)
HAB(I)=HABP(II)
HBA(I)=HABP(II)
HBB(I)=HBBP(II)
SAB(II)=SABP(II)
HAB(II)=HABP(II)
HBA(II)=HABP(II)
HBB(II)=HBBP(II)
57 CONTINUE
IF (IPCH.EQ.0) GO TO 73
DO 74 I=1,NTI
PUNCH 52, TIME(I),HAB(I),HBB(I)
74 PUNCH 52, SAB(I),HAB(I),HBA(I)
73 CONTINUE
PRINT 400, (LABEL(I),I=1,20)
PRINT 81
61 FORMAT(' NPZ TIME...R SAB...HAB...HBA HAA...HBB //')
DO 62 IT=1,NTI
62 PRINT 93, TIME(IT),R(IT),SAB(IT),HAB(IT),HBA(IT),HAA(IT),HBB(IT)
PRINT 94, Z2,EKEV,V,VR,RHO
IF IJCODE.EQ.1) CALL CDUEQNT,2)
IF IJCODE.NE.0) GO TO 66
PRINT 87
67 FORMAT(' ',///' NPZ TIME...R CA...CB...PROB...UNIT //')
Y(1)=1.000
Y(2)=G.000
Y(3)=0.000
Y(4)=0.000
CALL DIFDCTIME(1),TIME(2)/2.000,Y(0.2000,4,I,0-6)
DO 68 IT=2,NT
CALL DCQCTIME(1),TIME(IT),Y,HM,4,1.0-6)
PROB=Y(3)*Y(4)+Y(4)*Y(4)
UNIT=PROB*Y(1)*Y(2)+Y(2)*Y(2)-1.000
UNIT=UNIT+2.000*SAB(IT)*DCPLX(Y(3),-Y(4))*DCPLX(Y(3),Y(4))
/COEXPICTIME(IT)*(EALP-EBA)
68 PRINT 95, TIME(IT),R(IT),Y(1),Y(2),Y(3),Y(4),PROB,UNIT
PRB(2,LEV,IP0)=PROB
BRP(2,LEV,IP0)=R(2)*EB(IP0)
PRMP(2,LEV,IP0)=DCPLX(Y(3),Y(4))
PRINT 99, PRB(2,LEV,IP0),BRP(2,LEV,IP0),EIMPT(LEV),EB(IP0)
86 CONTINUE
IF IJCODE.EQ.0) GO TO 85
PRINT 81
DO 83 I=NT1,NT
SBA(I)=DCNJ(SAB(I))
SS=1.000-SAB(I)*SBA(I)
A11=-EALP*(HAA(I)-SAB(I))*HBA(I)/SS
A12=HAB(I)-SAB(I)*HBB(I)/SS
A21=HBA(I)-SBA(I)*HAA(I)/SS
A22=-EBA*(HBB(I)-SBA(I)*HAB(I))/SS
PRINT 3, TIME(I),R(I),A11,A12,A21,A22
83 CONTINUE
85 CONTINUE
53 CONTINUE
EKEV=EKEV+Z2*Z2
V=V+Z2
RHO=RHO+Z2
DO 56 I=1,NTI
TIME(I)=TIME(I)/Z2/Z2
56 TIME(I)=TIME(I)
1001 CONTINUE
IF IJCODE.EQ.0) GO TO 1000
DO 87 INC=1,2
DO 88 I=1,NRO
XXX(I)=S(I)
FFF=1.000-PPP*PAB(INDX,LEV,I)

```



```

NMX=NA1+N31
NN3=MMX+3
C=DCMPLX(0.000,0.000)
CI=DCMPLX(0.000,1.000)
CR=DCMPLX(1.000,0.000)
PL(1)=CR
FM(1)=C
D3=DSQRT(3.000)
GMA2=V*H*O/2.000
P(1)=0.000
P(2)=1.000
P(3)=-1.000
Z(1)=0.000
Z(2)=2A-A2
Z(3)=2B-B2
DLNVI(1)=0.000
DD 14 J=1,3
14 CVI(2,1)=C.000
IF(IPB.GT.1) GO TO 499
IF(ILEV.GT.1) GO TO 499
TIME(NNT1)=F1+4*(NNT1-1)/50.000
R1(NNT1)=OSQRT(V*V+TIME(NNT1)*TIME(NNT1)+RHO*RHO)

DF(1)=0.000
DF(2)=1.000
DG(1)=1.000
DGI(2)=1.000
DD 15 I=2,29
DPI(1)=DPI(1)+1.000
15 DGI(1)=DPI(1)+DGI(1)
DD 16 I=1,NA
NE=2*NXAL(1)+1
A1=(2.000*A*PI(1))*N1/DG(NE)
16 ACOEF(1)=ACOEFL(1)+OSQRT(DABS(A1))
DD 17 J=1,N3
NJ=2*NXB(1,1)+1
S1=(2.000*C*E*PI(1))*N2/DG(NJ)
17 BCOEFL(1)=BCOEFL(1)+OSQRT(DABS(S1))

A(1,1)=1.000
A(2,2)=1.000
B(1,2)=1.000
B(2,3)=-1.000/3.000
DD 20 K=2,NH3,2
AK=OF(K+1)
A(K+1,1)=1.000/(AK+1.000)
B(K+1,2)=3.000/(AK+1.000)/(AK+3.000)
KK=A+1
AKK=OF(KK+1)
A(KK+1,2)=3.000/(AKK+2.000)
B(KK+1,3)=-3.000/(AKK+2.000)/(AKK+4.000)
DD 20 L=2,KK,2
AL=OF(L+1)
ADM=(2.000*AL+1.000)/(2.000*AL-3.000)
A(K+L,L+1)=(2.000+AK-AL)*A(K+1,L-1)/(1.000+AK+AL)*AB
AL=AL+1.000
AB=(2.000*AL+1.000)/(2.000*AL-3.000)
B(K+L,L+2)=(3.000+AK-AL)*B(K+1,L)/(2.000+AK+AL)*AB
LL=L+1
ALL=AL
A(KK+1,LL+1)=(2.000+AKK-ALL)*A(KK+1,LL-1)/(1.000+AKK+ALL)*AB
ALL=ALL+1.000
AB=(2.000*ALL+1.000)/(2.000*ALL-3.000)
B(KK+1,LL+2)=(3.000+AKK-ALL)*B(KK+1,LL)/(2.000+AKK+ALL)*AB
20 CONTINUE

499 CONTINUE
DD 500 I=1,NNT1
LTT=NT-(I-1)
GMA1=V*V*TIME(I)/2.000
R2=R1(LT)/2.000
SAB10=C
HAB10=C
HAB10=C
SAB11=C
HAB11=C
HAB11=C
DD 510 I=1,NA
NP=NXAL(1)+1
SAB10=C
HAB10=C
HAB10=C
SAB11=C
HAB11=C
HAB11=C

```

```

HBAJL=C
DO 520 J=1,NB
NQ=NEC(J)
DPOS1=IAXP(1)+SXP(J)*R2
DNG3=IAXP(1)-SXP(J)*R2
AKK=AP+NC
SMM=NP+NL+2
SAXO=C
HABO=C
HAXO=C
SAX1=C
HAX1=C
HAX1=C
DO 530 I=X1,NLQ
DO 9 M=1,J
JPOS(M)=CPOS1+DLN(V(M)*R2
DNEG(M)=DNEG1+DLN(V(M)*R2*P(H)
DLM(M)=1.00+XX(LX)/CPOS(M)
DM=OSGRT(DLN(M)*DLN(M)-1.00)
DX=0.00
IF(CPOS(M).LT.1.30+02) DX=CEXP(-DPOS(M))
DPAD(M)=DX/CPGS(M)
DPAL(M)=DX/DPGS(M)+DM
DM=0.00
IF(DNEG(M).LT.1.30+02) DN=DNEG(M)
TCOSX=DCMPLX(GHA+DLN(M),DN)
TSINX=DCMPLX(GH+GMA,0.00)
RD=R2*DLN(M)
Z2=Z(M)
VV2,M)=Z2*F1.00+RD*(CV(1,M)*RD+CV(2,M)+RD+CV(3,M))
VV3,M)=P1)*Z2*(CV(1,M)+RD+CV(2.00)+CV(2,M)+RD+3.00*CV(3,M))
VV4,M)=Z2*(R2*DLN(V2,M)*F0+3.00*CV(3,M))
VV5,M)=P1)*Z2*(R2*DLN(V2,M)+CV(3,M)
IF(M.GT.1).AND.(DLN(V(M)).LE.1.00+00) GO TO 91
T=OSGRT(TSINX*TSINX+TCOSX*TCOSX)
X=TCOSX/T

JL(1)=COSTW(T)/T
JL(2)=JL(1)-CCOS(T)/T
PL(2)=X
PH(2)=COSRT(1.00-X**2)
JL(3)=3.00*JL(2)/T-JL(1)
PL(3)=(3.000*X*PL(2)-PL(1))/2.000
PH(3)=3.00*X*PH(2)-2.00*PH(1)
FLM(1,M)=A(1,1)*JL(1)*PL(1)
FLM(1,M)=A(1,2)*JL(2)*PH(2)*C1
FLM(1,M)=A(1,3)*JL(3)*PL(3)*C1
FLM(1,M)=B(1,3)*JL(3)*PH(3)
GO 10 N=2,NP,M,2
N1=N+1
FN1=CP(N1+1)
JL(N1+1)=(2.000*FN1-1.000)*JL(N1)/T-JL(N1-1)
PL(N1+1)=(12.000*FN1-1.000)*X*PL(N1)-FN1*PL(N1-1)+FN1*(N1-1)/FN1
PH(N1+1)=(12.000*FN1-1.000)*X*PH(N1)-FN1*PH(N1-1)/(FN1-1.000)
FLM(N1,M)=A(N1,1)*JL(N1)*PL(1)
FLM(N1,M)=B(N1,2)*JL(2)*PH(2)*C1
N2=N1+1
FN2=CF(N2+1)
JL(N2+1)=(2.000*FN2-1.000)*JL(N2)/T-JL(N2-1)
PL(N2+1)=(12.000*FN2-1.000)*X*PL(N2)-FN2*(N2-1.000)*PL(N2-1)/FN2
PH(N2+1)=(12.000*FN2-1.000)*X*PH(N2)-FN2*PH(N2-1)/(FN2-1.000)
FLM(N2,M)=A(N2,2)*JL(2)*PH(2)*C1
FLM(N2,M)=B(N2,3)*JL(3)*PH(3)
NN=N1
DO 10 L=2,N1,2
AL=OF(L+1)
FLM(N,M,N1)=FLM(N,M,N1)+A(N+1,L+1)*JL(L+1)*PL(L+1)
FLM(N,M,N1)=FLM(N,M,N1)+B(N+1,L+2)*JL(L+2)*PH(L+2)*C1
LL=PL-L
ALL=OF(LL+1)
FLM(N,M,NN+1)=FLM(N,M,NN+1)+A(NN+1,LL+1)*JL(LL+1)*PL(LL+1)*C1
FLM(N,M,NN+1)=FLM(N,M,NN+1)+B(NN+1,LL+2)*JL(LL+2)*PH(LL+2)
10 CONTINUE
GO TO 9
91 N1=NN+1
DO 92 N=1,N1
FLM(N,M,N)=FLM(N,M,N)
92 FLM(N,M,N)=FLM(N,M,N)
9 CONTINUE
100 CONTINUE

DO 35 K=1,NXX
DO 36 L=1,NXX
GSAO(K,L)=OPAD(1)*FLMO(1,L)
GSAO(K,L)=AZ*GSAO(K,L)+OPAD(2)*VV(2,Z)*FLMO(2,L)

```



```

,+VV(3,2)*FL*0(L+L+1)+VV(4,2)*FL*0(L+L+2)+VV(5,2)*FL*0(L+L+3)
GHBAD(K,L)=BZ*GSABD(K,L)+DPRO(3)*VV(2,J)*FL*0(L+L)
,+VV(3,3)*FL*0(L+L+1)+VV(4,3)*FL*0(L+L+2)+VV(5,3)*FL*0(L+L+3)
GSAB(K,L)=DPFL(I)*FL*0(L+L)
GHBAD(K,L)=BZ*GSAB(K,L)+DPL(2)*VV(2,2)*FL*0(L+L)
,+VV(3,2)*FL*0(L+L+1)+VV(4,2)*FL*0(L+L+2)+VV(5,2)*FL*0(L+L+3)
GHBAD(K,L)=BZ*GSAB(K,L)+PAL(1)*VV(2,J)*FL*0(L+L)
,+VV(3,3)*FL*0(L+L+1)+VV(4,3)*FL*0(L+L+2)+VV(5,3)*FL*0(L+L+3)
36 CONTINUE
  DO 35 L=1,J
    DPRO(L)=DPRO(L)+DL*NL
37  DPL(L)=DPL(L)+DL*NL
    SABD=C
    HSBFD=C
    HSBFD=C
    SABD=C
    HSBFD=C
    DO 540 IP=1,NP
      SABD=C
      HSBFD=C
      SABD=C
      HSBFD=C
      DO 540 IP=1,NP
        SABD=C
        HSBFD=C
        SABD=C
        HSBFD=C
        QI=1,GOO
        DO 550 IQ=1,NQ
          NI=NP+NG+1-IP-IQ
          NZ=IP+IQ-1
          CCQ=OG(INC)/OG(IQ)/OG(NQ-1Q+1)*QI
          SABQI=SABD1+GSAB(L,N1,N2)+CCQ
          IF(NL.EQ.1) GO TO 551
          HSBQI=HSBD1+GHB(L,N1,N2)*CCQ
          HBAQI=HBAQI+GHBAL(NL-1,N2)*CCQ*(OF(INC)-OF(IQ))/OF(NQ)
551 CONTINUE
        SABR=C
        HSBR=C
        HSBR=C
        CR=1,GOO
        DO 545 IR=1,2
          RI=NP+NQ+IP-IP-IQ
          RZ=IP+IQ+IR-2
          SARIR=SABD1+SABD(R1,P2)+CR
          IF(NL.EQ.1) GO TO 545
          HBAR=HSDR+HSDO(N1-1,N2)+CR
          HBAR=HBAR+HSDO(N1-1,P2)+CR
545 CR=CR
          SABQI=SABQI+SABR*CCQ
          HSBQI=HSDI+HSDI*HSDR*CCQ
          HBAQI=HBAQI+HBAI*CCQ*(OF(INC)-OF(IQ))/OF(NQ)
550 QI=QI
          CCQ=OG(NP)/OG(IP)/OG(NP-IP+1)
          SABPD=SABPD+SABQI*CCQ
          HSBPD=HSDPD+HSDQI*CCQ
          HBAQI=HBAQI+HBAQI*CCQ
          SABPI=SABPI+SABQI*CCQ
          HSBPI=HSDPI+HSDQI*CCQ
          HBAPI=HBAPI+HBAQI*CCQ
540 CONTINUE
          SABXQ=SABXQ+SABPD*HXC(IX)
          HSBXQ=HSDXQ+HSDPD*HX(IX)
          HBAQI=HBAQI+HBAQI*HX(IX)
          SABXI=SABXI+SABPI*HX(IX)
          HSBXI=HSDXI+HSDPI*HX(IX)
          HBAXI=HBAXI+HBAPI*HX(IX)
530 CONTINUE
          CCQ=BCQF(2)*RZ*(NXA(1)+NXB(1))
          SABJO=SABJO+SABQI*CCQ
          HSBJO=HSDJO+HSDQI*CCQ
          HBAQI=HBAQI+HBAQI*CCQ
          SABJI=SABJI+SABQI*CCQ
          HSBJI=HSDJI+HSDQI*CCQ
          HBAJI=HBAJI+HBAQI*CCQ
520 CONTINUE
          CCI=ACD(PI)*RZ
          SABDI=SABDI+SABQI*CCI
          HSBDI=HSDI+HSDQI*CCI
          SABII=SABII+SABQI*CCI
          HSBII=HSDI+HSDQI*CCI
          SABII=SABII+SABQI*CCI
          HSBII=HSDI+HSDQI*CCI
510 CONTINUE
          SABZ=SABD1*RZ
          HSBZ=HSD1/Z/Z
          HDALZ=DCGAN(I+HDAI0)/Z/Z

```

```

SABX=SAB11+R2
HABX=HAB11/22/22
HBAX=OCCNJJ1-HBA11/22/22

```

```

FORM LINEAR COMBINATIONS
COLTA=V*TIME(11)/P(111)
SOLTA=RHG/R(111)
SABP(11)=SABX*COLTA+SAB1*5OLTA
HABP(11)=HABX*COLTA+HAB1*5OLTA
HBAP(11)=HBAX*COLTA+HBAL*5OLTA
SABP(111)=SABX*5OLTA+SAB2*COLTA
HABP(111)=HABX*5OLTA+HAB2*COLTA
HBAP(111)=HBAX*5OLTA+HBAL*COLTA
SABP(1111)=OCCNJG(5SABP(111))
HABP(1111)=OCCNJG(5HABP(111))
HBAP(1111)=OCCNJG(5HBAP(111))
SABP(11111)=OCCNJG(SABP(111))
HABP(11111)=OCCNJG(HABP(111))
HBAP(11111)=OCCNJG(HBAP(111))

```

500 CONTINUE

```

CALL MHS(ACDEF,AXP,NXB,NA,3,HAB)
CALL HHP(BCDEF,BXP,NXB,NB,2,HBPX,HBPZ)

```

```

RETURN
END

```

```

SUBROUTINE MHS(ACDEF,AXP,NXB,NC,NV,HH)
IMPLICIT REAL(8)-D=1
COMMON INP(11)/V,RH,RP,FI,PI,NT,INT,MNTI
COMMON INP(12)/I(150),TIME(150),ZL,Z2
COMMON P(NT)/OL,NV(1),VC(1,3),AZ,BA,Z(1)
COMMON CCNST/5(125,25),T(25,25),OPE(30),GG(30)
DIMENSION COEF(NC),CXP(AC),NXC(NC)
DIMENSION F(30),FF(30),GA(30),GG(30)
DIMENSION C(13),HH(150)
C=D-300
ZL=BA
IF(NV.EQ.2) Z2=AZ
Z2=Z(NV)
OL=OL(NV)
CV(1)=VC(1,NV)
CV(2)=VC(2,NV)
CV(3)=VC(3,NV)
DO 100 I=1,MNTI
ITT=NT-IT-1)
RZ=R(11)/2.000
HI=C
DO 200 I=1,NC
HJ=C
RL=NXC(I)
NI=NI+I
DO 300 J=1,NC
HP=C
NJ=NXC(J)
NM=NI+NJ
A=(CXP(11)+CXP(J))42
BA=
AA=A+OL*HR
BB=B-OL*HR
NKG=NM+3=1

GX=C
FFX=C
GG=C
IF(1.000+5).LE.I,200+02) GX=DEXP(-2.000+5)
IF(1.000+5).LE.I,200+02) GG=CXP(1-2.000+5)
IF(DABS(BB-BA)) .LE.1.00+02) FFX=DEXP(BB-BA)
F(1)=1.000/A
FF(1)=FFX/AA
G(1)=1.000-GX/5
GG(1)=1.000-GG/50
GM=1.000
DO 10 K=2,NM3
FK=(OF(K)+F(K-1))/A+F(1)
FF(K)=(OF(K)+FF(K-1))/AA+FF(1)
GK=(OF(K)+G(K-1)+GM-GX)/5
GG(K)=(OF(K)+GG(K-1)+GM-GG)/50
10 GM=GM

DO 400 IP=1,N11
HO=C
DO 500 IC=1,NJ

```

```

N=NN+J-IP-10
M=IP-10
Q=PP (N) *GG (M)
Q1=CVE (1,N) * (N+1) *GG (N) -P (N) *GG (N+1)
Q2=CVE (2,N) *P (N+2) *GG (N) -2.000 *P (N+1) *GG (N+1) +P (N) *GG (N+2)
Q3=CVE (3,N) *P (N+1) *GG (N) -1.000 *P (N+2) *GG (N+1)
  -P (N+1) *GG (N+2) -P (N) *GG (N+3)
Q=ZZI *P (N) *GG (N) +ZZ2 * (Q1+Q2+Q3)
CQ=OG (N,1) /DG (1,1) /GG (N,1)
500 CONTINUE
CP=OG (N,1) /DG (1,1) /DG (N,1) +P (2)
HP=HPHQ *CP
400 CONTINUE
CJ=CDEF (J) * (RZ *NN)
HJ=HJ+HP *CJ
300 CONTINUE
CI=CDEF (I)
HPI=HJ+CI
200 CONTINUE
HH (IT) =HH (I) /2.000 /ZZ /ZZ
HH (IT) =HH (IT)
100 CONTINUE

RETURN
END

SUBROUTINE HPI (CDEF,XP,NXC,NC,NV,HPPX,HPIZ)
IMPLICIT REAL*8 (A-H,O-Z)
COMMON I,IPC,T1,V,RHO,RN,T1,P1,NT,NNT,NNT1
COMMON J,IPC,T2/R1 (150),TIME (150),Z1,Z2
COMMON G,CNST/5 (25,25),T (25,25),DF (30),OG (30)
COMMON OR, CDEF (NC),CXP (NC),NXC (NC)
DIMENSION P (30),FF (30),G (30),GG (30)
DIMENSION C V (3),HPPX (150),HPIZ (150)
COMMON /PTN1 L/DL4V (3),VC (3),AZ,8Z,Z (3)
C=0.000
ZZ1=8Z
IF (NV.EC.2) ZZ1=AZ
ZZ2=1/NV
DL=DL+V (NV)
CV (1)=VC (1, NV)
CV (2)=VC (2, NV)
CV (3)=VC (3, NV)
DO 100 I=T1,NNT1
ITT=NNT-I-1
RZ=RL (IT) /2.000
H1=C
H11=C
DO 200 I=1,NC
HJ=C
HJ1=C
N1=NXC (I)
DO 300 J=1,NC
HP=C
HP1=C
HJ=NXC (J) -1
N1=NXC (I) +NXC (J)
NHO=NH*3
A=(CXP (I) +CXP (J)) *RZ
B=A
AA=A+DL *RZ
BB=B+DL *RZ
C=B+C
GGX=C
FFX=C
IF (I2.000*J).LE.1.200+J2) GX=CEXP (-2.000*B)
IF (I2.000*B) .LE.1.200+J2) GUX=DEXP (-2.000*B*B)
IF (DABS (J3-A)) .LE.1.00+J2) FFX=DE+PI (B-A)
F (I) =1.00/FX
FF (I) =FF *A/A
G (I) =1.00-GX /B
GG (I) =1.00-GGX /BB
GM=1.000
DO 10 K=1,NH3
F (K) =DF (K) *F (K-1) /A+FF (I)
FF (K) =DF (K) *FF (K-1) /A+FF (I)
G (K) = (DF (K) *G (K-1) +GM) *A /B
GG (K) = (DF (K) *GG (K-1) +GM) *GGX /BB
10 GM=GM
DO 400 IP=1,N1
H2=C
H21=C
DO 500 IQ=1,NJ

```

```

HRO=C
HRI=C
CR=1.000
DO #00 IR=1,2
HSD=C
HSI=C
CS=1.000
DO 700 IS=1,2
N=NXC(I)*NXC(J)+IR+IS-IP-IQ-2
M=[P+IQ+(R+S-3)
QQ=FF(N)*GG(M)
Q=(CV(I)*FF(N)+GG(M)-FF(N)*GG(M+1))
Q2=CV(I)*FF(N+2)*GG(M)-2.000*FF(N+1)*GG(M+1)+FF(N)*GG(M+2))
Q3=CV(I)*FF(N+3)*GG(M)-3.000*FF(N+2)*GG(M+1)
  +FF(N+1)*GG(M+2)+FF(N)*GG(M+3))
Q=Z1*F(N)*G(M)+Z2*(Q+Q2+Q3)
HSD=HSD+C
N=NXC(I)*NXC(J)+4-2*IR-IP-1Q
M=[P+IQ+2*(S-3)
QQ=FF(N)*GG(M)
Q1=CV(I)*FF(N+1)*GG(M)-FF(N)*GG(M+1))
Q2=CV(I)*FF(N+2)*GG(M)-2.000*FF(N+1)*GG(M+1)+FF(N)*GG(M+2))
Q3=CV(I)*FF(N+3)*GG(M)-3.000*FF(N+2)*GG(M+1)
  +FF(N+1)*GG(M+2)+FF(N)*GG(M+3))
Q=Z1*F(N)*G(M)+Z2*(Q+Q2+Q3)
HSI=HSI+C*CS
700 CS=-CS
HRO=HRO+HSD
HRI=HRI+HSI*CR
800 CR=-CR
CG=CG(I)/CG(IQ)/CG(N)-IQ+I)
MQO=HOO+RO*CI
RQI=HQI+RI*CO
500 CONTINUE
CP=CG(I)/CG(IP)/CG(N)-IP+I)
HP=HPQ+HQ*CP
HP I=HP I+H2I*CP
400 CONTINUE
CJ=CDEF(J)*(R2*NM)
HJQ=HJQ+HP*CJ
HJI=HJI+PI*CJ
300 CONTINUE
CJ=CDEF(I)
HJQ=HJQ+JP*CI
HJI=HJI+HJI*CI
200 CONTINUE
HZ=3.000*HIZ/2.000/Z2/Z2
HX=3.000*HIX/4.000/Z2/Z2
CD=V*V*TIME(I)*T1*H(I)/AL(I)/R1(I)
SDP=HCR*HCO/A1(I)/R1(I)
HHP(I)=CO*HX+DO*HE
HMP(I)=CO*HIX+DO*HX
HNP(I)=HHP(I)
HMP(I)=HMP(I)
100 CONTINUE
RETURN
END
SUBROUTINE DER(F,Y,YP)
IMPLICIT REAL*8 (A-H,O-Z)
COMPLEX*16 S5,A,8,AUDT,BOOT,ENT,CR,E
COMPLEX*16 S12,S21,H22,H21,SAB,S94,PAB,H8A
COMMON/MATRX/S12(150),H12(150),H21(150),H11(150),H22(150)
COMMON/IMPCT/V,VRNG,RM,TZ,PL,NT,NWF,NNT1
COMMON/WFV/EALP,ZA
COMMON/WP/EOTA,ZB
COMMON/IMPCT2,ZX(150)
DIMENSION Z(150),ANG( 5),VAL( 5),Y(4),YP(4)
CN1=OCMP(LX(3),O00,-1.000)
DO 301 I=1,NT
301 Z(I)=S12(I)
CALL DATSMT,TIME,Z,NT,1,ARG,VAL,5)
CALL DAL(IT,ARG,VAL,Z,5,1,E-5,1ER)
DO 302 I=1,NT
302 Z(I)=S21(I)+CN1
CALL DATSMT,TIME,Z,NT,1,ARG,VAL,5)
CALL DAL(IT,ARG,VAL,Z,5,1,E-5,1ER)
SAB=OCMP(LX(1),Z)
DO 303 I=1,NT
303 Z(I)=Z(I)
CALL DATSMT,TIME,Z,NT,1,ARG,VAL,5)
CALL DAL(IT,ARG,VAL,Z,5,1,E-5,1ER)
DO 304 I=1,NT

```

```

304 Z(1)=HZ(1)*CNI
CALL DATSM(T,TIME,Z,NT,1,ARG,VAL,S)
CALL DAL(1,T,ARG,VAL,Z2,S,1,E-S,IER)
HAB=DCNPLX(Z1,Z2)
DO 305 I=1,NT
305 Z(I)=HZ1(I)
CALL DATSM(T,TIME,Z,NT,1,ARG,VAL,S)
CALL DAL(1,T,ARG,VAL,Z1,S,1,E-S,IER)
DO 306 I=1,NT
306 Z(I)=H21(I)*CNI
CALL DATSM(T,TIME,Z,NT,1,ARG,VAL,S)
CALL DAL(1,T,ARG,VAL,Z2,S,1,E-S,IER)
HBA=DCNPLX(Z1,Z2)
DO 307 I=1,NT
307 Z(I)=H11(I)
CALL DATSM(T,TIME,Z,NT,1,ARG,VAL,S)
CALL DAL(1,T,ARG,VAL,Z1,S,1,E-S,IER)
HAB=Z1
DO 304 I=1,NT
308 Z(I)=H21(I)
CALL DATSM(T,TIME,Z,NT,1,ARG,VAL,S)
CALL DAL(1,T,ARG,VAL,Z2,S,1,E-S,IER)
HBB=Z2
SBA=DCNJS(SAB)
ENT=DCNPLX(0.000,T*E(ETA-EALP))
SS=(1.000-SAB*SSA)*10.000,1.000)
SS=1.000/SS
A=DCNPLX(Y(1),Y(2))
B=DCNPLX(Y(3),Y(4))
ADDT=SS*(A*(HAA-SAB*HBA)+B*(HAS-SAB*HBS)*CDEXP(ENT))
BDOT=SS*(A*(HBB-SBA*HAB)+B*(HBA-SBA*HAA)*CDEXP(-ENT))
YP(1)=ADCT
YP(2)=ADCT*CHI
YP(3)=BDCT
YP(4)=BDCT*CHI
RETURN
END
SUBROUTINE DCUPEQIN,NCODE)
IMPLICIT REAL*8 (A-H,C-Z)
COMPLEX*16 GG,SU,A,X,ENT,U,CHI,PRMP
COMPLEX*16 X2B(400),XSA(600)
COMPLEX*16 C1(600),C2(600),DELTA(600)
COMPLEX*16 S12,S21,W12,W21
COMPLEX*16 SAB(400),SBA(600),HAB(400),HSA(600)
COMPLEX*16 ALP(600),ATA(600),AA(600),BB(600),CA(600),CB(600)
COMPLEX*16 Y1,Y2,Y3
COMMON/MATRIX/S12(150),S21(150),H11(150),H22(150)
COMMON/OPTV/LENET,HN,IPNCH,IREO,IPNT1,IPNT2,NITP,NDAB,NCAS
DIMENSION HA(600),HB(600)
DIMENSION A(600),VAL(10),TIME(600),R(600),Z(150)
COMMON/IMPCT/VA,RMC
COMMON/IMPCT2/BA(150),T(150)
COMMON/IMPCT3/EB(20),EINPT(10),NRG,NEV,LEV,IPB
,PRB(2,10,20),BAPB(2,10,20),PRMP(2,10,20)
COMMON/AF/EALP,ZA
COMMON/AF/EETA,ZB

CNI=DCNPLX(0.000,-1.000)
SET UP TIME VECTOR
TI=TI(1)
HM=10.00 C*TI/(E31.000*HM)
K=0
HH=HH+1
92 CONTINUE
DO 91 I=1,HH
91 TIME(K*HH+I)=TI+(I-1)*HM
K=K+1
IF(K.GT.4) GO TO 93
TI=TIME(K*HH+1)
HM=Z.000
GO TO 92
93 CONTINUE
NNT=5*HH
NNT1=NNT+1
NT=2*NNT+1
DO 98 I=1,NNT1
II=NNT-(I-1)
TIME(II)=TIME(II)
R(II)=CDSQRT(RND**2*(V+TIME(II))*2)
R(II)=R(II)
98 CONTINUE
EALP=Z5*V*V
NR=2*H-1

```

```

      DO 300 K=1,NNTL
      KK=NT-(K-1)
      DO 301 I=1,N
301  Z(I)=S1Z(I)
      CALL DATSMITIME(K),T,Z,N,I,ARG,VAL,5)
      CALL DAL1 (TIME(K),ARG,VAL,Z1,5,1.E-5,IER)
      DO 302 I=1,N
302  Z(I)=S1Z(I)*CM1
      CALL DATSMITIME(K),T,Z,N,I,ARG,VAL,5)
      CALL DAL1 (TIME(K),ARG,VAL,Z2,5,1.E-5,IER)
      SAA(K)=DCMPLX(Z1,Z2)
      DO 303 I=1,N
303  Z(I)=H2Z(I)
      CALL DATSMITIME(K),T,Z,N,I,ARG,VAL,5)
      CALL DAL1 (TIME(K),ARG,VAL,Z1,5,1.E-5,IER)
      DO 304 I=1,N
304  Z(I)=H2Z(I)*CM1
      CALL DATSMITIME(K),T,Z,N,I,ARG,VAL,5)
      CALL DAL1 (TIME(K),ARG,VAL,Z2,5,1.E-5,IER)
      HAA(K)=DCMPLX(Z1,Z2)
      DO 305 I=1,N
305  Z(I)=H2I(I)
      CALL DATSMITIME(K),T,Z,N,I,ARG,VAL,5)
      CALL DAL1 (TIME(K),ARG,VAL,Z1,5,1.E-5,IER)
      DO 306 I=1,N
306  Z(I)=H2I(I)*CM1
      CALL DATSMITIME(K),T,Z,N,I,ARG,VAL,5)
      CALL DAL1 (TIME(K),ARG,VAL,Z2,5,1.E-5,IER)
      HBA(K)=DCMPLX(Z1,Z2)
      DO 307 I=1,N
307  Z(I)=H3I(I)
      CALL DATSMITIME(K),T,Z,N,I,ARG,VAL,5)
      CALL DAL1 (TIME(K),ARG,VAL,Z1,5,1.E-5,IER)
      HAA(K)=Z1
      DO 308 I=1,N
308  Z(I)=H2Z(I)
      CALL DATSMITIME(K),T,Z,N,I,ARG,VAL,5)
      CALL DAL1 (TIME(K),ARG,VAL,Z2,5,1.E-5,IER)
      HBB(K)=Z2
500  CONTINUE

      DC=1.000
      IF(NCCOE.EQ.2) DC=-1.000
      DO 600 I=1,NNTL
      II=NT-(I-1)
      SBA(I)=DC*CNJG(SAB(I))
      SAA(I)=DC*CNJG(SAB(I))*DC
      SBA(I)=DC*CNJG(SBA(I))*DC
      HBA(I)=DC*CNJG(HAB(I))*DC
      HAA(I)=DC*CNJG(HAB(I))*DC
      HBA(I)=HAA(I)
      HBB(I)=HBB(I)

      S5=1.000-SAB(I)*SAA(I)
      HAA(I)=HAA(I)-SAB(I)*HBA(I)/S5
      HBB(I)=HBB(I)-SBA(I)*HAB(I)/S5
      IF(1.EQ.NNT) GO TO 600
      HAA(I)=DC*CNJG(HAA(I))
      HBB(I)=DC*CNJG(HBB(I))
600  CONTINUE

      IF(1PNT1.EQ.0) GO TO 11
      PRINT 520
520  FORMAT(' ',///50A,'INTERPLATED MATRIX ELEMENTS'///)
      PRINT 521
521  FORMAT(' TIME...R SAA...HAB...HBA...HAA...HBB '///)
      DO 507 I=1,NNT1,NT1P
507  PRINT 508,TIME(I),P(I),SAB(I),HAB(I),HAA(I),HBB(I)
508  /GAMATL1Z1X,P10,58,2X,41P011,4X,1P011,4X,2X)
      11  CONTINUE

      NT=NT-1
      DELTAX(I)=60.000,0.000)
      ALP(I)=1.E+000,0.000)
      STA(I)=10.000,0.000)
      DO 700 J=2,NTI
      XJ=TIME(I,J)
      XZ=TIME(I,J)
      X3=TIME(I,J+1)
      Y1=AA(I,J-1)
      Y2=AA(I,J)
      Y3=AA(I,J+1)
      ALP(J)=ALP(I,J-1)*SUM(X1,X2,X3,Y1,Y2,Y3)
      Y1=0B(I,J-1)

```

```

Y2=BB(J)
Y3=BB(J+1)
BTA(J)=BTA(J-1)+SUM(X1,X2,X3,Y1,Y2,Y3)
700 DELTA(J)=ALP(J)-BTA(J)
X3=TIME(NT)
X2=TIME(NT1)
X1=TIME(NT1-1)
Y1=AA(NT)
Y2=AA(NT1)
Y3=AA(NT1-1)
ALP(NT)=ALP(NT1)+SUM(X1,X2,X3,Y1,Y2,Y3)
Y1=BB(NT)
Y2=BB(NT1)
Y3=BB(NT1-1)
BTA(NT)=BTA(NT1)+SUM(X1,X2,X3,Y1,Y2,Y3)
DELTA(NT)=ALP(NT)-BTA(NT)

DO 800 K=1,NT
DELTA(K)=DELTA(K)-TIME(K)*EALP-ZETA)
SS=L,DOO-SAB(K)*SBA(K)
Y3=COEXP(DELTA(K)/CR1)
XAB(K)=(HAB(K)-SAB(K)*HBB(K))*CM1*Y3/SS
XBA(K)=(HBA(K)-SBA(K)*HBA(K))*CM1/Y3/SS
OA(K)=(L,DOO,0,000)
800 OB(K)=(C,DOO,2,000)

SS3=0,000
DO 1000 K=1,LIMIT
OA(1)=(L,DOO,0,000)
OB(1)=(C,DOO,0,000)
DO 900 J=2,NT1
X1=TIME(J-1)
X2=TIME(J)
X3=TIME(J+1)
Y1=XBA(J-1)*OA(J-1)
Y2=XBA(J)*OA(J)
Y3=XBA(J+1)*OA(J+1)
900 OB(J)=OB(J-1)+SUM(X1,X2,X3,Y1,Y2,Y3)
X3=TIME(NT)
X2=TIME(NT1)
X1=TIME(NT1-1)
Y1=XBA(NT)*OA(NT)
Y2=XBA(NT1)*OA(NT1)
Y3=XBA(NT1-1)*OA(NT1-1)
OB(NT)=OB(NT1)+SUM(X1,X2,X3,Y1,Y2,Y3)
DO 950 J=2,NT1
X1=TIME(J-1)
X2=TIME(J)
X3=TIME(J+1)
Y1=XAB(J-1)*OB(J-1)
Y2=XAB(J)*OB(J)
Y3=XAB(J+1)*OB(J+1)
950 OA(J)=OA(J-1)+SUM(X1,X2,X3,Y1,Y2,Y3)
X3=TIME(NT)
X2=TIME(NT1)
X1=TIME(NT1-1)
Y1=XAB(NT)*OB(NT)
Y2=XAB(NT1)*OB(NT1)
Y3=XAB(NT1-1)*OB(NT1-1)
OA(NT)=OA(NT1)+SUM(X1,X2,X3,Y1,Y2,Y3)
IF(IIPNTZ,EO,0) GO TO 13
PRINT 21, K1
21 FORMAT(11 ITERATION=*,(3//)
PRINT 125
125 FORMAT(4X,4X,'TIME',2X,'OA',3X,'OB'//)
DO 22 I=1,NT,NCAB
22 PRINT 23, TIME(I),OA(I),OB(I)
23 FORMAT(2X,F12.0X,4X,E16.7)
13 CONTINUE

SS1=0,000
SS2=0,000
DO 960 I=1,NT
SS1=SS1+CBASS(OA(I)-OB(I))
960 SS2=SS2+CBASS(OB(I))
SSZ=SS1/SS2
1000 CONTINUE

2000 CONTINUE
PRINT 3
3 FORMAT(///' R UA..UB XAB..XBA CA..CB..PROC..UNITARITY'//)
DO 50 I=1,NT,NCAB
CA(I)=OA(I)*L*EXP((C,DOO,-L,000)*ALP(I))

```

```

CB11)=0811)*COEXP(10.000,-1.000)*BTA(11)
PROB=CB(11)*OCUNJG(CB11)
ENN=TIME(11)*CALP=ESTAI
ENT=DCMPLX(0.000,-ENN)
UNIT=PROB*CA(11)*CCNJG(CA11)
U=OCNJG(CA(11)*CB(11)*SAB(11)*COEXPIENT)
UNIT=UNIT*U=OCUNJG(U)
UNIT=1.000-UNIT
SS=1.000-SAB(11)*SBA(11)
X1=(HBA(11)-SAB(11)*SBA(11))/SS-EALP
X2=(HBB(11)-SBA(11)*HBA(11))/SS-EUTA
Y1=(HBA(11)-SAB(11)*HBA(11))/SS
Y2=(HBA(11)-SBA(11)*HBA(11))/SS
30 PRINT 60, R(1),X1,X2,Y1,Y2,CA(11),CB(11),PROB,UNIT
60 FORMAT(1X,F9.3,12(1X,1P09.21)

SP=PROB*(BI(IP))
PRINT 229,SP,EC(IP),E[MYT(LEV)
229 FORMAT(' ',PHCB*RD='',E12.5,' AT RHD=',F8.4,' EKEV=',F10.3/)
PRB(INCODE,LEV,IP)=PROB
BRPB(INCODE,LEV,IP)=SP
PRNP(INCODE,LEV,IP)=CB(11)
RETURN
END

```


APPENDIX III

Appendix III includes the publication of which this work is an extension.

Two-state atomic expansion methods for electron capture from multielectron atoms by fast protons

C. D. Lin, S. C. Soong,* and L. N. Tunnell

Department of Physics, Kansas State University, Manhattan, Kansas 66506

(Received 19 May 1977; revised manuscript received 13 October 1977)

The two-state, two-center atomic expansion method of Bates for charge transfer is generalized to calculate cross sections of electron capture from inner shells of multielectron atoms by fast protons. In the limit of small capture probabilities, the connections of the present approach with various first-order Born theories are investigated. It is shown that these Born methods for electron capture of multielectron atoms can be obtained from the present approach by further approximations. The method is applied to obtain cross sections of electron capture from C, N, O, Ne, and Ar atoms by fast protons in the energy region where the projectile velocity is nearly equal to the *K*-shell electron orbital velocity of these atoms. Results of the calculations are compared with experimental measurements.

I. INTRODUCTION

The transfer of an electron from target to projectile during ion-atom collisions is the subject of recent experimental and theoretical investigations. It is known that this process plays an important role in vacancy production in ion-atom collisions.¹

For collisions in which the projectile velocity is much smaller than the characteristic orbital velocity of the active electron to be transferred, the molecular theory (MO) of Fano and Lichten² has been applied successfully to explain qualitatively the observed low-energy ion-atom collision phenomena.³ Recent developments by Briggs and Macek,⁴ and by Taulbjerg et al.⁵ have put the MO theory in quantitative form for *K*-shell vacancy transfer in symmetric and asymmetric ion-atom collisions.

For fast collisions such that the projectile velocity is comparable to or greater than the characteristic orbital velocity of the active electron, the capture of bound electrons from the target atom is less well understood. Whereas the first Born approximation or its variations have been useful in describing excitation and ionization in fast collisions,⁶ considerable contention still persists in the application of the first Born theory in rearrangement collisions, particularly for the electron-capture process.^{7,8} Even in the simplest resonant charge-transfer process, $p + \text{H}(1s) \rightarrow \text{H}(1s) + p$, the various first Born theories predict substantially different capture cross sections. Attempts to generalize these first-order Born theories to multielectron ion-atom collisions create even further questions.

Historically, the $p + \text{H}(1s) \rightarrow \text{H}(1s) + p$ resonant charge exchange has been calculated in the Oppenheimer,⁹ Brinkman, and Kramers (OBK)¹⁰ approxi-

mation. In the OBK approximation, the nuclear-nuclear interaction was completely neglected in evaluating the first Born transition amplitude. This is justified in that the nuclear-nuclear interaction can only deflect the trajectory of the projectile and does not change substantially the total electron-capture cross sections. Later, similar first-order approximations were adopted by Bates and Dalgarno,¹¹ and by Jackson and Schiff¹² (JS), but with the internuclear potential also included in the first Born amplitude.¹¹ As argued by Bates and Dalgarno, the complete nuclear-nuclear interaction is included in the perturbation on the grounds that this would compensate to some extent for the nonorthogonality of the wave functions of the initial and final states, and would consequently lead to more realistic cross sections.¹³ Interestingly, the cross sections calculated in this method are much smaller than those calculated by the OBK method and agree much better with experimental data.

Recently, both the OBK and JS methods have been generalized to calculate electron-capture cross sections in multielectron ion-atom collisions.^{14,15} Like the prediction in the proton-hydrogen resonant capture, the OBK approximation always predicts cross sections much higher than experimental results. Diverse efforts have been attempted to correct this either by reducing the OBK prediction by a semiempirical factor,^{16,17} by semiempirical method,¹⁸ or by introducing different amounts of core-core interactions.¹⁹

The straightforward generalization of the JS method includes the interaction between the two bare nuclei in the perturbation.^{14,15,17} This method apparently fails because the predicted capture cross sections are a few orders of magnitude too high. For example, cross sections for the

capture of *K*-shell electrons of Ar atoms by protons are predicted to be about 320 times larger than experimental data.¹⁶

Much of the discrepancy mentioned in the above is due to the fact that no proper allowance had been made for the nonorthogonality of the initial- and final-state wave functions. Bates¹⁷ was the first to note that if the nonorthogonality is properly treated, the difficulty formally associated with the choice of internuclear potential can be resolved.

In this paper, we extend the method of Bates to electron capture in multielectron ion-atom collisions within the independent-electron approximation. This approximation treats only the electron to be transferred as active; the others are treated as passive and provide only screening during the collision process.

In Sec. II, the Bates method is reviewed. The connections of Bates method, in the limit of small capture probability, to the different first Born methods are discussed in Sec. III. In Sec. IV, this method is applied to the capture of *K*-shell electrons of C, N, O, Ne, and Ar atoms by fast protons. The validity of the present method is discussed in Sec. V.

II. ATOMIC EXPANSION METHOD

Developed by Bates in 1958, the atomic expansion method was designed to properly account for the nonorthogonality of the initial- and final-state wave functions in the electron-capture process.

In the Bates method, the motion of the electrons and the nuclei in ion-atom collisions is separated by using the perturbed-stationary-state (pss) method¹⁸; the motion of the nuclei is treated classically. The attractive nuclear field experienced by the electrons during the collision depends upon the trajectories of the two nuclei. In this paper, we are dealing with high-velocity projectiles; thus straight-line trajectories will be adopted.

To study electron-capture problems in multi-electron ion-atom collisions, many approximations can be made if only the capture of inner-shell electrons is to be treated. In principle, the Bates approach can be used to deal with multi-electron wave functions. However, it has been shown that electron correlation and exchange effects are not very important for the electron-capture process in the proton-helium system.^{16,19} We thus expect the independent-electron model to be adequate, particularly for capture from the inner shells of atoms.

In this approximation, the wave function of the active electron is governed by the time-dependent

Schrödinger equation

$$\left(H_e - i \frac{\partial}{\partial t} \right) \Psi(\vec{r}, t) = 0, \quad (1)$$

where

$$H_e = -\frac{1}{2} \nabla^2 - Z_A/r_A - Z_B/r_B \quad (2)$$

is the effective Hamiltonian of the active electron. In Eq. (2), Z_A and Z_B are the effective charges experienced by the electron; r_A and r_B are the positions of the electron with respect to the target *A* and to the projectile *B*, respectively. Atomic units will be used.

Equations (1) and (2) are to be solved with proper boundary conditions at $t = -\infty$. The method adopted by Bates is to expand $\Psi(\vec{r}, t)$ in terms of the traveling eigenstates of the target and of the projectile. The following derivation can be found in the paper of Bates¹⁷ or in the book by McDowell and Coleman.⁹ We will summarize it below for later discussion.

The time-dependent wave function $\Psi(\vec{r}, t)$ can be expanded generally as

$$\begin{aligned} \Psi(\vec{r}, t) = & \sum_a \alpha_a(t) \phi_a(\vec{r}_A) \exp[-i(\frac{1}{2} \vec{v} \cdot \vec{r} + \frac{1}{2} v^2 t + \epsilon_a t)] \\ & + \sum_b \beta_b(t) \phi_b(\vec{r}_B) \\ & \times \exp[-i(-\frac{1}{2} \vec{v} \cdot \vec{r} - \frac{1}{2} v^2 t + \epsilon_b t)], \quad (3) \end{aligned}$$

where $\phi_a(\vec{r}_A)$ [$\phi_b(\vec{r}_B)$] is the stationary eigenfunction of the target [projectile] with eigenenergy ϵ_a [ϵ_b], \vec{v} is the velocity of the projectile in the laboratory frame and \vec{r} is the position vector of the electron with respect to the midpoint of the internuclear axis.¹⁹ In Eq. (3), the velocity-dependent exponents are introduced to preserve translational invariance.

To describe electron capture, the simplest approximation to Eq. (3) is to retain only the two states which are relevant to the capture process, the initial state of the target and the final state of the projectile. To simplify the notation, we rewrite Eq. (3) (in a self-evident way) as

$$\begin{aligned} \Psi(\vec{r}, t) = & a(t) \phi_A \exp[-i(\frac{1}{2} \vec{v} \cdot \vec{r} + \frac{1}{2} v^2 t + \epsilon_A t)] \\ & + b(t) \phi_B \exp[-i(-\frac{1}{2} \vec{v} \cdot \vec{r} - \frac{1}{2} v^2 t + \epsilon_B t)]. \quad (4) \end{aligned}$$

Substitution of Eq. (4) into Eq. (1) yields a set of coupled equations:

$$i(1 - \sigma^2) \dot{a} = a(\lambda_{AA} - \sigma_{AB} \lambda_{BA}) + b(\lambda_{AB} - \sigma_{BA} \lambda_{AA}) \sigma^{i\omega}, \quad (5)$$

$$i(1 - \sigma^2) \dot{b} = b(\lambda_{BB} - \sigma_{BA} \lambda_{AB}) + a(\lambda_{BA} - \sigma_{AB} \lambda_{BB}) \sigma^{-i\omega},$$

where $\omega = \epsilon_A - \epsilon_B$ and

$$\begin{aligned}
 s_{AB} &= \int \phi_A^* \phi_B e^{i(\mathbf{r}^2/\tau)} d\tau, \\
 s_{BA} &= \int \phi_B^* \phi_A e^{i(\mathbf{r}^2/\tau)} d\tau, \\
 h_{AB} &= \int \phi_A^* (-Z_A/r_A) \phi_B e^{i(\mathbf{r}^2/\tau)} d\tau, \\
 h_{BA} &= \int \phi_B^* (-Z_B/r_B) \phi_A e^{i(\mathbf{r}^2/\tau)} d\tau, \\
 h_{AA} &= \int \phi_A^* (-Z_A/r_A) \phi_A d\tau, \\
 h_{BB} &= \int \phi_B^* (-Z_B/r_B) \phi_B d\tau,
 \end{aligned}
 \quad (6)$$

and where the integration is over the electronic coordinates. The identities $s_{BA} = s_{AB}^*$ and $s^2 = s_{AB} s_{BA}$ are obvious.

Introducing the transformation

$$\begin{aligned}
 a(t) &= d_A(t) \exp\left(-i \int_{-\infty}^t \alpha(t') dt'\right), \\
 b(t) &= d_B(t) \exp\left(-i \int_{-\infty}^t \beta(t') dt'\right).
 \end{aligned}
 \quad (7)$$

Eq. (5) are simplified to

$$\begin{aligned}
 i \dot{d}_A &= \frac{h_{AB} - s_{BA} h_{BA}}{1 - s^2} e^{i \omega t} d_B, \\
 i \dot{d}_B &= \frac{h_{BA} - s_{AB} h_{AB}}{1 - s^2} e^{-i \omega t} d_A,
 \end{aligned}
 \quad (8)$$

where

$$\alpha = \int_{-\infty}^t [\alpha(t') - \beta(t')] dt'
 \quad (9)$$

and

$$\begin{aligned}
 \alpha(t) &= (h_{AA} - s_{AB} h_{BA}) / (1 - s^2), \\
 \beta(t) &= (h_{BB} - s_{BA} h_{AB}) / (1 - s^2).
 \end{aligned}
 \quad (10)$$

Equations (8) are to be solved with the boundary conditions $d_A(-\infty) = 1$, $d_B(-\infty) = 0$ for each impact parameter ρ and each energy. The total capture cross section per atom is obtained from

$$Q = 2\pi N_A \int_0^\infty \rho d\rho p(\rho),
 \quad (11)$$

where $p(\rho) = |b(-\infty)|^2$ is the capture probability and N_A is the number of equivalent electrons in the target shell from which the active electron is captured.

III. CONNECTIONS WITH OTHER BORN APPROXIMATIONS

For collisions in which the capture probabilities are small, the capture amplitude can be solved

from Eqs. (8) by first-order approximation. If we set $d_A(t) = b$, then $d_B(t = \infty)$ is given by

$$d_B(+\infty) = -i \int_{-\infty}^{\infty} \frac{h_{BA} - s_{BA} h_{AB}}{1 - s^2} e^{-i \omega t} dt.
 \quad (12)$$

In Eq. (12), the transition amplitude $d_B(+\infty)$ can be easily shown to be independent of any arbitrary internuclear potentials added to the definitions of the matrix elements h_{BA} and h_{AB} . This is due to the fact that the nonorthogonality of initial and final states has been properly accounted for in Eq. (5) through the introduction of overlap integrals s_{AB} and s_{BA} .

The δ term in Eq. (12) represents the distortion of the electron wave function in the nuclear field of the projectile and the target in the two-state atomic expansion approximation. If this distortion is neglected, then Eq. (12) becomes

$$d_B(+\infty) = -i \int_{-\infty}^{\infty} \frac{h_{BA} - s_{BA} h_{AB}}{1 - s^2} e^{-i \omega t} dt.
 \quad (13)$$

For high-velocity collisions, $s^2 \ll 1$, Eq. (13) can then be written explicitly as

$$\begin{aligned}
 d_B(+\infty) &= -i \int_{-\infty}^{\infty} dt d\tau \phi_B \left[-\frac{Z_B}{r_B} - h_{AB} \right] \\
 &\quad \times \phi_A \exp[-i(\mathbf{r} \cdot \mathbf{v} - \omega t)],
 \end{aligned}
 \quad (14)$$

in a form similar to the first Born transition amplitude with $(Z_B/r_B) - h_{AB}$ as the interaction "potential." For capture from the K shell of target A to the K shell of projectile B , h_{AA} is

$$h_{AA} = (Z_B/R)^2 [1 + (1 - Z_A/R) e^{-2R/a_0}].
 \quad (15)$$

For the charge-exchange $p + H(1s) - H(1s) + p$, $Z_A = Z_B = 1$, Eq. (14) becomes identical to the distorted-wave approximation for electron capture derived by Bassel and Gerjuoy.¹⁸ Thus, Eq. (14) is the generalization of their method to arbitrary Z_A and Z_B . Incidentally, Eq. (14), or more rigorously, Eq. (13), can also be derived from the usual first Born theory if the final-state wave function is required to be orthogonal to the initial-state wave function. Thus, we show that in the limit of small capture probabilities, the two-state atomic expansion method of Bates, the distorted-wave approximation of Bassel and Gerjuoy and the first Born theory are all equivalent if the orthogonalized final state is used in the first Born theory.

To explore the meaning of Eq. (14) in more detail, we plot, in Fig. 1, $-R h_{AA}/Z_B$ as a function of $Z_A R$, where R is the internuclear separation. The function h_{AA} approaches zero as $Z_A R \rightarrow 0$ and approaches $-Z_B/R$ as $Z_A R \rightarrow \infty$. If

FIG. 1. Plot of $-RA_{AA}/Z_B$ as a function of Z_A/R .

k_{AA} is chosen to be zero in Eq. (14), we recover the usual OBK approximation. From Eq. (13), this is equivalent to neglecting the nonorthogonality of initial and final states as was done in the OBK approximation (by setting $k_{AA} = 0$). On the other hand, if the large- R limit of k_{AA} is used in Eq. (14), the expression in the squared bracket becomes $[-Z_B/v_B + Z_B/R]$. In the $\beta + H(1s) - H(1s) + \beta$ capture problem, it becomes $[-1/v_B + 1/R]$ and the second term resembles the internuclear interaction between the protons. This is equivalent to the method of JS in which the internuclear potential is included in the first Born transition amplitude. Therefore, we can interpret that the introduction of the internuclear interaction into the first Born transition amplitude has the effect of partially accounting for the nonorthogonality of the initial and final states in the $\beta + H(1s) - H(1s) + \beta$ reaction at intermediate and large R . However, this similarity cannot be generalized to ion-atom collisions of arbitrary Z_A and Z_B . The large R limit of k_{AA} is Z_B/R instead of the internuclear interaction $Z_A Z_B/R$. This partially explains why the straightforward generalization of the JS method to ion-atom collisions by including a full internuclear interaction results in unrealistic capture cross sections. Incidentally, the large- R limit of k_{AA} has also been introduced recently¹⁵ in the Born amplitude, under the assumption of almost complete screening of the target nucleus charge by the passive electrons. This assumption is not valid for the capture of K -shell electrons. It is better to interpret Z_B/R as an approximation of the nonorthogonality contribution to the Born amplitude for electron capture and has no relation with the internuclear potential.

It is not difficult to understand why the JS or the Born method of Ref. 15 usually gives better absolute total capture cross section than the OBK approximation. In Fig. 1, k_{AA} is well approximated by its large- R limit $-Z_B/R$ for R near or greater than the K -shell radius. Thus, if the total electron capture comes primarily from large impact parameter β , such $\beta Z_A > 1$, then the JS or the Born method of Ref. 15 will give

reasonable total capture cross sections [as compared with that obtained from Eq. (13)]. However, it must be realized that both methods will fail at small β or, correspondingly, at large scattering angles. Also, if the total capture cross section comes primarily from small impact parameters, then the total cross sections calculated from these two methods will be wrong.

It might then be speculated that the OBK method is a better approximation for collisions at small impact parameters. This is not quite true. For small impact parameters, the distortion of the active electron wave function by the projectile is very large and cannot be reasonably approximated by any first-order theory, even such as Eqs. (8) and (13).

IV. K-SHELL ELECTRON CAPTURE OF C, N, O, Ne, AND Ar ATOMS BY FAST PROTONS

The two-state atomic expansion method has previously been applied only to simple atomic systems. (See the review by Bransden.³) By comparing with experimental data or with more elaborate calculations, it is concluded that the simple two-state calculations predict reasonable capture cross sections when the projectile velocity is not very far away from the characteristic orbital velocity of the active electrons.

Theoretical calculations of electron-capture cross sections from multielectron atoms have been limited to the OBK or other Born methods.^{17,18} The results of these calculations are often unreliable. We have applied the two-state atomic expansion method, under the independent-particle approximation as outlined in Sec. II, to calculate the electron-capture cross sections of the K shell of carbon, nitrogen, oxygen, neon, and argon atoms by fast protons.

The numerical method is straightforward. A screened hydrogenic $1s$ wave function with effective charge $Z_A = Z - \sigma$, where Z is the nuclear charge of the target, is used for the target atom and a bare nuclear charge Z_B is used for the projectile. The matrix elements of Eq. (8) are evaluated by transforming the two-centered integrand to prolate spheroidal coordinates (λ, μ, ϕ) ,¹⁹ integrations over ϕ and μ can be carried analytically. The integration over λ is done using 24-point Gauss-Laguerre quadrature, although the 32-point formula has been used also to check the accuracy of the integration. The capture amplitude $b(-\infty)$, or equivalently $d(+\infty)$, is obtained by solving the coupled Eqs. (8), either by direct numerical integration or by an iterative method. The latter method is more suitable for calculating small amplitudes. In particular, the first it-

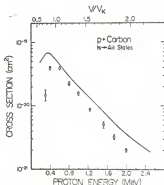


FIG. 2. Electron-capture cross sections from the K shells of carbon atoms by fast protons. The values are the total capture cross sections per target atom, including capture to the excited state of hydrogen atoms. The solid curve is the result of the present calculation. Experimental data are from Redero *et al.*, Ref. 32. Also shown are the values of WV_K , the ratio of the projectile velocity V to the characteristic K -shell orbital velocity of the target atom, defined by $V_K = \sqrt{2I_K}$, where I_K is the K -shell ionization energy.

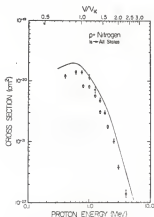


FIG. 3. Same as in Fig. 2, except for nitrogen atoms. Experimental data: \circ , from Redero *et al.*, Ref. 32; \square , from Cooke *et al.*, Ref. 32.

erative solution for $d_{\beta}(t, \mathbf{r})$ is then given by Eq. (12). Depending upon the systems, usually two or three iterations are enough for desirable accuracy. In solving Eqs. (8), we use experimental K -shell ionization energy for ϵ_A and $-Z_B^2/2$ for ϵ_B . By choosing ϵ_A and Z_B separately, the unitarity condition is not imposed in the calculation. This choice of ϵ_A is desirable because the capture probability, as given by its first-order solution Eq. (12), is dominated by the oscillatory function $e^{i\mathbf{k}\cdot\mathbf{r}}$ in the integrand, as well as the damped oscillation in the matrix elements of $-Z_B/r_B - \delta_{kA}$. This explains why the ODK approximation (obtained by letting $\delta_{kA} \rightarrow 0$) usually predicts correct energy dependence for the total capture cross sections, even though the absolute values are often wrong.

The calculated total capture cross sections from the K shells of C, N, O, Ne, and Ar atoms by protons are displayed in Figs. 2-6. They are the total capture cross sections per target atom, including capture to the excited states of the projectile. The theoretical values shown in the figures are obtained from the calculated $Is-Is$ nu-

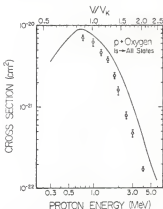


FIG. 4. Same as in Fig. 2 except for oxygen atoms. Experimental data from Cooke *et al.*, Ref. 32.

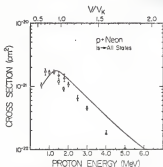


FIG. 5. Same as in Fig. 3 except for neon atoms. Experimental data: \circ , from R  dbr   *et al.*, Ref. 23; \square , Cocks *et al.*, Ref. 22.

ues by multiplying 1.2, corresponding to the high velocity $1/v^2$ scaling.²⁰ Experimental data shown on these figures are from Macdonald *et al.*,²¹ Cocks *et al.*,²² and from R  dbr   *et al.*²³ For

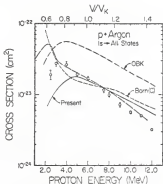


FIG. 6. Same as in Fig. 3 except for argon atoms. Other theoretical results: short-dashed lines, the Born (C) method of Ref. 15, dash-dotted lines, the OBK results of Ref. 15. Long-dashed lines, continuous distorted-wave (CDW) results of Ref. 24. Experimental data are from Macdonald *et al.*, Ref. 21.

C, N, and O, atoms, the experimental data are obtained from measuring capture in CH_4 , N_2 and O_2 gases. The experimental K -shell capture cross sections are not expected to change much by any molecular binding effect.

It can be seen from Figs. 2-6 that the calculated values are generally in good accord with experimental data. In Fig. 6, the results of the OBK approximation, the Born method of Omidvar *et al.*,¹⁵ and the continuum distortion-wave method of Belic and McCarroll¹⁴ are also shown for comparison. The OBK predictions shown in Fig. 6 are about three times too large when compared with experimental data. The Born method of Omidvar *et al.*¹⁵ predicts cross sections in reasonable agreement with data at higher energies but the predicted energy dependence differs from the experimental data. The continuum distorted-wave method of Belic and McCarroll¹⁴ also predicts cross sections in excellent agreement with experimental data at the high-energy side,²⁴ but the energy dependence at the low-energy side is also incorrect.

V. DISCUSSION

From the results of Figs. 2-6, it is clear that the simple two-state expansion method is capable of predicting capture cross sections in reasonable agreement with experimental data. However, further improvement of the model is possible. In the following we discuss the limitation of the present method and possible further improvement.

A. Atomic model

In Eqs. (1) and (2), we use the active-electron approximation by disregarding the effects of passive electrons. It is possible to formulate a many-electron theory of electron capture based upon the Bates formulation. In fact, such a theory has been written explicitly by Meezane²⁵ recently for the two-electron systems. However, the complexity of such a theory for general N -electron problem will make such a formulation impractical in view of the numerical difficulties.

Improvement in the atomic model within the independent-electron approximation can be proceeded by using a more realistic potential $V(r_A)$ for the target atom. For example, the Green-Seitlin-Zachor (GSZ) potential of Green *et al.*²⁶ can be introduced into the Hamiltonian (2).²⁶ These potentials predict the K -shell ionization energy accurately. We can thus use the eigenstates and eigenenergies generated from this potential in the expansion (4), thus preserving the unitarity relation in the coupled Eqs. (6) and (8). It is hoped that the choice of the more realistic potential will

improve the computed cross sections in the region where the cross section peaks. However, it is not expected that the improvement in the atomic model alone will make the theoretical calculations agree with experimental data over the entire energy range considered. The convergence of the truncated atomic expansion has to be investigated too.

B. Scattering model

To study the limitation of the two-state atomic expansion method, we examine the well-studied simple reaction $p + H(1s) \rightarrow H(1s) + p$. At the low-velocity limit, the potential curves of the quasi-molecule H_2^+ are exactly known. These potential curves describe the distortion of the atomic electron wave function by the projectile in the adiabatic limit. By comparing the potential curves calculated by the two-state atomic expansion with the exact H_2^+ potential curves,³⁹ we can conclude that the two-state representation is adequate for $R \gg 1.0$, but not smaller R . Therefore, we can expect the two-state atomic expansion method adequate for describing the collision $p + H(1s) \rightarrow H(1s) + p$ at impact parameters $p \gg 1.0$, but not at smaller impact parameters. If the total capture cross section comes primarily from the impact parameters $p \gg 1.0$, then the total capture cross section obtained from the two-state atomic expansion will be adequate. This occurs at the intermediate energy region where the projectile velocity nearly matches the orbital velocity of the target electron. As the velocity of the projectile increases, the capture has to occur at smaller

impact parameters for the projectile to pick up electrons close to the target nucleus, then the two-state atomic expansion becomes inadequate.⁴⁰

Within the method of Bates, the charge exchange $p + H(1s) \rightarrow H(1s) + p$ has been studied by the multi-state atomic expansion method⁴¹ by using the Sturmian basis set⁴² and by the pseudostate method.⁴³ In the multistate expansion method of Ref. 41, excited hydrogenic orbitals are used in the expansion of Eq. (3). It was found that the electron-transfer cross sections are not changed substantially by the inclusion of the excited states. However, this does not imply that the two-state calculation has converged in all the cases studied. It actually happens that the excited states included in the expansion are not important for this particular reaction. This can be easily understood from the discussion in the previous paragraph. It was shown there that the inadequacy of the two-state atomic expansion occurs at small $R < 1.0$ where the electronic motion cannot be represented by the excited-state wave functions of the target or the projectile because of the diffuse nature of these functions, but can only be represented by the continuum functions. The Sturmian basis set and the pseudostates are all chosen in the hope that the continuum states are thus partially accounted for. In Table I, we compare the two-state calculation of McCarroll⁴⁴ and the pseudostate calculation of Cheshire *et al.*⁴³ for the reaction $p + H(1s) \rightarrow H(1s) + p$. We can see the two-state calculations are quite adequate for $E_p < 100$ keV, but as E_p increases, the two-state calculations overestimate the capture cross sections by a factor of 2 as the contributions of capture from small impact parameters to the total cross section increase.

From Table I and the discussion above, it becomes clear that the two-state approximation is best in the energy region where $v_p \approx v_e$. The method becomes inadequate as the projectile energy increases, eventually reducing to the OBK approximation at extremely high energies. It is interesting to mention that this implies all the first Born approximations for electron transfers are inadequate, even at high energies. This is not inconsistent with the conclusion of Drisko⁴⁵ that the second Born term is more important than the first Born term in the extreme limit of high energies.

By examining the results of our calculations in Figs. 2-6, our values at the high-energy side are about a factor of 2 higher than experimental data. Thus one might speculate that the continuum states are also very important in our calculations. At this moment we tend to believe this is not the case. The discrepancy probably can be reduced

TABLE I. Comparison of the two-state calculations^a and the pseudostate calculations^b for the total capture cross sections for $p + H(1s) \rightarrow H(1s) + p$ reactions. The cross sections are given in cm^2 . $A(2) = A \times 10^{-20}$.

Energy (keV)	Two-state ^a	Pseudostate ^b
4	1.15(-15) ^c	1.15(-15)
10	1.79(-16) ^c	7.77(-16)
15	5.60(-16)	5.81(-16)
20	4.18(-16) ^c	4.14(-16)
25	2.78(-16)	2.93(-16)
40	1.51(-16) ^c	1.15(-16)
60	4.98(-17) ^c	4.26(-17)
100	1.01(-17)	8.59(-18)
300	1.71(-19)	8.51(-20)
1000	5.12(-22)	2.62(-22)

^a Two-state calculations from McCarroll, Ref. 41.

^b Pseudostate calculations from Cheshire *et al.*, Ref. 42.

^c Interpolated from Ref. 41.

by including a few more atomic states of the target atom into expansion (3). It is noted that some excited orbitals of the target atoms have radii smaller or comparable to the radius of the 1s orbital of the hydrogen atom. The restriction of the two-state atomic expansion with basis functions differing substantially in the size of orbitals might have forced those amplitudes which would have otherwise ended up in the direct excitation channels into the electron-capture channel. The validity of this speculation has to be substantiated by actual calculations.

In summary, we applied the two-state atomic expansion method to compute the electron-capture cross sections of C, N, O, Ne, and Ar atoms. Comparisons of this method with other first-order Born methods are made to elucidate the region of validity of these methods. The limitation and possible further improvement of the present

model is also discussed.

Note added in proof. The revised experimental electron capture cross sections for protons on carbon atoms at low energies, in units of 10^{18} cm², are 0.61 ± 0.05 at 400 keV, 0.98 ± 0.08 at 300 keV, and 0.8 ± 0.08 at 250 keV of proton energies (J. R. Macdonald, private communication). These revised values are in good agreement with our calculations in Fig. 2.

ACKNOWLEDGMENTS

One of us (C.D.L.) acknowledges useful discussions with C. L. Cooke, J. M. Macdonald, and J. H. McGuire. This work is supported in part by Division of Basic Energy Sciences, U. S. Department of Energy. One of us (S.C.S.) is also supported partially by U. S. Army Research Office, Durham, North Carolina.

*Present address: Physics Dept., Hong Kong Baptist College, Hong Kong.

¹For a recent review, see P. Richard, in *Atomic Inner-Shell Processes*, edited by B. Grassman (Academic, New York, 1979), Vol. 1.

²U. Fano and W. Liebman, *Phys. Rev. Lett.* **14**, 627 (1975).

³G. G. Keessel and B. Frazier, *Case Studies in Atomic Physics*, edited by E. W. McDowell and M. R. G. McDowell (Amsterdam, North-Holland, 1973), Vol. 3. Y. S. Briggs and J. H. Macek, *J. Phys. B* **5**, 579 (1972). See also the review by J. S. Briggs in *Rep. Prog. Phys.* **35**, 217 (1976).

⁴K. Taulbjerg, J. S. Briggs, and J. Vaaben, *J. Phys. B* **5**, 1351 (1976).

⁵M. R. G. McDowell and J. P. Coleman, *Introduction to the Theory of Ion-Atom Collisions* (North-Holland, Amsterdam, 1976).

⁶See the review by R. A. Stapleton, *Theory of Charge Exchange* (Wiley-Interscience, New York, 1972).

⁷B. H. Bracken, *Rep. Prog. Phys.* **21**, 349 (1973).

⁸V. R. Opperholzer, *Phys. Rev.* **21**, 349 (1953).

⁹H. C. Brinkman and H. A. Kramers, *Proc. Acad. Sci. (Amsterdam)* **23**, 973 (1930).

¹⁰D. R. Bates and A. Dalgaard, *Proc. Phys. Soc. Lond.* **A** **65**, 919 (1953).

¹¹D. Jackson and R. Schiff, *Phys. Rev.* **55**, 359 (1953).

¹²In Ref. 12, the authors concluded that including the internuclear potential term will improve the convergence of the Born series. See also the remarks on p. 381 of Ref. 6.

¹³For earlier works, see Ref. 8.

¹⁴K. Ouldriz, J. E. Golden, J. H. McGuire, and L. Weaver, *Phys. Rev. A* **13**, 590 (1976).

¹⁵V. B. Barst, *Phys. Rev. Lett.* **27**, 634 (1976).

¹⁶A. Halpern and J. Law, *Phys. Rev. A* **12**, 1776 (1975).

¹⁷A. Halpern and J. Law, *Phys. Rev. Lett.* **31**, 4 (1973).

¹⁸V. S. Nikolaev, *Zh. Eksp. Teor. Fiz.* **21**, 1262 (1956) [*Sov. Phys. JETP* **24**, 847 (1967)].

¹⁹G. Lapicid and W. Lotensky, *Phys. Rev. A* **15**, 598 (1977).

²⁰For example, the Born (G) method of Ref. 15.

²¹D. R. Bates, *Proc. R. Soc. A* **274**, 294 (1955).

²²H. S. W. Massey and R. A. Smith, *Proc. R. Soc. A* **142**, 142 (1933).

²³L. T. Sin Fai Lam, *Proc. Phys. Soc. Lond.* **92**, 47 (1967).

²⁴T. C. Winter and C. C. Lin, *Phys. Rev. A* **10**, 2141 (1974).

²⁵K. E. Banyard and B. J. Sauster, *Phys. Rev. A* **10**, 129 (1977).

²⁶However, it can be shown that the resulting coupled equations are independent of the choice of origin so long as the origin is on the internuclear axis. See Ref. 22.

²⁷R. H. Bassel and E. Gerjuoy, *Phys. Rev.* **117**, 749 (1960).

²⁸See p. 212 of Ref. 6.

²⁹The approximate $1/a^3$ rule is discussed on p. 279 of Ref. 6. See also Ref. 25.

³⁰J. R. Macdonald, C. L. Cooke, and W. W. Eidsen, *Phys. Rev. Lett.* **22**, 648 (1974).

³¹C. L. Cooke, R. K. Gardner, B. Cunsutte, T. Bratton, and T. K. Saylor, *Phys. Rev. A* **15**, 2243 (1977).

³²M. Reuther, H. Pedersen, and J. R. Macdonald, in *Abstracts of the Tenth International Conference on the Physics of Electronic and Atomic Collisions*, Paris, 1977, edited by M. Barat and J. Reinhardt (Commissariat à l'Energie Atomique, Paris, 1977).

³³Oz Belkic and R. McCarroll, *J. Phys. B* **10**, 1923 (1977).

³⁴It must be pointed out, however, the authors in Ref. 34 apparently use the binding energy of the target to be $-1/2$, with $Z_p = 18$ for Ar. Their CBK results are in disagreement with the CBK results given in Refs. 15 and 21. Thus, it is not clear that the good agreement between calculations and data in the high-energy side given in Fig. 7 of Ref. 34 is exactly meaningful.

- ²A. Messine, *Phys. Rev. A* **15**, 666 (1977).
- ³A. E. S. Green, D. L. Schiff, and A. S. Zachor, *Phys. Rev.* **154**, 1 (1969); A. E. S. Green, *Adv. Quantum Chem.*, **2**, 221 (1973).
- ⁴Calculation of MO potential curves upon the GSE potential has been recently discussed by J. Eichler and U. Wille [*Phys. Rev. A* **11**, 1973 (1975)].
- ⁵M. J. Antal, M. B. McElroy, and D. G. Anderson, *J. Phys. B* **3**, 1513 (1973).
- ⁶A physically intuitive model would be to include in expansion (2) the eigenfunctions of the united atom He⁺ for collisions at small impact parameters. See Ref. 29 above and C. D. Lin (unpublished) (1977).
- ⁷L. Wilet and D. F. Gallaher, *Phys. Rev.* **147**, 13 (1966).
- ⁸D. F. Gallaher and L. Wilet, *Phys. Rev.* **153**, 139 (1963); R. Shakeshaft, *Phys. Rev. A* **14**, 1626 (1976).
- ⁹T. M. Cheshire, D. F. Gallaher, and A. J. Taylor, *J. Phys. B* **3**, 813 (1970).
- ¹⁰R. McCarroll, *Proc. R. Soc. A* **164**, 547 (1961).
- ¹¹R. H. Drisko, thesis (Carnegie Institute of Technology, 1959) (unpublished).

ELECTRON TRANSFER IN ION-ATOM COLLISIONS

by

LAURA NORMAN TUNNELL

B.S., East Texas State University, 1976

A MASTER'S THESIS

submitted in partial fulfillment of the

requirements for the degree

MASTER OF SCIENCE

Department of Physics

KANSAS STATE UNIVERSITY
Manhattan, Kansas

1979

ABSTRACT

The two state, two center atomic expansion method of Bates is applied within the independent electron approximation to charge transfer processes involving multielectron atoms. Usage of a realistic potential enabled a description of capture from both inner and outer shells of multielectron targets to be given. The theory is expected to be valid for projectile velocities near the characteristic orbital velocity of the active electron.

Comparison is made with an earlier work in which a screened hydrogenic model was employed to describe the transfer of electrons from the K shell of multielectron targets to the K shell of bare projectiles. It was concluded that the simple hydrogenic model could be used for high energy, asymmetric collision systems.

This is the first effort to describe capture from outer shells of multielectron targets in which a realistic atomic model is used. The method is applied to electron transfer from the outer shells of neon, argon, and krypton atoms to the K shell of hydrogen. Results of the calculations are compared with experimental data and further improvements in the theory are discussed.